UNIVERSITÀ DEGLI STUDI DI NAPOLI "FEDERICO II"

Tesi di Dottorato

"New insights into the Pathogenesis of Inflammatory Myopathies in Animals"

Coordinatore
Ch.mo Prof.
Cringoli Giuseppe

Candidato
Dott.
Prisco Francesco

Tutor
Ch.mo Prof.
Paciello Orlando

Co-Tutor
Ch.ma Prof.ssa
Serenella Papparella

Sapere aude!
Orazio (Epistole I, 2, 40)

Index

Index

Ringraziamenti

-

Lists of abbreviations

ACR	American College of Rheumatology
APP	Amyloid precursor protein
ART	Antiretroviral therapy
BLAST	Basic local alignment search tool
βAPP	Amyloid-β precursor protein
CL	Cutaneous leishmaniasis
COX	Cytochrome oxidase
C_q	Quantification cycle
CTPA	Calcium-translocating P-type ATPase
DCs	Dendritic cells
DM	Dermatomyositis
DMD	Duchenne muscular dystrophy
ER	Endoplasmic reticulum
ET	Engel trichrome
EULAR	European League Against Rheumatism
FCoV	Feline Coronavirus
FeLV	Feline Leukemia Virus
FIV	Feline Immunodeficiency Virus
GAPDH	Glyceraldehyde 3-phosphate dehydrogenase
GNE	UDP-N acetylglucosamine 2-epimerase/N-acetylmannosamine kinase
HCM	Hypertrophic cardiomyopathy
HE	Hematoxylin and eosin
hIBM	Hereditary inclusion body myositis
HIV	Human Immunodeficiency Virus
IBM	Inclusion body myositis
IFAT	Immunofluorescent antibody test
IFN	Interferon
IHC	Immunohistochemistry
IIF	Indirect immunofluorescence assay
IIM	Idiopathic Inflammatory Myopathies
IL	Interleukin
IM	Inflammatory Myopathies
IMNM	Immune-mediated necrotizing myopathies
IQ	Interquartile
JDM	Juvenile DM
LC-MS/MS	Liquid Chromatography-Tandem Mass Spectrometry

List of abbreviations

MAAs	Myositis-associated autoantibodies
MMM	Masticatory muscle myositis
mMyBP-C	Masticatory myosin binding protein-C
MSAs	Myositis-specific autoantibodies
NADH-TR	Nicotinamide adenine dinucleotide-tetrazolium reductase
NXP2	Nuclear matrix protein 2
PM	Polymyositis
QF	Quadriceps femoris muscle
ROI	Region of interest
SDH	Succinate dehydrogenase
SERCA1	Sarcoplasmic/endoplasmic reticulum calcium ATPase 1
SIV	Simian Immunodeficiency Virus
SR	Sarcoplasmic reticulum
TB	Triceps brachii muscle
TGF-β	Transforming growth factor-β
T_H	T helper
TIF1γ	Transcription intermediary factor 1γ
TL1A	Tumor necrosis factor-like ligand 1A
TLRs	Toll-like receptors
TNF	Tumor necrosis factor
TNFSF15	Tumor necrosis factor superfamily member 15
TWEAK	TNF-related weak inducer of apoptosis
VCP	Valosin-containing protein, a type II ATPase
VEGI	Vascular endothelial growth inhibitor
VL	Visceral leishmaniasis
WS	White striping myopathy

List of figures

List of figures

List of tables

Abstract

Inflammatory Myopathies (IMs) are a large and heterogeneous group of acquired disorders of the skeletal muscle characterized by the presence of inflammatory cells directly responsible for initiating and maintaining myofiber injury.

IMs are poorly characterized in veterinary medicine. A relatively large body of descriptive knowledge is available, however, many of the factors responsible for disease initiation and perpetuation remain less well-defined and the understanding of these mechanisms is mainly based on biological plausibility from animal models and human medicine.

The majority of these disorders are considered to be autoimmune disorders in which skeletal muscle is inappropriately targeted by the immune system. Autoimmune diseases develop as a result of chronic inflammation owing to interactions between genes and the environment. However, the mechanisms by which autoimmune diseases evolve remain poorly understood. Numerous evidences support that the innate immune system (including cytokines and chemokines) and adaptive immune system (including autoantibodies and antigen-specific T cells) are involved in IM pathogenesis. Furthermore, several non-immune-mediated mechanisms contribute to the pathogenesis of these disorders, including cell-stress pathways, free radicals, altered energy metabolism, protein homeostasis and mitochondrial damages.

Autoantibodies are present in approximately 60-70% of human patients with IM and often specific autoantibodies are strongly associated with specific form of IMs. The role of autoantibodies in causing muscle

damage and dysfunction is still debated, however, they have proven to be immensely useful biomarkers for the diagnosis, monitoring and prognosis of IMs. Therefore, there is great interest in the identification of myositis-specific autoantibodies.

In the present Ph.D. thesis:

1. we have identified novel pathogenetic mechanisms underlying leishmania-associated inflammatory myopathy in dogs. In particular, we identified circulating autoantibodies that recognize the muscle protein sarcoplasmic/endoplasmic reticulum calcium ATPase 1 (SERCA1) as the main antigen, supporting the autoimmune mechanism underlying this myopathy and the antigen mimicry pathogenesis;
2. we morphologically and molecularly characterize the white striping myopathy of the broiler chicken and, based on our results, we hypothesize an associated immune-mediated mechanism;
3. we describe the morphological and molecular findings of the inflammatory myopathy associated with natural Feline Immunodeficiency Virus infection in cats and identify circulating anti-skeletal muscle autoantibodies.

General Background

Inflammatory Myopathies in Veterinary Medicine

Inflammatory Myopathies (IMs) or Myositis are a large and heterogeneous group of acquired disorders of the skeletal muscle characterized by the presence of inflammatory cells directly responsible for initiating and maintaining myofiber injury.[1–3]

The term myositis has been inappropriately applied to various other muscular disorders in veterinary medicine, such as exertional and nutritional myopathy, in the horses. These two disorders are necrotizing myopathies, not IMs.[1] It is very important to distinguish between a true myositis and a degenerative myopathy in which there is a secondary inflammatory response.[1] In the normal response to the myofiber necrosis, the necrotic fiber is infiltrated by macrophages recruited from the circulating monocyte population, which phagocytose the cellular debris.[1] Severe acute necrotizing myopathy can also be accompanied by a certain degree of infiltrating lymphocytes, plasma cells, neutrophils, and eosinophils. Cytokines released from damaged muscle fibers are likely to recruit a variety of inflammatory cells under various circumstances, but these cells are not involved in causing

the muscle cell damage.[1] Moreover, lymphocytic myositis must also be distinguished from lymphoma involving skeletal muscle.[1]

IMs are poorly characterized in veterinary medicine. A relatively large body of descriptive knowledge is available[4–7], however, many of the factors responsible for disease initiation and perpetuation remain less well-defined and the understanding of these mechanisms is mainly based on biological plausibility from animal models and human medicine.[5]

The etiology and the pathomechanisms underlying IMs are still largely unknown. The majority of these disorders have an unknown cause and are defined as Idiopathic IMs (IIMs), others have been associated with the exposition to infectious or non-infectious agents and are defined as secondary IMs.[2,8] These two groups do not have a sharp division because different infectious or non-infectious agents do not cause IM directly but indirectly with still unknown mechanisms. As these mechanisms are defined, IMs classified as IIMs are moved to the secondary IM group.[2,8]

The majority of these disorders are considered to be autoimmune disorders in which skeletal muscle is inappropriately targeted by the immune system.[2,4,9] A relation between these immune disorders and the exposition to different infectious and non-infectious agents has been reported both in humans[2], dogs[10], cats[11], horses[12] and has also been proposed in sheep.[13]

Classification of Inflammatory Myopathy

Classification criteria are meant to identify uniform and comparable groups of IMs for both clinical and research purposes.[14] This classification

criteria continually evolve and reflect epidemiologic and molecular knowledge advances on IMs.[14,15]

In 2017 the European League Against Rheumatism (EULAR) and American College of Rheumatology (ACR) developed and validated with a robust methodology the new diagnostic criteria for IMs in human medicine.[15] Several clinicopathological classification criteria for IM have been defined and associated with a remarkable calculation system for the probability of IM diagnosis. If the calculated probability of diagnosis of an IM is greater than or equal to 55% the disorder will be further classified as follow (Fig. 1).[15]

IM in adults (>18 years old) are classified into three major subgroups including polymyositis (PM), dermatomyositis (DM) and inclusion body myositis (IBM). DM includes a further subgroup defined as Amyopathic DM and characterized by the presence of typical skin findings without muscle weakness. According to this classification scheme, PM subset includes immune-mediated necrotizing myopathies (IMNM).[15]

According to the 2017 EULAR/ACR classification system, IMs in children (<18 years old) are divided in juvenile DM (JDM) and in a less defend and heterogeneous group named “other juvenile myositis”.[15]

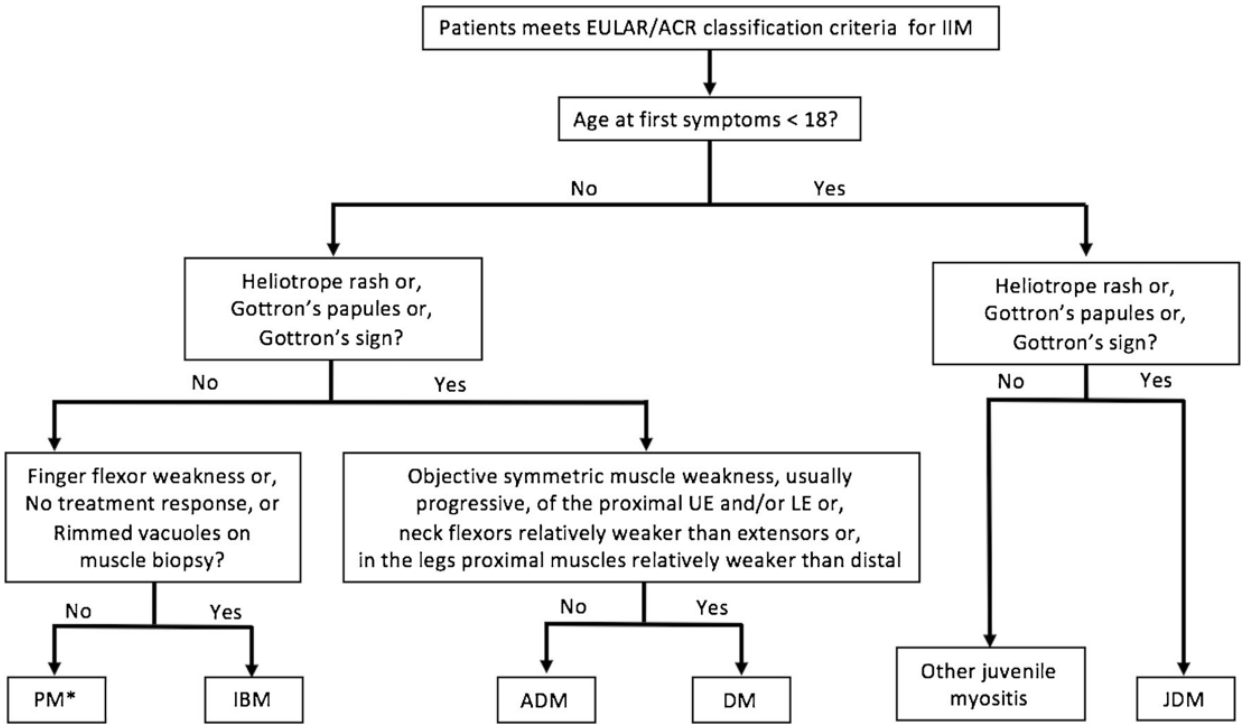

Figure 1. Subgroups of human IMs according to the 2017 EULAR/ACR classification criteria.[15] **The PM subset includes immune-mediated necrotizing myopathies (IMNM). PM, polymyositis; IBM, inclusion body myositis; ADM, amyopathic dermatomyositis; DM, dermatomyositis; JDM, juvenile dermatomyositis.*

A well-structured classification system such as the one used in human medicine is not currently available in veterinary medicine. Among animals, IMs are best studied in dogs and classified according to the scheme that we propose in figure 2. The most common canine IMs include the highly specialized immune-mediated masticatory muscle myositis (MMM) and the PM, otherwise, extraocular myositis and DM occur less commonly.[4] Homologous to the human IBM and IMNM are not yet well reported in dogs but few case reports of canine myopathies that share many features with these IM subtypes has been published.[4,16] Different IMs, mainly with a disease phenotype similar to PM, have been described also in horses[12], cats[11] and sheep[13].

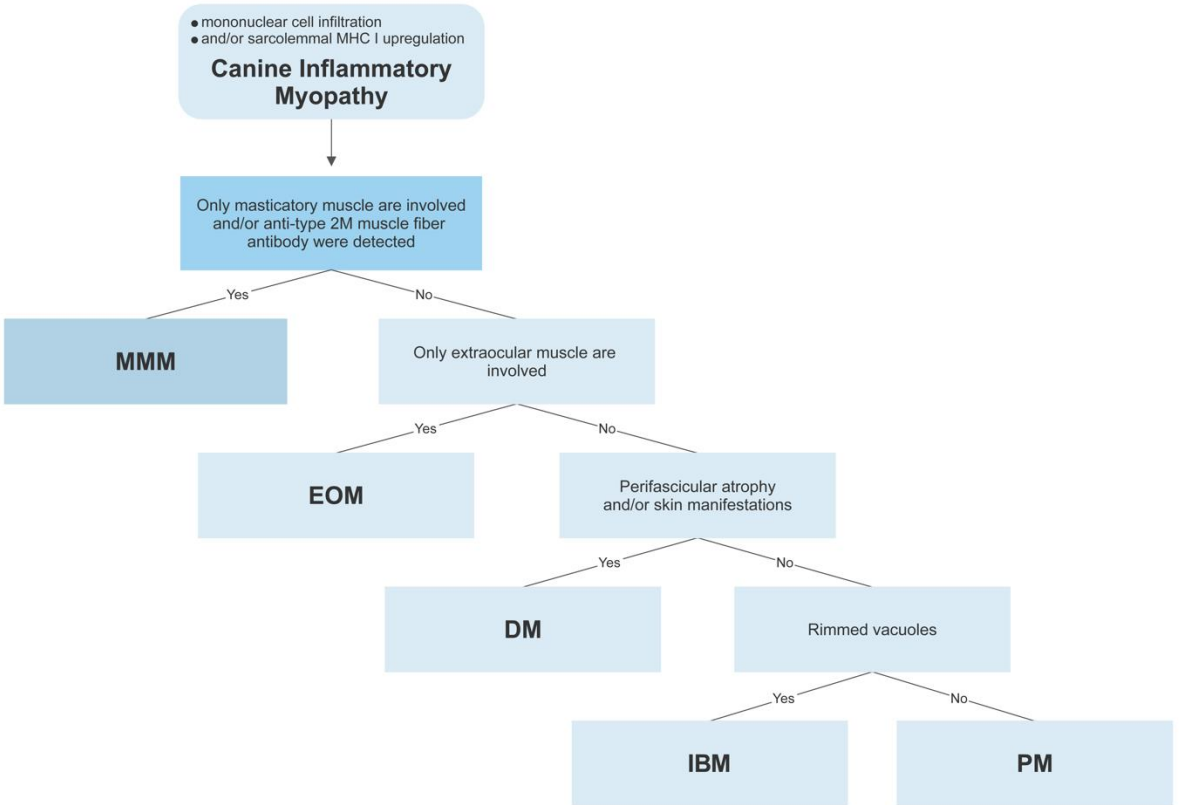

Figure 2. Subgroups of canine IMs according to the most recent classification criteria.[4,16] *MMM, masticatory muscle myositis; EOM, extraocular myositis; PM, polymyositis; IBM, inclusion body myositis; DM, dermatomyositis.*

Risk factors

The pathogenic mechanisms of most immune-mediated diseases relate to chronic organ inflammation that can be caused by specific interactions between genetic and environmental risk factors (Fig. 3).[2] However, how these factors determine the activation of the immune system is still far from clear.[2]

Genetic risk factors

Several genetic risk factors have been described in humans;[2] The HLA 8.1 ancestral haplotype is a key risk factor for major IM phenotypes in some populations, and several genetic variants associated with other autoimmune diseases have been identified as IM risk factors.[2] No naturally occurring genetic risk variants have been identified in other animals so far. However, the overrepresentation of some canine breeds (e.g. Boxer and Newfoundland) in relatively large clinicopathological studies allow to hypothesize that the genetic variants play a role at least in this specie.[7,17]

Also based on knowledge of genetic risk factors, different transgenic animal models of IMs have been generated. These models include a murine model based on inducible, muscle-specific overexpression of MHC I (HT double-transgenic mice). This model has proven invaluable for the assessment of the relationship between muscle weakness/dysfunction and

activation of ER stress pathways both of which occur before the onset of histopathologically evident mononuclear cell infiltration.[6]

Transgenic and knockout mice models for the human hereditary inclusion body myositis (hIBM) have also been generated. These models are based on muscle-specific overexpression of amyloid-β precursor protein (βAPP) or mutations of genes encoding GNE (UDP-N acetylglucosamine 2-epimerase/N-acetylmannosamine kinase, an enzyme involved in sialic acid synthesis) and VCP (valosin-containing protein, a type II ATPase). Another animal model used by several investigators for the study of hIBM is the nematode *Caenorhabditis elegans* with overexpression of the human APP proteolytic fragment Aβ.[6]

Other transgenic models used for the study of IMs include animals with structural protein defect resulting in muscular dystrophies. The pathologies that characterize these models are not classifiable as IMs, but some investigators have used these models to explore some pathways of the associated inflammation assuming that some pathomechanisms are common to IM. Examples involve SJL/J mice, a strain that develops an age-dependent dysferlinopathy closely mimicking the pathology of human disease, and mdx mice, a model of Duchenne muscular dystrophy (DMD) characterized by a mutation of the cytoskeletal protein dystrophin resulting in sarcolemmal instability, muscle necrosis and in an associated inflammatory component.[6]

Environmental risk factors

The pathogenesis of IMs cannot be explained solely by genetic risk factors. Many of the variants identified have a relatively small effect on disease risk individually.[2] It has been hypostasized that the physiological effect of these genes might depend on their activation or modification by environmental factors.[2]

Multiple lines of evidence suggest that the environmental component have an influence on autoimmune diseases; there are strong temporal associations between certain exposures (infectious agents and drugs in particular) and the subsequent development of some autoimmune diseases; in some individuals, disease improves after removing a suspected environmental agent (dechallenge) and/or worsens or reoccurs after re-exposure to the suspected agent (rechallenge).[2]

Environmental risk factors are less well studied than genetic factors but might include parasites, viruses, bacteria, ultraviolet radiation, cigarette smoke exposure and a growing list of drugs (including biologic agents) and dietary supplements.[2,12,13,18]

A number of specific infectious agents are implicated in IMs pathogenesis on the basis of reported occurrences of the infection-induced disease in animals.[2,4,19] Examples include *Leishmania spp*. in dogs[10,18,20], mice[21] and Syrian hamsters[19,22]; *Theileria equi* and *Babesia caballi* in horses[12]; *Sarcocystis tenella* in sheep[13] *Trypanosoma cruzi* in mouse[6]; *Feline Immunodeficiency Virus (FIV)* in cats[11,23]; *Ross River virus* and *Coxsackie B virus* in mouse,[6] etc.

Non-infectious agents are less reported in veterinary medicine, probably due to the major difficulties of realizing epidemiological studies in animals. However, numerous evidences of epidemiological correlation between IMs and ambient pollutions or drugs have been reported in humans and several of these associations are also supported by experimental studies based on animal models.[2,24]

Data from relevant animal models have shown the plausibility of multiple environmental agents potentially triggering autoimmune disease.[2,10,12,13,20] Notably, mercury induces systemic autoimmune disease in rats and mice, several mineral oil components and certain other hydrocarbons can induce acute inflammatory arthritis in some rat strains, and there is also a clear association between infection with a limited number of pathogens and the development of specific autoimmune diseases in different animal species.[24,25] Furthermore, evidences that other environmental factors, such as dioxins, organochlorine pesticides, silica, etc., may promote autoimmunity are also reported.[25]

Moreover, interesting epidemiological studies in human populations and experimental studies with animal models revealed that perinatal factors affecting mothers during gestation, including air pollution, cigarette smoke and exposure to dust and/or solvents, could be important risk factors for IM, in particular for juvenile dermatomyositis.[2,25]

It is likely that the existing associations between environmental agents and autoimmune disorders are more numerous. The main difficulty in identifying these associations probably lies in the fact that after certain disease-initiating exposures, several years can pass before the autoimmune disease manifests.[2]

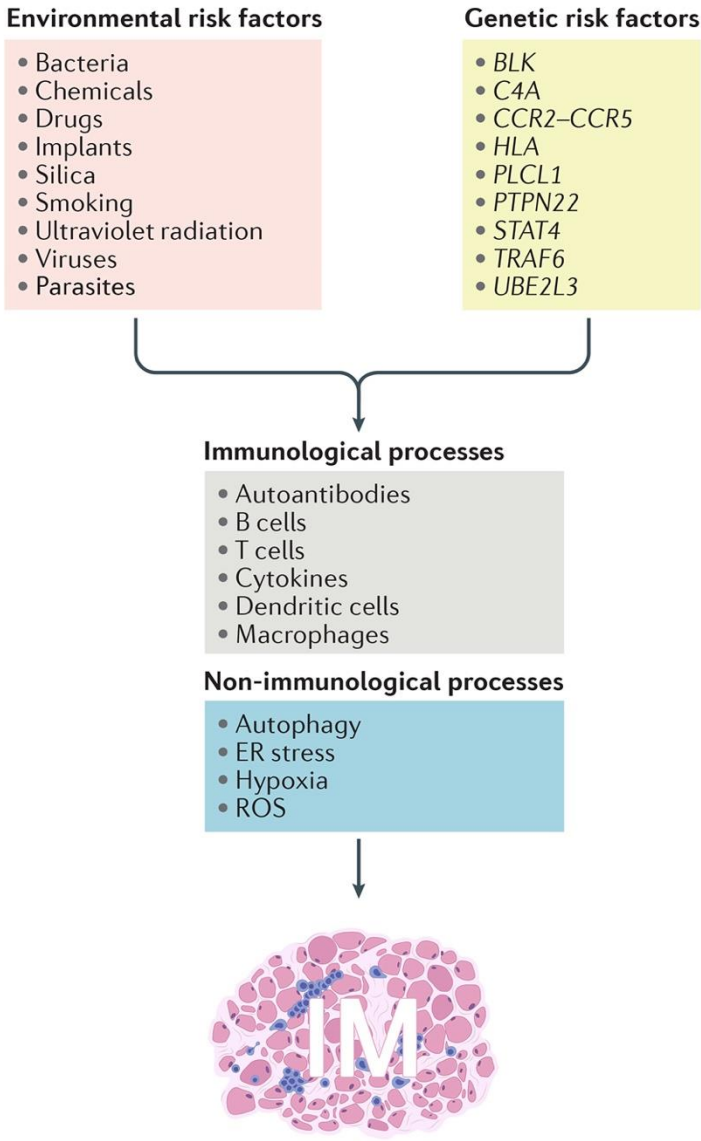

Figure 3. Possible pathways involved in inflammatory myopathies pathogenesis in humans and other animals *(modified from Miller et al., 2018).*[2] *Inflammatory Myopathy (IM) could result from different pathogenic mechanisms, including immunological and non-immunological processes, because of the*

interactions between genetic and environmental risk factors. Some combinations of genotypes and environmental exposures induce certain mechanisms and disease phenotypes, whereas other combinations might have no effect or could be protective. C4A, complement 4A; ER, endoplasmic reticulum; ROS, reactive oxygen species.

Disease mechanisms

Although the disease mechanisms for IMs are ill-defined, numerous evidences support that the innate immune system (including cytokines and chemokines) and adaptive immune system (including autoantibodies and antigen-specific T cells) are involved. Furthermore, several non-immune-mediated mechanisms contribute to IMs pathogenesis, including cell-stress pathways, free radicals, altered energy metabolism, protein homeostasis and mitochondrial damages.[2,13]

Immune-mediated Disease Mechanisms

Generally, muscles of animals with IM are mainly infiltrated by both T and B lymphocytes.[4,5]

T cells are mainly cytotoxic $CD8^+$ effector T cells associated with a smaller number of $CD4^+$ helper T cells.[2,4,5] The invasion of $CD8^+$ effector T cells into non-necrotic muscle fibers is considered a characteristic histological feature of PM and IBM both in humans and in animals.[2,13] Furthermore, in humans it has been shown that muscles affected by IM also

contain some unique subsets of highly cytotoxic, apoptosis-resistant, pro-inflammatory T cells, such as $CD28^{null}$ ($CD244^{+}$) T cells (both $CD4^{+}$ $CD28^{null}$ and $CD8^{+}$ $CD28^{null}$ T cells).[2]

γδ-T cells have been reported in forms of IM both in humans and in animals.[2,26] In humans, investigators suggested a potential link between γδ T cells and autoantibody responses in IM demonstrating that these γδ T cells recognize the same antigens that are recognized by myositis specific antibodies.[2,27]

Regulatory T (T_{reg}) cells (defined by FOXP3 expression) are described in human IMs and their role appears to be the counterbalance of muscle inflammation.[2]

Recent studies have demonstrated the presence of B cells, plasma cells and immunoglobulin transcripts in the muscle of both humans and animals with IMs, indicating a humoral component in those disorders.[2,5,13]

Autoantibody

Autoantibodies are present in more than half of all human patients with IM and often are strongly associated with specific form of IMs.[2,5] Traditionally, autoantibodies found in patients with myositis are described as being myositis-specific autoantibodies (MSAs) or myositis-associated autoantibodies (MAAs), depending on their prevalence in other related conditions. Alternatively, MSA and MAA could be combined into a single entity such as myositis-related autoantibodies.[5,28]

The role of autoantibodies in causing muscle damage and dysfunction is debated because most of the autoantigens are intracellular and thus not easily accessible to circulating autoantibodies.[28,29]

An intriguing aspect of MSAs is that the detection of more than one of such autoantibodies in the same patient are extremely rare, although MAAs can sometimes coexist. As such, MSAs are ideal biomarkers, not only for identifying homogeneous subsets of myositis but also for exploring more precisely the potential environmental and genetic factors contributing to the disease.[28,29] So, although cause and effect relationships between autoantibodies and disease phenotype and activity currently are not clear, the strong associations of MSAs with distinct genotypes, clinical phenotypes, interferon expression patterns and disease severity are immensely useful for the diagnosis and prognosis of IMs.[2]

Very little is known about the presence of autoantibodies in IM in veterinary medicine, however, some noteworthy examples are available.[5] Notably, the MMM in dogs is characterized by circulating anti-type 2M fibers antibodies, and these play an important role in the diagnosis of this muscular disorder. MMM is characterized by circulating autoantibody directed against both masticatory muscle myosin heavy and light chains.[30] Additionally, an interesting study by Wu et al. showed that the main antigens of the autoantibodies in canine MMM include also a masticatory myosin binding protein-C (mMyBP-C).[31]

Circulating autoantibodies mainly directed against sarcolemmal structures have been reported in horses with chronic piroplasmosis.[12]

Furthermore, recently we reported circulating anti-muscle autoantibodies also in dogs with Leishmania-associated myopathy.[20] In

Chapter 1 of this thesis it will be illustrated how we have defined Sarcoplasmic/endoplasmic reticulum calcium ATPase 1 (SERCA1) as the main antigen recognized by circulating antibodies.

Innate-Immune Disease Mechanisms

Antigen processing and presentation by professional antigen-presenting cells, such as dendritic cells (DCs), are critical to initiating the adaptive immune response, and the muscle microenvironment of IM is enriched with both myeloid and plasmacytoid DCs.[2,5] The relative proportion of lymphocytes and macrophages in skeletal muscle seems to vary in different entities, for example, in canine PM the number of macrophages is usually very low compared with the number of lymphocytes, differently, in white striping myopathy in broiler chickens macrophages predominate over T and B cells.[5,26]

Skeletal muscle, as well as muscle-infiltrating cells, express abundant innate immune receptors, including Toll-like receptors (TLRs). Activation of innate immune receptors can lead to activation of NF-κB signaling and pro-inflammatory cytokine and chemokine secretion, which, in turn, further recruit immune cells into a milieu that is already ripe for antigen processing and presentation by dendritic cells. These immune cells and cytokines can then further activate T helper 1 (T_H1), T_H17 and T_H2 cells, as well as $CD8^+$ cytotoxic T cells and $CD28^{null}$ T cells, which potentially damage muscle cells.[2,26] Such mediators include T_H1 cytokines (TNF, IFNγ, IL-12 and IL-2), T_H2 cytokines (IL-4 and IL-13), T_H17 cytokines (IL-17,

IL-22, IL-23, TNF-related weak inducer of apoptosis (TWEAK) and IL-6), T_{reg} cytokines (IL-10 and transforming growth factor-β (TGFβ)) and innate immune cytokines (IL-1α, IL-1β and type I interferons (IFNα and IFNβ)). These cytokines coordinate various innate and adaptive immune response pathways, and some of them can cause muscle damage and weakness, depending on the stage of the disease.[2,26]

Non-immune-mediated Disease Mechanisms

Mounting evidence suggests that several non-immune-mediated mechanisms also occur in IMs.[2] In general, these mechanisms fuel inflammation via a positive feedback loop, affect muscle contraction and are responsible for muscle weakness, imbalance muscular protein homeostasis and lead to atrophy and mostly irreversible structural damage of muscle fibers.[2]

Non-immune-mediated disease mechanisms involved in IMs include endoplasmic reticulum (ER)-stress, free radicals, protein homeostasis imbalance, the heat shock response, dysregulation of autophagy and mitochondrial abnormalities.[2]

ER stress mechanisms include the unfolded protein response and the ER overload response, both activated in all forms of IMs.[2] The unfolded protein response includes several pathways that reduce the protein overload and subsequent accumulation of unfolded proteins in the ER. The ER overload response modulates inflammation by upregulating NF-κB signaling.[2]

Free radicals are key factors in muscle fiber damage in all forms of IM, and these molecules are speculated to contribute directly to muscle weakness.[2]

Protein dyshomeostasis, malfunction of the autophagic machinery and the associated heat-shock response are mechanisms well described in the pathogenesis of the human IBM. This pathology is characterized by the accumulation into muscle fibers of a variety of unwanted and defective proteins that should be removed from the cell, including β-amyloid and its associated proteins.[2]

Furthermore, also mitochondrial abnormalities, such as cytochrome c oxidase deficiency, are often described as part of the pathomechanism of IMs both in humans and in animals.[2,13] These dysfunctions potentially participate in the production of free radicals or in ER stress further fueling these two non-immune-mediated pathways.[2,13]

Link with the Cardiac Muscle Pathology

Cardiac involvement in IM was first reported by Oppenheim in 1899.[32] Currently, more and more evidence has accumulated in support of a link between IMs and cardiac involvement.[33] Since the myocardium shares many structural and functional features with skeletal muscle, it is hypostasized that the same pathogenetic mechanism can participate both in IM and myocarditis. However, the full extent of this link and the mechanisms behind it are still poorly understood.[34]

In humans, cardiac involvement is more commonly reported in patients with PM/DM, while patients with IBM have a lower risk.[33] Morphologically, in PM/DM the myocardium shows an inflammation similar to that of skeletal muscle.[33] An increased risk of myocardial infarction and venous thromboembolism has also been reported in patients with IMs.[35] However, cardiac disease in IMs is most commonly subclinical and the literature suggests that rhythm disturbances are the most common subclinical cardiac manifestation of PM/DM, while congestive heart failure is the most frequently reported cardiac complication, and occurs in 10-15% of patients.[33] Congestive heart failure can develop at any time in the course of skeletal muscle disease, and even in remission state.[33]

Cardiac involvement has also been reported in different infectious agents-related IMs in animals, such as in dogs and Syrian hamsters with *Leishmania spp*. infection, in seep infected with *Sarcocystis spp*., in horses with piroplasmosis and in cats with Feline Immunodeficiency Virus infection.[5]

Cardiac involvement in IMs is a feared event because it is one of the most common causes of death.[5,33,35]

Cancer-associated Myositis

In human medicine, an increased risk of cancer in patients with IM has been reported. Cancer-associated myositis is typically defined as the development of malignancy within 3 years of diagnosis of IM.[28,36]

An increased risk for malignancy has been reported in IM with adult-onset but not in juvenile-onset disease. PM and DM are the most commonly associated with malignancy and DM of recent onset showed even higher risk.[28,36]

The association between DM and malignancy is particularly strong in those humans with antibodies to transcription intermediary factor 1γ (TIF1γ; also known as TRIM33) or nuclear matrix protein 2 (NXP2; also known as MORC3). Indeed, between 50% and 75% of adult humans with anti-TIF1γ autoantibodies will have an associated cancer. While, although anti-NXP2 autoantibodies are also associated with the development of cancer, such detailed information is not available because they are rare in humans IMs with adult onset and the association with malignancy has been difficult to study.[28,36]

Information regarding the association of IMs and cancer in Veterinary Medicine is sparse; only few case reports and case series are available. Notably, in dogs, few reports have linked polymyositis with lymphoma, thymoma, myeloid leukemia, bronchogenic carcinoma, tonsillary carcinoma, anaplastic round cell tumor and plasmacytoma.[37]

Lymphoma is the most commonly associated with IM in dogs and, interestingly, Boxers are overrepresented.[7,37] In the reported cases, at the time of diagnosis of the IM, no evidence of neoplastic cells was found in the biopsy sections, whereas at the time of diagnosis of neoplasia, neoplastic cells were observed in the muscle biopsies.[7] This finding suggests that IM might be a preneoplastic syndrome in this breed.[7]

Animal Models of Inflammatory Myopathy

Despite the large body of descriptive knowledge, many of the factors responsible for IMs initiation and perpetuation remain less well-defined. Animal models have proven to be tremendously helpful in mechanistic studies and allow researchers to overcome the inevitable restrictions of human research. Although many of these models reproduce isolated aspects of the skeletal muscle pathology found in human IMs, none exactly replicate the totality of human disease. Moreover, since the pathomechanism underlying IMs remains unclear, both in human and veterinary medicine, therapeutic approaches, in general, comprise unspecific immunosuppression strategies that have been met with limited success. Therefore, a deeper understanding of the underlying mechanisms is critically required to assist in the development of targeted therapies.[6]

Models of IMs (Table 1) include infection-induced models, genetically based models of immune-mediated pathways, genetically based models of nonimmune pathways, antigen-induced models and a diet-triggered model.[6]

Infection-induced models of myositis are animal models generated using the mechanism of induction of IMs by specific infectious agents. Some examples include mice infected with Ross River virus, Coxsackie B virus or *Trypanosoma cruzi*[6]; *Leishmania spp.* infection in mouse[21] and Syrian hamsters[19] etc.

Genetically based models of immune-mediated myopathy include several models characterized by structural proteins defect resulting in muscular dystrophies with subsequent muscle inflammation. These models

are used to highlight specific inflammatory pathways potentially common to IMs and muscular dystrophies.[6]

Genetically based models of nonimmune pathways include models of the hereditary and sporadic IBM, generally characterized by aberrant amyloid precursor protein (APP) expression and the already mentioned murine model based on inducible muscle-specific overexpression of MHC I (HT double-transgenic mice).[6]

Antigen-induced models of inflammatory myopathy are models in which IM is generated with an antigen/adjuvant immunization strategy with the attempt to model (auto)immune pathways contributing to the pathogenesis of these diseases. The strategy consists of immunizing the animal against autoantigens implicated in human IMs (most employ myosin or myosin-associated proteins) and resulting in an autoimmune disorder targeting the skeletal muscle.[6]

To date, only one model of diet-triggered IM has been described. Rabbits fed with cholesterol-enriched diets exhibit pathological features that resemble IBM. The high dietary cholesterol increases APP and Aβ and induces IBM-like pathology. This model has opened new perspectives for the study of protein dyshomeostasis in the pathogenesis of IMs.[24,38]

Table 1. *Induced experimental models of Inflammatory Myopathy.*[6,21,24,38]

Model	Host	Disease phenotype	Muscle infiltrate and other features	Gender[a]
Infection-induced				
Ross River virus	Mouse	PM	M, NK, $CD4^+$, $CD8^+$	Undefined
Chikungunya virus	Mouse	PM	M, NK, $CD4^+$, $CD8^+$	Undefined
Coxsackievirus B1	Mouse	PM	Mononuclear	Undefined
Trypanosoma cruzi	Mouse	PM	M, $CD4^+$, $CD8^+$	Female
Leishmania spp.	Syrian hamster, Mouse	PM	$CD4^+$, $CD8^+$	Undefined
Genetic/transgenic				
Aβ	Nematode	Neuromuscular deficit	Amyloid aggregates	Hermaphrodite
βAPP	Mouse	hIBM	Myofibrillar deposits, N	Undefined
GNE	Mouse	hIBM/DMRV	Rimmed vacuoles, inclusion bodies	Undefined
VCP	Mouse	IBMPFD	Rimmed vacuoles, mononuclear cells	Undefined
MHC I	Mouse	JDM (early); PM (late)	M	Female (male delayed)
Synaptotagmin VII	Mouse	PM	$CD3^+$, M, Ly-$6G^+$ and ANA	Female
mdx/dystrophin	Mouse	Dystrophy, myositis	M, $CD4^+$, $CD8^+$, N	Male>female[b]
SJL/J—EAM	Mouse	Dysferlinopathy, myositis	M[c], $CD4^+$, $CD8^+$	Male, female
Antigen-induced				
Myosin	Mouse, rat	PM	$CD4^+$, $CD8^+$, M	Female
C protein	Mouse, rat	PM	M, $CD4^+$, $CD8^+$	Female
HRS/CFA (subcutaneous)	Mouse	ILD, myositis	$CD3^+$	Male=female
HRS/soluble (intramuscular)	Mouse	PM	$CD3^+$	Male=female
Laminin	Rat	PM	$CD4^+$, $CD8^+$, M	Female
Diet-triggered				
Diet with 2% cholesterol	Rabbit	sIBM	M and intracellular deposits (Aβ, Tau)	Female

[a] Reported gender in experiments; gender restriction unknown unless indicated

[b] Adult (6-month-old) mice

[c] Macrophages predominate in spontaneous myopathy of SJL/J mice; EAM induction increases the percentage of $CD4^+$, $CD8^+$ T cells

*A*β proteolytic fragment of APP; β*APP* β-amyloid precursor protein; *CD3*$^+$ $CD3^+$ T cell; *CD4*$^+$ $CD4^+$ T cell; *CD8*$^+$ $CD8^+$ T cell; Ly-$6G^+$ Ly-$6G^+$ neutrophils and eosinophils; ANA antinuclear antibody; *CFA* Complete Freund's Adjuvant; *DMRV* distal myopathy with rimmed vacuoles; *EAM* experimental

autoimmune myositis (myosin induced); *GNE* UDP-*N* acetylglucosamine 2-epimerase/*N*-acetylmannosamine kinase; *hIBM* hereditary inclusion body myositis; *sIBM* sporadic inclusion body myositis; *HRS* histidyl-tRNA synthetase; *IBMPFD* inclusion body myopathy with Paget's disease of bone and frontotemporal dementia; *ILD* interstitial lung disease; *JDM* juvenile dermatomyositis; *M* macrophage; *MHC* major histocompatibility complex; *N* neutrophil; *NK* natural killer cell; *PM* polymyositis; *VCP* valosin-containing protein.

Specific Background

New Perspectives in Natural Occurring Animal Models of Inflammatory Myopathies

In recent years, the regulation about laboratory animal is becoming more and more strict. According to the principle of the three Rs, Replace, Reduce and Refine, the use of naturally occurring (or spontaneous) animal models is becoming more significant.[39] The potential advantages of using naturally occurring animal models of human disease are: domestic animals share the same environments as humans; the life cycle of the domestic animals is usually shorter compared with humans; some animals have large numbers of offspring, facilitating hereditary studies.[40] Some limitations of naturally occurring animal models compared with laboratory animals are: the genetic variability in a study group is higher; animal pedigrees are not always verified so the exact parentage is not always known; specific mating between animals cannot be arranged.[40]

In the following sub-chapters, we provide an overview of the most recently described natural occurring animal models of IMs.

Canine Inflammatory Myopathy Associated with Leishmania Infantum Infection

In dogs, *Leishmania infantum* infection is associated with an IM with many similarities with the human PM.[10,18] This pathology has also been experimentally reproduced in Syrian hamsters and mice.[19,21]

IM in these dogs is often subclinical.[41] The most common clinical signs of leishmaniasis are skin lesions, lymphadenopathy, hepatosplenomegaly, weight loss, onychogryphosis and ocular lesions. Rarely, these signs can be associated with clinically evident neuromuscular signs, such as paraparesis.[41] With electromyography, fibrillation potentials, positive sharp waves and complex repetitive discharges can generally be detected even in asymptomatic dogs.[41]

Morphologically, the inflammatory infiltrate in skeletal muscle is mainly perivascular in the perimysium and multifocally surrounds the muscle fibers in the endomysium. The inflammatory cells are mainly CD8+ T lymphocytes and macrophages with fewer CD4+ T lymphocytes.[10,41] Marked variation in fiber size, including atrophic and hypertrophic fibers, and different disseminated necrotic muscle fibers can usually be observed. Aspects of muscle regeneration can also be observed, including myotubes and type 2C fibers.[10] In the chronic stages, endomysial and perimysial thickening due to fibrosis can be observed. Usually, many muscle fibers show immunohistochemical sarcolemmal expression of MHC class I and class II.[10] Moreover, CD8+ T lymphocytes invade histologically normal muscle fibers expressing MHC class I antigens (CD8/MHC-I complexes) supporting an immune-mediated pathogenetic hypothesis.[10]

Dogs infected with *Leishmania infantum* also show myocarditis characterized by an inflammatory infiltrate similar to that reported in

skeletal muscle. Interstitial fibrosis and sarcolemmal expression of MHC class I and MHC class II antigens have also been reported.[18]

Several pathogenetic mechanisms have been hypothesized[10]; however, the most supported is an antibody-mediated autoimmune mechanism.[20] We hypothesize that the autoantibodies produced by dogs with leishmaniasis may be directed against one or more proteins shared by skeletal and cardiac muscle, triggering immune-mediated damage in both tissues.[10,18] Further arguments regarding this mechanism will be provided in the Chapter 1 of this thesis.

Inflammatory Myopathy in Horses Associated with Piroplasmosis

Equine piroplasmosis is a protozoal disease caused in horses by two apicomplexan hemoprotozoa, *Theileria equi* and *Babesia caballi*.[12] Equine piroplasmosis has been associated with an IM characterized by circulating anti-muscle antibodies.[12]

Clinically, horses with chronic piroplasmosis can develop poor performance and muscle atrophy. The serum activity of CK, AST and LDH is usually slightly elevated.[12]

Histologically, the main myopathic change is a multifocal lymphocytic infiltrate often organized in cuffs around the perimysial and endomysial blood vessels and less frequently expanding multifocally into the endomysium. The inflammatory infiltrate is mainly composed of both CD8+ and CD4+ T lymphocytes, fewer macrophages and rare scattered

CD79α+ B lymphocytes.[12] Various degrees of atrophy of nonangular fibers, necrotic fibers invaded by macrophages, mild perimysial fibrosis were also observed. Mitochondrial abnormalities include ragged blue fibers observed with SDH stain and fibers with a moth-eaten appearance observed with COX and NADH stains.[12] Muscle fibers immunohistochemically overexpress MHC I and MHC II.[12]

Increased mRNA levels of IL-12, TNF-α, and IFN-γ were found in the muscles of affected animals, while no changes in IL-10 mRNA levels were observed. Moreover, DNA from *Theileria equi* or *Babesia caballi* was not detected by RT-PCR in muscle samples affected.[12]

Involvement of the heart during piroplasmosis has been well established in dogs, but there is little sporadic information in the literature on heart involvement during piroplasmosis in horses.[42,43] Further studies are needed to better clarify the involvement of the heart in this species.

Inflammatory Myopathy in Cats Associated with Feline Immunodeficiency Virus Infection

Feline Immunodeficiency Virus (FIV) infection is associated with an IM and a myocarditis in adult cats.[11,44] HIV is similarly implicated in a form of IM and myocarditis in humans.[44–46] This model has so far been poorly characterized and there is little information in the literature, however, the characteristics of this myopathy are comparable to human PM.[11,44]

No clinical signs have been associated with this IM, however, an increase in serum CK values has been reported.[11] Needle electromyography may be characterized by mild to moderate abnormal spontaneous activity. Furthermore, a mixture of positive acute waves and fibrillation potentials can be detected in a multifocal pattern.[11]

The pelvic limb muscles are more frequently affected than the thoracic limb muscles. The vastus lateralis is the most frequently affected muscle while the brachial triceps is the least affected muscle.[11]

Histologically, this IM is characterized by perivascular and endomysial multifocal infiltration of CD8+ T lymphocyte. Sometimes, these lymphocytes infiltrate non-necrotic myofibers. Myofiber necrosis and phagocytosis has also been reported.[11]

FIV infection in adult cats has also been associated with myocarditis. Clinical manifestations included dyspnea, lethargy, anorexia and vomiting.[44] Histologically is characterized by a coalescing multifocal inflammatory infiltrate mainly composed of lymphocytes and, to a lesser extent, of macrophages, neutrophils and plasma cells. A variable degree of interstitial fibrosis has also been reported.[44] Hypertrophic cardiomyopathy (HCM) is also described in cats associated with FIV infection.[44]

Inflammatory Myopathy in Sheep Associated with Sarcocystis tenella Infection

For years, it has been argued that *Sarcocystis* infection almost always did not cause injury to the ruminant's muscle or is associated with an eosinophilic myositis in the case of cyst rupture. We have defined that *Sarcocystis tenella* infection is associated with an IM in sheep.[13]

In intermediate hosts, such as sheep, infection is commonly asymptomatic and the presence of muscle cysts is considered an incidental finding.[13] However more than 95% of infected animals show subclinical myopathy.[13]

Histologically, this myopathy is characterized by a multifocal inflammatory endomysial infiltrate mainly composed of CD8+ lymphocytes, occasionally centered around parasitic and non-parasitic fibers and rarely arranged in perivascular cuffs. Variability of fiber diameter and different disseminated necrotic muscle fibers invaded by macrophages are reported.[13]

We also reported widespread sarcolemmal immunopositivity for MHC I and MHC II in almost all cases and variable expression of MHC I antigen on the cyst wall.[13] Moreover, occasionally CD8+ cells invade non-necrotic parasitized and non-parasitized fibers.[13]

Sheep naturally infected with *Sarcocystis tenella* also show myocarditis characterized by an inflammatory infiltrate similar the that found in skeletal muscle.

Inflammatory CD8+ T lymphocytes infiltrate, sarcolemmal immunopositivity to MHC I and CD8+ T lymphocytes invading non-

necrotic muscle fibers suggest that parasitized muscle fibers might play an active role in antigen presentation and stimulating inflammatory response.[13]

Objectives

The overall aim of this Ph.D. thesis was to provide a broader understanding and documentation of pathomechanisms underlying inflammatory myopathies in animals, to better define the characteristics of these pathologies in veterinary medicine and propose new spontaneous animal models of human diseases.

The specific objectives were:

1. Investigate the autoimmune pathomechanism underlying inflammatory myopathy associated with leishmania infection in dogs.

2. Describe the morphological and molecular findings of the inflammatory myopathy associated with natural Feline Immunodeficiency Virus infection in cats and provide insight on the underlying pathomechanisms.

3. Describe the morphological and molecular findings of the white strip myopathy in broiler chickens and investigate the underlying pathomechanisms.

References

1. Zachary JF. *Pathologic Basis of Veterinary Disease*. Sixth Edit. (Zachary JF, ed.).; 2017.
2. Miller FW, Lamb JA, Schmidt J, Nagaraju K. Risk factors and disease mechanisms in myositis. *Nat Rev Rheumatol*. 2018;14(5):255-268. doi:10.1038/nrrheum.2018.48
3. Lundberg IE, De Visser M, Werth VP. Classification of myositis. *Nat Rev Rheumatol*. 2018;14(5):269-278. doi:10.1038/nrrheum.2018.41
4. Shelton GD. From dog to man: The broad spectrum of inflammatory myopathies. *Neuromuscul Disord*. 2007;17(9-10):663-670. doi:10.1016/j.nmd.2007.06.466
5. Prisco F, Papparella S, Paciello O. The correlation between cardiac and skeletal muscle pathology in animal models of idiopathic inflammatory myopathies. *Acta Myol*. 2020;XXXIX:315-321. doi:10.36185/2532-1900-035
6. Ascherman DP. Animal models of inflammatory myopathy. *Curr Rheumatol Rep*. 2012;14(3):257-263. doi:10.1007/s11926-012-0245-7
7. Evans J, Levesque D, Shelton GD. Canine inflammatory myopathies: A clinicopathologic review of 200 cases. *J Vet Intern Med*. 2004;18(5):679-691. doi:10.1892/0891-6640(2004)18<679:CIMACR>2.0.CO;2
8. Podell M. Inflammatory myopathies. *Vet Clin North Am Small Anim Pract*. 2002;32(1):147-167. doi:10.1016/S0195-5616(03)00083-4
9. Moran EM, Mastaglia FL. Cytokines in immune-mediated inflammatory myopathies: Cellular sources, multiple actions and therapeutic implications. *Clin Exp Immunol*. 2014;178(3):405-415. doi:10.1111/cei.12445
10. Paciello O, Oliva G, Gradoni L, et al. Canine inflammatory myopathy associated with Leishmania Infantum infection. *Neuromuscul Disord*. 2009;19(2):124-130. doi:10.1016/j.nmd.2008.10.013
11. Podell M, Chen E, Shelton GD. Feline immunodeficiency virus associated myopathy in the adult cat. *Muscle Nerve*. 1998;21(12):1680-1685. doi:10.1002/(SICI)1097-4598(199812)21:12<1680::AID-MUS9>3.0.CO;2-F

12. Pasolini MP, Pagano TB, Costagliola A, et al. Inflammatory Myopathy in Horses With Chronic Piroplasmosis. *Vet Pathol*. 2018;55(1):133-143. doi:10.1177/0300985817716262
13. Pagano TB, Prisco F, De Biase D, et al. Muscular Sarcocystosis in Sheep Associated With Lymphoplasmacytic Myositis and Expression of Major Histocompatibility Complex Class I and II. *Vet Pathol*. December 2019:030098581989125. doi:10.1177/0300985819891257
14. Leclair V, Lundberg IE. New Myositis Classification Criteria—What We Have Learned Since Bohan and Peter. *Curr Rheumatol Rep*. 2018;20(4). doi:10.1007/s11926-018-0726-4
15. Lundberg IE, Tjärnlund A, Bottai M, et al. 2017 European League Against Rheumatism/American College of Rheumatology classification criteria for adult and juvenile idiopathic inflammatory myopathies and their major subgroups. *Ann Rheum Dis*. 2017;76(12):1955-1964. doi:10.1136/annrheumdis-2017-211468
16. King J, Lecouteur RA, Aleman M, et al. Vacuolar myopathy in a dog resembling human sporadic inclusion body myositis. *Acta Neuropathol*. 2009;118(5):711-717. doi:10.1007/s00401-009-0588-y
17. Hankel S, Shelton GD, Engvall E. Sarcolemma-specific autoantibodies in canine inflammatory myopathy. *Vet Immunol Immunopathol*. 2006;113(1-2):1-10. doi:10.1016/j.vetimm.2006.03.025
18. Costagliola A, Piegari G, Otrocka-Domagala I, et al. Immunopathological features of canine myocarditis associated with leishmania infantum infection. *Biomed Res Int*. 2016;2016. doi:10.1155/2016/8016186
19. Paciello O, Wojcik S, Gradoni L, et al. Syrian hamster infected with Leishmania infantum: a new experimental model for inflammatory myopathies. *Muscle Nerve*. 2010;41(3):355-361. doi:10.1002/mus.21502
20. Prisco F, De Biase D, Piegari G, et al. Pathomechanism highlights of leishmania-associated myopathy in the dog. *J Comp Pathol*. 2019;166:110. doi:10.1016/j.jcpa.2018.10.033
21. Silva-Almeida M, Carvalho LOP, Abreu-Silva AL, d'Escoffier LN, Calabrese KS. Leishsmania (Leishmania) amazonensis infection: Muscular involvement in BALB/c and C3H.HeN mice. *Exp Parasitol*. 2010;124(3):315-318.

doi:10.1016/j.exppara.2009.11.006
22. Melby PC, Chandrasekar B, Zhao W, Coe JE. The Hamster as a Model of Human Visceral Leishmaniasis: Progressive Disease and Impaired Generation of Nitric Oxide in the Face of a Prominent Th1-Like Cytokine Response. *J Immunol*. 2001;166(3):1912-1920. doi:10.4049/jimmunol.166.3.1912
23. Prisco F, De Biase D, Ilsami A, et al. Feline Immunodeficiency Virus-Associated Myopathy in Cats: An Autoimmune Disorder? *J Comp Pathol*. 2020;174:148. doi:10.1016/j.jcpa.2019.10.026
24. Afzali AM, Ruck T, Wiendl H, Meuth SG. Animal models in idiopathic inflammatory myopathies: How to overcome a translational roadblock? *Autoimmun Rev*. 2017;16(5):478-494. doi:10.1016/j.autrev.2017.03.001
25. Germolec D, Kono DH, Pfau JC, Pollard KM. Animal models used to examine the role of the environment in the development of autoimmune disease: Findings from an NIEHS Expert Panel Workshop. *J Autoimmun*. 2012;39(4):285-293. doi:10.1016/j.jaut.2012.05.020
26. Prisco F, Biase D De, Ilsami A, et al. Histological and immunohistochemical characterization of white striping myopathy in broiler chickens. In: Olbia (Italy): 73° Convegno SISVET-AIPVET; 2019.
27. Bruder J, Siewert K, Obermeier B, et al. Target specificity of an autoreactive pathogenic human γδ-T cell receptor in myositis. *J Biol Chem*. 2012;287(25):20986-20995. doi:10.1074/jbc.M112.356709
28. McHugh NJ, Tansley SL. Autoantibodies in myositis. *Nat Rev Rheumatol*. 2018;14(5):290-302. doi:10.1038/nrrheum.2018.56
29. Dubowitz V, Sewry CA, Oldfors A, Lane RJM. *Muscle Biopsy: A Practical Approach*. 4th Editio. Saunders; 2013.
30. Shelton GD, Cardinet GH, Bandman E. Canine masticatory muscle disorders: A study of 29 cases. *Muscle Nerve*. 1987;10(8):753-766. doi:10.1002/mus.880100812
31. Wu X, Li Z, Brooks R, et al. Autoantibodies in Canine Masticatory Muscle Myositis Recognize a Novel Myosin Binding Protein-C Family Member. *J Immunol*. 2007;179(7):4939-4944. doi:10.4049/jimmunol.179.7.4939
32. Opinc A, Makowski M, Makowska J. Patients with Idiopathic Inflammatory Myopathies and Primary involvement of Heart Muscle and Cardiovascular Complications. *Biomed J Sci Tech Res*.

2018;5(2):4467-4470. doi:10.26717/BJSTR.2018.05.001184
33. Jayakumar D, Zhang R, Wasserman A, Ash J. Cardiac Manifestations in Idiopathic Inflammatory Myopathies: An Overview. *Cardiol Rev*. 2019;27(3):131-137. doi:10.1097/CRD.0000000000000241
34. Myhr KA, Pecini R. Management of Myocarditis in Myositis: Diagnosis and Treatment. *Curr Rheumatol Rep*. 2020;22(9):1-7. doi:10.1007/s11926-020-00925-4
35. Diederichsen LP. Cardiovascular involvement in myositis. *Curr Opin Rheumatol*. 2017;29(6):598-603. doi:10.1097/BOR.0000000000000442
36. Yang Z, Lin F, Qin B, Yan L, Renqian Z. Polymyositis/dermatomyositis and malignancy risk: A metaanalysis study. *J Rheumatol*. 2015;42(2):282-291. doi:10.3899/jrheum.140566
37. Gianella P, Avallone G, Bellino C, et al. Primary cutaneous undifferentiated round cell tumor with concurrent polymyositis in a dog. *Can Vet J*. 2012;53(5):549-553.
38. Chen X, Ghribi O, Geiger JD. Rabbits fed cholesterol-enriched diets exhibit pathological features of inclusion body myositis. *Am J Physiol Integr Comp Physiol*. 2008;294(3):R829-R835. doi:10.1152/ajpregu.00639.2007
39. Lairmore MD, Khanna C. Naturally Occurring Diseases in Animals: Contributions to Translational Medicine. *ILAR J*. 2014;55(1):1-3. doi:10.1093/ilar/ilu022
40. Michell B, Clinical C, Foundation S, Binns M, Trust AH. Spontaneous animal models of human disease. *Vet Rec*. 2005;156(18):559-560. doi:10.1136/vr.156.18.559
41. Amélia A, Gomes D, Laurenti MD, et al. Subclinical muscle injuries in dogs infected with Leishmania (Leishmania) infantum chagasi. *Brazilian J Vet Pathol*. 2012;5(3):108-115.
42. Lobetti RG. Cardiac involvement in canine babesiosis : review article. *J S Afr Vet Assoc*. 2005;76(1):4-8. doi:10.4102/jsava.v76i1.386
43. Diana A, Guglielmini C, Candini D, Pietra M, Cipone M. Cardiac arrhythmias associated with piroplasmosis in the horse: A case report. *Vet J*. 2007;174(1):193-195. doi:10.1016/j.tvjl.2006.04.003
44. Rolim VM, Casagrande RA, Wouters ATB, Driemeier D, Pavarini SP. Myocarditis caused by Feline Immunodeficiency Virus in Five

Cats with Hypertrophic Cardiomyopathy. *J Comp Pathol*. 2016;154(1):3-8. doi:10.1016/j.jcpa.2015.10.180

45. Hiniker A, Daniels BH, Margeta M. T-cell-mediated inflammatory myopathies in HIV-positive individuals: A histologic study of 19 cases. *J Neuropathol Exp Neurol*. 2016;75(3):239-245. doi:10.1093/jnen/nlv023
46. Sani MU. Myocardial disease in human immunodeficiency virus (HIV) infection: A review. *Wien Klin Wochenschr*. 2008;120(3-4):77-87. doi:10.1007/s00508-008-0935-3

Chapter 1

Canine Inflammatory Myopathy due to Leishmania infantum infection is associated with circulating autoantibodies recognizing SERCA1 as major antigen

Based on:

Pathomechanism highlights of leishmania-associated myopathy in the dog. Prisco Francesco, De Biase Davide, Piegari Giuseppe, Oriente Francesco, Cimmino Ilaria, Pavone Luigi Michele, Ruoppolo Margherita, Costanzo Michele, Santoro Pasquale, Paciello Orlando. J Comp Pathol. 2019;166:110. doi:10.1016/j.jcpa.2018.10.033

Canine Inflammatory Myopathy due to Leishmania infantum infection is associated to circulating autoantibodies recognizing SERCA1 as major antigen. Francesco Prisco, Davide De Biase, Giuseppe Piegari, Francesco Oriente, Ilaria Cimmino, Luigi Michele Pavone, Margherita Ruoppolo, Michele Costanzo, Pasquale Santoro, Serenella Papparella, Orlando Paciello. Submitted article.

1.1 Introduction

IMs have been related to different spontaneous infections both in humans[2], dogs[13], cats[14], horses[15], and a relation has also been proposed in sheep.[10] Notably, *Leishmania infantum* infection has been related to a form of IM in dogs, experimentally reproduced in Syrian hamsters and mice.[13,16–18]

Around 70 animal species, including humans, have been found as natural reservoir hosts of Leishmania parasites[19], however, infected dogs constitute the main domestic reservoir of the parasite and play a key role in transmission to humans.[20]

Leishmania infantum (syn. *L. chagasi*) has been identified as the main etiologic agent of canine leishmaniasis. However, other Leishmania species (e.g., *L. donovani*, L. *braziliensis*, *L. tropica*, *L. major*, etc.) are able to infect and induce pathology both in dogs and in other animals. [20–23]

The pathogenesis of Leishmania infection in dogs is extremely complex and is the result of the interaction among vector (e.g. repeated infectious bites), parasite (virulence), and host (e.g. genetic background, immune response, coexisting diseases).[22] The wide variability of these factors results in a wide range of clinicopathological presentations ranging in severity from self-healing cutaneous leishmaniasis (CL) to fatal disseminated visceral leishmaniasis (VL) leading to organ damage and dysfunction.[21,22]

Other than IM, the clinicopathological picture of *Leishmania infantum* infected dogs may include various combinations among exfoliative

and/or ulcerative dermatitis, with or without nasodigital hyperkeratosis and onychogryphosis, glomerulonephritis, myocarditis, anterior uveitis, keratoconjunctivitis sicca, epistaxis, and/or polyarthritis.[13,16,22] Although the pathogenetic mechanisms underlying these features are not yet clear, one of the best-characterized mechanisms is the presence of circulating immune complexes[24] and the production of autoantibodies directed against different structures, including antinuclear[25], antiplatelet[26] and smooth-muscle autoantibodies.[27]

The leishmania related IM can be classified as a canine PM.[5,6] Myopathic features related to leishmania infection are necrosis, regeneration, fibrosis and infiltration of lymphocytes (mainly CD8+) and macrophages. As observed in other PMs[10,15,18,28], also the leishmania-related IM is further characterized by a wide sarcolemmal MHC class I and II overexpression.[13] Moreover, an interesting myopathic observation is the presence of morphologically normal MHC I-positive myofibers invaded by CD8-positive lymphocytes (CD8/MHC I complex) that strongly suggest an immune-mediated pathogenesis.[13,28]

Leishmania infection in dogs is also related to myocarditis that shares many histological characteristics with the leishmania-related myopathy.[16] The myocardium is often infiltrated by inflammatory cells that share morphological and immunophenotypical characteristics with those described for leishmania-related myopathy. Furthermore, MHC I and II overexpression on cardiomyocyte membrane is also reported.[16]

Due to the numerous shared pathological features between leishmania-related myopathy and cardiomyopathy and due to many

similarities between these two tissues, a common immune-mediated pathogenetic mechanism has been postulated.[6,16]

Based on our observation and the literature[2,5,13,16–18], we hypostasize that one of the main components of the pathogenesis of the canine leishmania-related myositis is the dysregulation of the adaptive immune system with the production of autoantibodies directed against muscle structures.

In the present study, we have recognized circulating autoantibodies against skeletal muscle in Leishmania-infected dogs and identified the main target antigen, which is a member of the sarcoplasmic reticulum calcium ATPase located on the sarcoplasmic reticulum and named sarcoplasmic/endoplasmic reticulum Ca^{2+}-ATPase 1 (SERCA1).

1.2 Materials and methods

1.2.1 Sera

35 leishmania-positive dog sera and 10 negative controls were selected from the sera bank of the Comparative Neuromuscular Laboratory of the Department of Veterinary Medicine of the University Federico II in Napoli. All sera were tested for anti-leishmanial antibody titer using immunofluorescent antibody test (IFAT) for *Leishmania spp*. Sera data were summarized in table 1.1. Upon arrival, sera were stored at -80 °C until further processed.

To reduce background signal in immunofluorescence and unspecific signals in immunoblot, groups of serum from 5 dogs were randomly pooled in 7 pools of leishmania-positive dogs and 2 groups of negative controls. IgG were purified from the pooled serum using the Protein A IgG Purification Kit (Thermo Fisher Scientific, Waltham, Massachusetts, USA) according to manufacturer instructions.

Table 1.1 Sera samples with corresponding anti-leishmanial antibody titer tested by Immunofluorescent antibody test (IFAT).

Serum #	IFAT
1,2	1/80
3-8	1/160
9-12	1/320
13-15	1/640
16-35	1/1280
36-45	Absent

1.2.2 Tissues

Normal quadriceps femoris fresh-frozen samples of dogs, mice and sheep were selected from the tissue archives of the Comparative Neuromuscular Laboratory of the Department of Veterinary Medicine of the University Federico II in Napoli. All selected muscles (Table 1.2) were

collected from animals serologically and parasitologically negative for *L. infantum*.

Table 1.2 Muscle samples.

Muscle #	Species	Breed/Strain	Sex	Age
1	Dog	Siberian husky	M	5 years
2	Dog	Mix	MC	12 years
3	Dog	Jack Russell terrier	M	9 years
4	Dog	Whippet	F	6 years
5	Dog	Mix	M	3,5 months
6	Mouse	C57	F	1 year
7	Mouse	C57	F	1 year
8	Mouse	C57	F	1 year
9	Sheep	Mix	F	4 years
10	Sheep	Mix	F	5 years
11	Sheep	Mix	F	7 years

1.2.3 Indirect immunofluorescent staining

Eight micrometers transversal cryosections were cut from selected muscle specimens and dried at room temperature for 45 minutes. Sections were fixed in acetone for 10 minutes at 4 °C. After 3 wash of 5 minutes in PBS, sections were incubated with 10% normal rabbit sera in PBS for 30

minutes at room temperature. To block endogenous dog IgG, after 3 wash of 5 minutes in PBS, sections of dog muscles were preincubated with F(ab')2 fragments of rabbit anti-dog IgG (H+L) (1:50; Rockland Immunochemicals, Limerick, PA, USA) for 1 hour. The latter step was avoided for the muscles of the other species. Sera pools from dogs were serially diluted in PBS (1:100, 1:300, 1:1000, 1:3000, 1:10000) and after 3 wash of 5 minutes in PBS, were added to each section for incubation overnight at 4 °C. Control sections were incubated with PBS. After washing three times with PBS for 5 minutes, FITC-conjugated rabbit anti-dog IgG (H+L) (1:300; Jackson Laboratories, West Grove, PA, USA) was added to each section, and incubated for 40 minutes at room temperature. Sections were washed three times with PBS for 5 minutes and mounted under coverslips in VECTASHIELD® H-1200 (Vector, Burlingame, CA, USA) to prevent fading of fluorescence.

A quantitative assessment of immunofluorescence-stained sections was performed for each dilution for each sera pool. Ten 40× fields were randomly photographed under an optical microscope (Leica DM6000B by Leica, Wetzlar, Germany) associated with a digital camera (Leica DFC450C digital camera by Leica). The intensity of the fluorescence signal was measured for each photo with Fiji (ImageJ, National Institutes of Health). The mean stain intensity of the 10 analyzed fields was calculated for each dilution for each sera pool.

1.2.4 Indirect immunofluorescent with colocalization

To evaluate the colocalization of detected autoantigens and SERCA1, cryosections were processed as described in the indirect immunofluorescent staining section up to the primary antibody. As first primary antibody was used the purified sera pool 1 from leishmania infected dogs diluted 1:1000 overnight at 4 °C. After washing three times with PBS for 5 minutes, FITC-conjugated rabbit anti-dog IgG (H+L) (1:300; Jackson Laboratories, West Grove, PA, USA) was added to each section, and incubated for 40 minutes at room temperature. After, slides were rinsed with PBS and a second primary mouse monoclonal antibody directed against SERCA1 ATPase (1:200; clone VE121G9, Thermo Fisher Scientific, Waltham, MA, USA) was applied for 2 hours at room temperature. A FITC fluorochrome-labeled rabbit anti-mouse secondary antibody was applied (1:300; Jackson Laboratories) on sections for 1 hour at room temperature. Slides were rinsed with PBS and mounted with VECTASHIELD® H-1200 (Vector).

1.2.5 Western blot analysis and Immunoprecipitation procedures

Tissue samples were homogenized in a Polytron (Brinkman Instruments, N.Y.). The homogenate was stirred for 2 hours at 4°C and then centrifuged at 14.000 rpm x 20 min. The supernatant was collected, and proteins were determined by the Bradford procedure.[29] Proteins from total homogenates were separated by SDS-PAGE. Briefly, cells were solubilized with lysis buffer containing 50mM HEPES, 150mM NaCl, 10mM EDTA,

10mM Na4P2O7, 2mM sodium orthovanadate, 50mM NaF, 1mM phenylmethylsulfonyl fluoride, 10µg/ml aprotinin, 10µg/ml leupeptin, pH 7.4, and 1% (v/v) Triton X-100. Lysates were clarified by centrifugation at 12,000g for 20 minutes at 4°C. The protein concentrations in the cell lysates were measured using a Bio-Rad DC (detergent compatible) assay. Aliquots of the lysates were precipitated with SERCA1 ATPase Abs coupled to protein G Sepharose for 2 hours at 4 °C. Immunoprecipitation and Western blot analysis have been performed as previously described.[29,30]

1.2.6 LC-MS/MS analysis for antigen identification

Protein extracts obtained from dog, mouse, and sheep muscle tissues were fractionated by SDS-PAGE. The gel was stained using the Gel Code Blue Stain Reagent (Thermo Fisher Scientific, Waltham, MA, USA) and a band approximately near to the 100 kDa molecular weight marker was excised from the gel lanes and subjected to in-gel digestion, as elsewhere reported.[42] Trypsin (Promega, Madison, WI, USA) was used as proteolytic enzyme. Then, peptide mixtures were analyzed by liquid chromatography–tandem mass spectrometry (LC-MS/MS) on an LTQ-Orbitrap XL (Thermo Scientific, Bremen, Germany) equipped with a nanoLC system, set as reported. Protein identification was carried out using Mascot (www.matrixscience.com) through the MS/MS Ions Search tool. *Canis lupus familiaris*, *Mus musculus*, and *Ovis aries* databases were selected as taxonomy.

1.2.7 Statistical Analysis

Fisher's Exact test was used to compare the difference of frequency of positivity to IF assay between leishmania-positive and negative pools. Spearman's rank correlation coefficient was used to evaluate the correlation between sera dilution and positivity to the IF assay.

1.3 Results

1.3.1 Leishmania-infected dogs have circulating antibodies against skeletal muscle

To investigate the presence of circulating autoantibodies anti-skeletal muscle in dogs with leishmaniasis we analyzed sera by using indirect immunofluorescence on sections of normal dog muscle. To reduce the background signal, the sera were pooled and purified. To prevent FITC-conjugated antibodies bound to endogenous dog IgG, present in blood vessels and the interstitial spaces, we pretreated normal dog muscle sections with F(ab')2 fragments of rabbit anti-dog IgG before incubation of the sections with serial dilutions of test serum.

Pooled sera from leishmania-infected dogs showed antibodies against skeletal muscle in titers up to over 1:10000 (Fig. 1). The IF showed mainly a sarcoplasmic positivity. At higher concentrations the sarcoplasm of all fiber was positive; differently, usually starting from the 1:1000 sera

dilution, a differential stain among fibers was evident with a checkerboard pattern. None of the control sera pools had detectable antibodies in this test.

Fisher's Exact test confirmed a statistically significant difference between leishmania positive and negative pools (p= 0,027778).

The IF positivity of pooled sera from leishmania-infected dogs was positively correlated with the dilution (r_s=0.662896; p=0.000014). In contrast, this correlation was not evident in the control sera (r_s=0.169621; p=0.598178; Fig. 2).

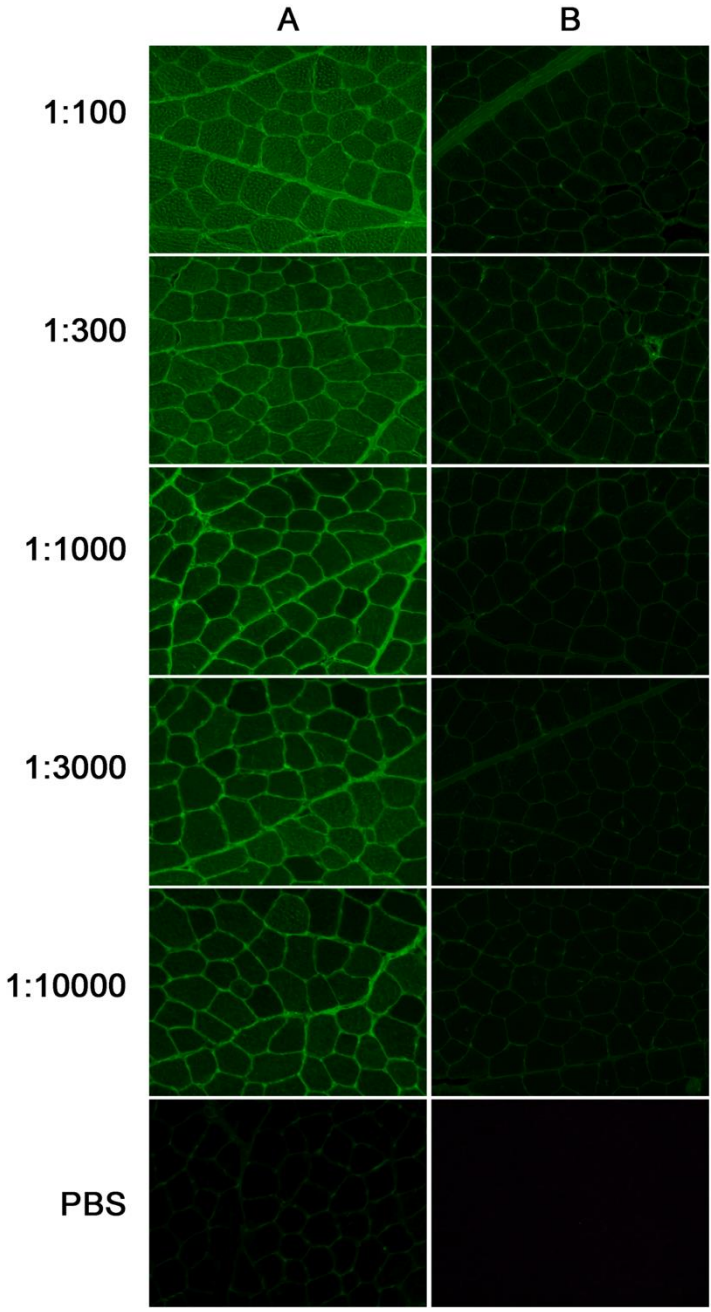

Figure 1.1 Indirect immunofluorescence using dog muscle and different dilutions of serum from a leishmania-infected dog (A) and normal dog (B). Sera

pool from leishmania-infected dogs showed antibodies against skeletal muscle in titers up to over 1:10000. At 1:100 and 1:300 dilution there are no evident differences in the staining of the sarcoplasm of the different muscle fibers; differently, starting from the 1:1000 sera dilution, a differential stain among fibers was evident with a checkerboard pattern.

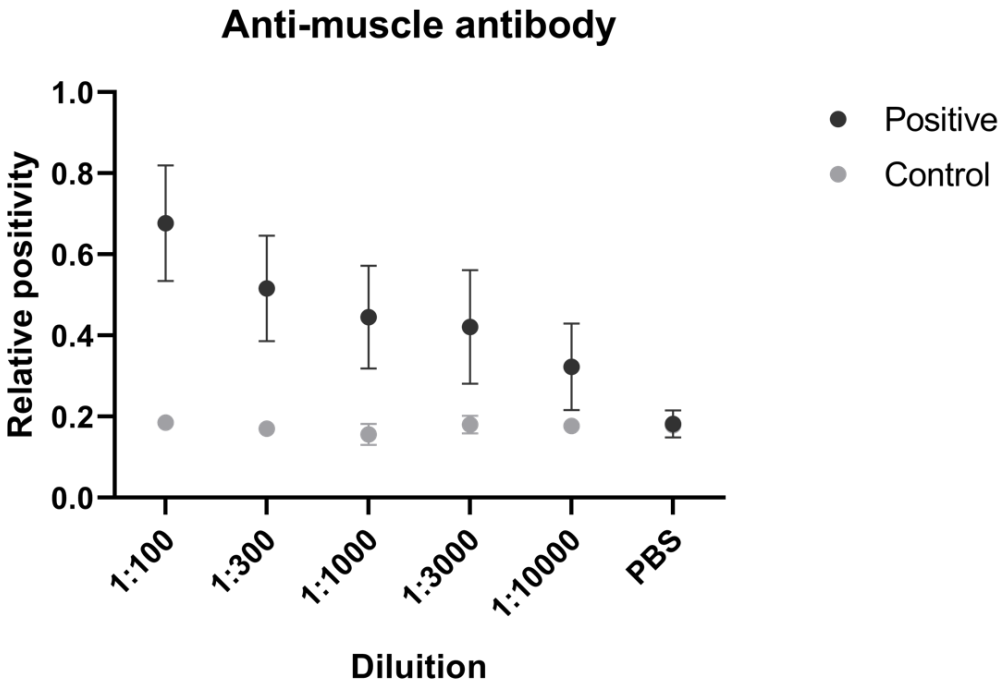

Figure 1.2 Quantitative assessment of immunofluorescence positivity. The IF positivity of pooled sera from leishmania-infected dogs is dilution-dependent (r_s=0.663; p=0.000014). In contrast, this association is not evident in the control sera (r_s=0.170; p=0.598).

1.3.2 Specificity of autoantibodies

We also performed indirect immunofluorescence on sections of normal sheep and mouse muscle to determine if the autoantibodies found in dogs with leishmaniasis are specific for canine muscle. Positivity has been demonstrated both in sheep and in mouse muscle with all pooled sera from leishmania-infected dogs. The IF positivity showed the same sarcoplasmic checkerboard pattern. The intensity of the staining was slightly lower on sheep muscle and significantly lower on mouse muscle. No staining has been found using pooled sera from normal control dogs on muscle from both species (Fig. 3).

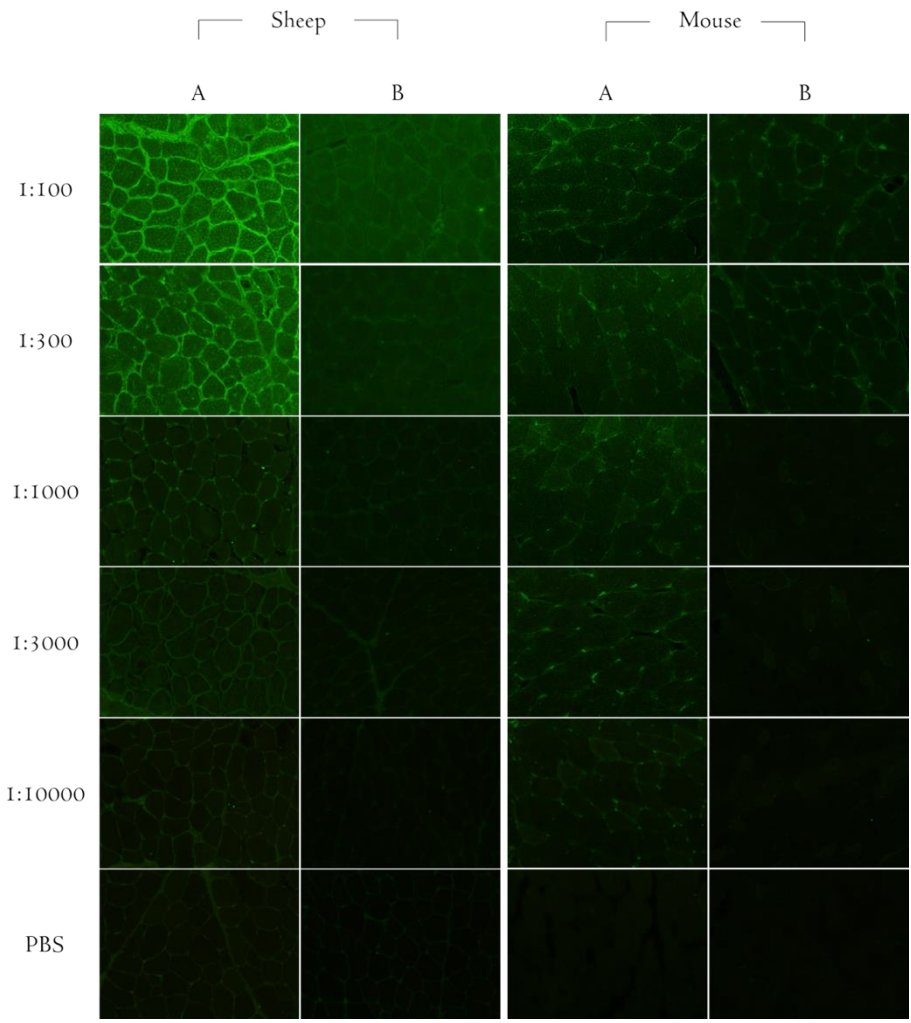

Figure 1.3 Indirect immunofluorescence using sheep and mouse muscle and different dilutions of serum from a leishmania-positive dog (A) and a control dog (B).

1.2.3 Antibodies in leishmania-infected dogs recognize a 100 kDa muscle protein

We performed immunoblot analysis using the sera from leishmania-infected dogs and normal muscle proteins extract to check the molecular weight of the unknown antigen(s). A band of about 100 kDa was identified in sera from leishmania-infected dogs. This 100 kDa protein was not detected in muscle extracts using the sera of normal dogs (Fig. 4). Additionally, proteins with a molecular mass less than and greater than 100 kDa were identified in immunoblotting, these proteins were not consistently identified by all sera.

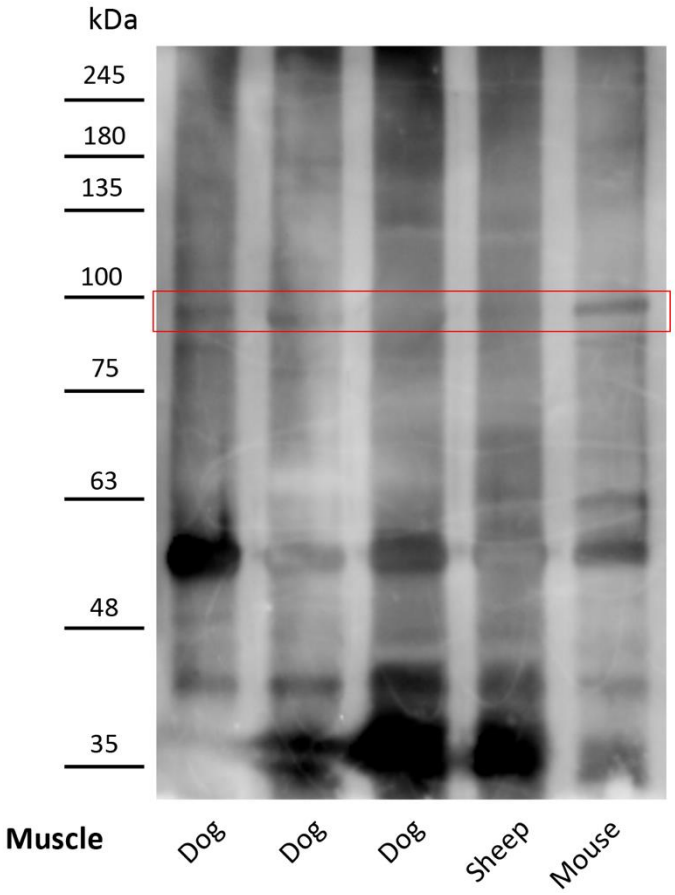

Figure 1.4 Autoantibodies in sera from leishmania-infected dogs (A) bind to a protein to about 100 kDa. This band was not detected in control dog sera (B). The muscle samples were named with D: Dog, S: Sheep and M: Mouse.

1.3.4 Isolation and characterization of the canine muscle protein recognized by the leishmania-infected dog sera

To individuate the target protein of the autoantibody, the protein extracts from normal canine muscles were fractionated by SDS-PAGE and the resulting gel bands with a molecular weight of about 100 kDa were excised, trypsinized and analyzed by LC-MS/MS. Mass spectrometry analysis led to the identification of a protein of about 100 kDa in the canine muscle protein extracts, the sarcoplasmic/endoplasmic reticulum calcium ATPase 1 (SERCA1, UniProt ID: E2RRB2). Thus, the canine SERCA1 was subjected to basic local alignment search tool (BLAST) analysis, showing that this protein is highly conserved across species, including humans and other primates, cat, ferrets, mouse, horse, pig, bovine, sheep, etc. Particularly, the alignment of SERCA1 the amino acid sequences of the dog, mouse and sheep resulted in a 96.17% and 95.77% of identity respectively.

A BLAST search revealed also that canine SERCA1 has significant overall homology (49.02%) to calcium-translocating P-type ATPase of Leishmania infantum (XP_001462838.2) and that these proteins share many identical tracts (Fig. 5).

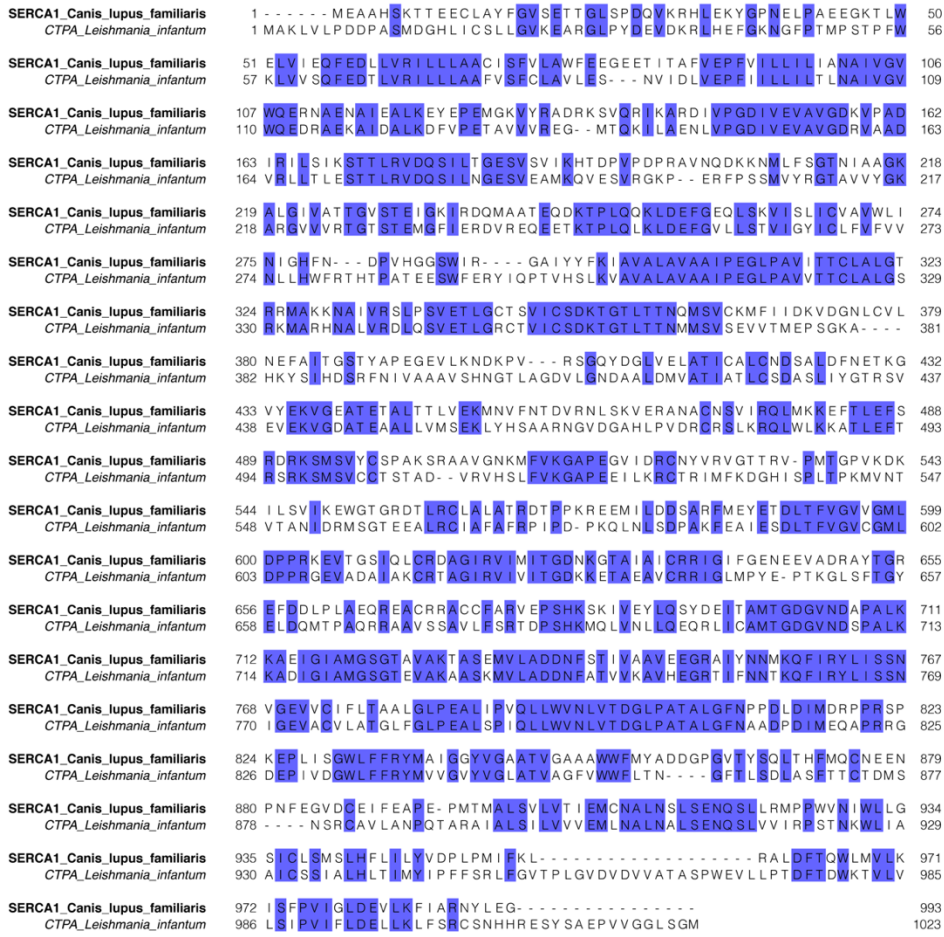

Figure 1.5 Protein sequence alignment. Canine sarcoplasmic/endoplasmic reticulum calcium ATPase 1 (SERCA1, UniProt ID: E2RRB2) is 49.02% identical to calcium-translocating P-type ATPase (CTPA, UniProt ID: A4HRZ6) of *Leishmania infantum*. Identical amino acids are highlighted with blue.

1.3.5 Muscle protein recognized by antibodies of leishmania-infected dogs colocalize with anti-SERCA1 Abs

To evaluate the colocalization of the muscle protein recognized by Abs of leishmania-infected dogs and SERCA1, we performed a double indirect immunofluorescence, analyzing sections of fresh frozen normal canine muscle. Muscle sections were incubated with sera of dogs infected with leishmania and with anti-SERCA1 Abs. Anti-SERCA1 Abs marked type II muscle fibers with a checkerboard pattern, and the staining partially colocalized with muscle protein recognized by Abs of leishmania-infected dogs (Fig. 6).

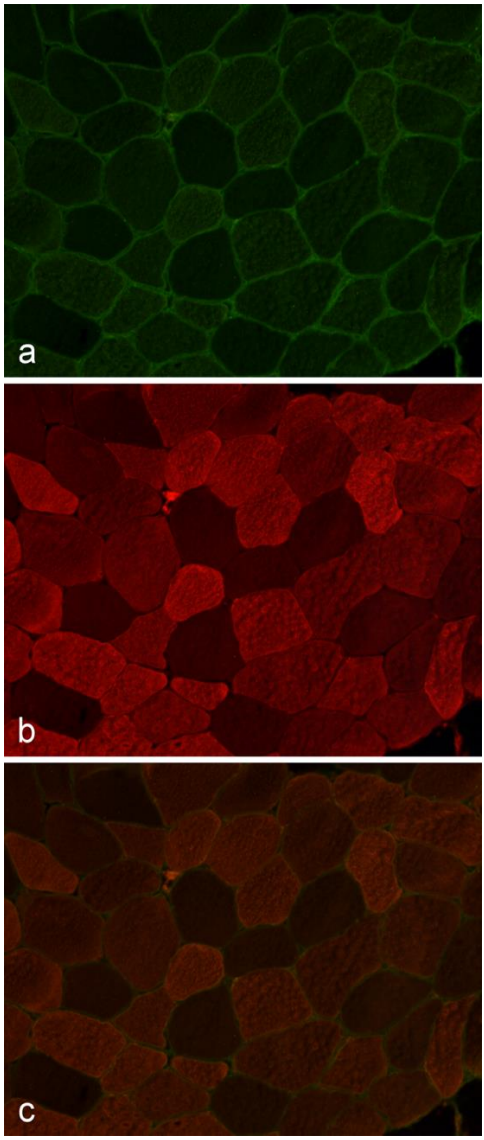

Figure 1.6 Double-color immunofluorescence with purified sera pool of leishmania-infected dogs (a: green, FITC) and commercial mouse anti-SERCA1 Ab (b: red, TRIC) and their colocalization (c: merge, orange color) on normal dog skeletal muscle section. A marked immunocolocalization between SERCA1 and the major antigen is evident.

1.3.6 Antibodies of leishmania-infected dogs recognize immunoprecipitated SERCA1

SERCA1 has been isolated through immunoprecipitation from normal muscle proteins extract using monoclonal antibody specific for SERCA1. The immunoprecipitated was tested in immunoblotting with leishmania-infected dog sera. A protein band consistent with canine SERCA1 was identified in sera from leishmania-infected dogs (Fig. 7). SERCA1 was not detected in muscle extracts using the sera of control dogs.

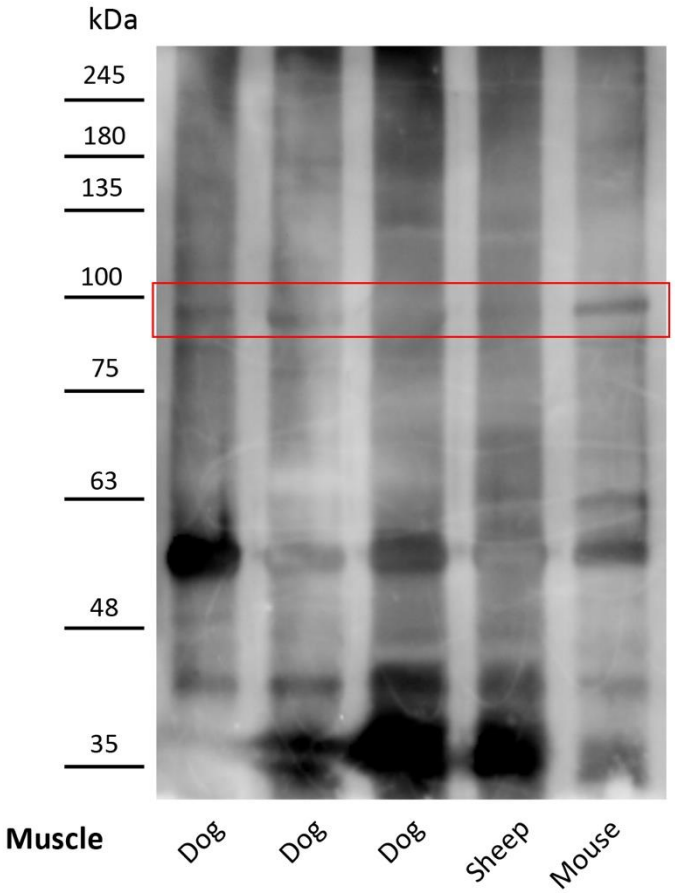

Figure 1.7 Immunoblot using total muscle protein samples immunoprecipitated with anti-SERCA1 antibody and sera of leishmania-infected dog. Muscle tissues were homogenized and solubilized. Total protein samples were immunoprecipitated with anti-SERCA1 antibody and immunoblotted with a serum of leishmania-infected dog. Autoantibodies in sera from leishmania-infected dogs bind to a protein of about 100 kDa consistent with canine SERCA1. The autoradiograph shown is representative of three different experiments. The muscle samples were named with D: Dog, S: Sheep and M: Mouse.

1.4 Discussion

In this study, we identified circulating IgG autoantibodies specific for the skeletal muscle in leishmania-infected dogs. We found mainly a sarcoplasmic positivity with indirect immunofluorescence and showed that antibodies present in the sera of leishmania-infected dogs bind different muscle proteins. We also identified the main target protein as SERCA1.

Circulating immune complexes and several autoantibodies have already been described in sera of *Leishmania spp.*-infected dogs.[31] In a study of 44 infected adult dogs, antinuclear antibodies have been reported in up to 30% of dogs with an indirect immunofluorescence method.[32] It has also been established that these antibodies are often directed against DNA-associated proteins, such as histones, and that are part of the pathogenetic mechanism of leishmania-associated glomerulonephritis.[25] In a large study of 260 dogs, anti-actin and anti-tubulin IgG has been reported respectively in 95% and 94% of dogs infected with *Leishmania donovani* using ELISA.[31] Furthermore, anti-mammalian basal membrane glycoproteins and cerebrosides antibodies have been also described.[31]

Circulating autoantibodies anti-skeletal muscle have also been found in other infectious-related IMs, such as piroplasmosis in the horses[15] and *Feline Immunodeficiency Virus* infection in cats.[33]

In the present study, we consistently found autoantibodies directed against SERCA1 in leishmania-infected dogs. The sarcoplasmic-endoplasmic reticulum calcium ATPase (SERCA) is responsible for transporting calcium (Ca^{2+}) from the cytosol into the lumen of the sarcoplasmic reticulum (SR) following the muscular contraction in both cardiac and skeletal muscle.[34] Structurally, the SERCA proteins are transmembrane proteins with a molecular mass of 110 kDa. There are three major isoforms of SERCA and several sub-isoforms: SERCA1 isoforms are expressed in the fast-twitch (type II) skeletal muscle fibers, explaining the observed checkerboard pattern at IF. SERCA2a is expressed specifically in cardiomyocytes, slow-twitch skeletal muscle fibers (type I) and vascular smooth muscle cells. Although SERCA2b is expressed ubiquitously and SERCA2c has been recently reported to be expressed in the left ventricles in humans. SERCA3 proteins can be expressed in various tissues including hematopoietic cell lineages.[34,35]

Since we found a positivity on sheep and mouse muscles, we assume that autoantibodies are directed to phylogenetically preserved muscle antigens. This data is also supported by the reported high homology between sheep and mouse SERCA1 evaluated by in silico analysis. The lower antibody titers against muscle from other species may indicate the existence of multiple antigens, some of which are species-specific, or suggest that the affinity of the antibodies for the antigen(s) in other species are lower.[7] The above hypotheses are not mutually exclusive, and they do not exclude the formulation of other hypotheses.

SERCA1 was the main antigen of the circulating autoantibodies in the sera tested. However, proteins with a molecular mass less than and greater than 100 kDa were identified in immunoblotting in individual dog sera. The significance of autoantibodies to these other Ags is not known, because they are not present in all cases. Future investigations are needed to understand the pathogenetic significance of these autoantibodies.

A plurality of autoantibody is reported in different IMs, including canine masticatory muscle myositis.[36,37] Therefore, different autoantigens are expected also in Leishmania-associated IM. Autoantibodies in IM are generally classified in myositis-specific autoantibodies (MSAs) or myositis-associated autoantibodies (MAAs), depending on their prevalence in other, related conditions. The identification of MSAs in Leishmania-associated myositis and myocarditis is important because they could be used as biomarker helping the diagnosis, prognosis and monitoring of these diseases. Muscle biopsy will remain the gold standard for diagnosing myositis; however, the evaluation of this biomarker(s) would be a useful tool for the clinician also helping the decision to perform a muscle biopsy.

The role of autoantibodies in causing muscle damage and dysfunction is debated because most of the autoantigens are intracellular and thus not easily accessible to circulating autoantibodies.[37,38] SERCA proteins, being expressed on the sarcoplasmic reticulum, are indirectly in contact with the extracellular milieu through the T-tubular system.

Among the various autoantibodies described during IM and myocarditis, autoantibodies to SERCA2a has been detected in humans with

myocarditis or dilated cardiomyopathy.[35,39] A model of experimental myocarditis has been generated immunizing mice with SERCA2a.[35,39] This model allowed us to define, through immunoperoxidase staining and transmission electron microscopy, that anti-SERCA2a antibodies gain access through the transverse tubules of the myocardium that are connected to the interstitial extracellular environment.[40] Considering the shared ultrastructural features between skeletal and cardiac muscle, we hypothesize that the same mechanism can explain how circulating autoantibodies can bind SERCA1.

SERCA1 is expressed in skeletal muscle but not in cardiac muscle.[34] Thus, the presence of autoantibodies directed to SERCA1 may justify myositis, but the link with leishmania-associated myocarditis is less direct. We can hypothesize that these autoantibodies partially cross-react with the other SERCA isoforms, expressed in the myocardium, or that there are other autoantibodies directed towards proteins shared by skeletal and cardiac muscle.

Different hypotheses have been formulated to justify the production of autoantibodies during infections.[13,16] One of the most solid is the antigen mimicry. It is hypothesized that the proteins of the infectious agent have epitopes in common with host proteins, therefore, the autoantibodies produced against these epitopes cross-react with the host proteins causing an autoimmune pathology.[13,16] This mechanism has been well established in human toxoplasmosis.[41] In humans, during *Trypanosoma cruzi* infection, circulating autoantibodies against β_1-adrenergic receptor were detected. These autoantibodies determinate an immune-mediated myocarditis.[41] The

production of such antibodies was explained by molecular mimicry between the immunodominant ribosomal protein PO of *Trypanosoma cruzi* and a functional epitope on the human β_1-adrenergic receptor.[41]

We hypostasize that antigen mimicry may justify the production of autoantibodies against SERCA1. This hypothesis is based on the high homology between the protein calcium-translocating P-type ATPase of *Leishmania infantum* and canine SERCA1 and on the identification of perfectly overlapping traits of amino acid sequence between these two proteins. Our results are not sufficient to prove this mechanism, however, they strongly support it. Further studies are needed to clarify the pathogenetic mechanisms underlying the production of anti-SERCA1 antibodies in leishmania infected dogs.

1.5 Conclusions

Our studies provide evidence that: 1) the leishmania-infected dogs have circulating IgG autoantibodies directed against skeletal muscle; 2) these autoantibodies are not species-specific; 3) the major recognized antigen is SERCA1; 4) antigen mimicry may justify the production of autoantibodies.

Other studies may further highlight pathomechanism underlying the IM in leishmania-infected dogs and may help to identify new biomarkers useful for the diagnosis, prognosis and monitoring of the disease.

Chapter 1 References

1. Zachary JF. *Pathologic Basis of Veterinary Disease*. Sixth Edit. (Zachary JF, ed.).; 2017.
2. Miller FW, Lamb JA, Schmidt J, Nagaraju K. Risk factors and disease mechanisms in myositis. *Nat Rev Rheumatol*. 2018;14(5):255-268. doi:10.1038/nrrheum.2018.48
3. Lundberg IE, De Visser M, Werth VP. Classification of myositis. *Nat Rev Rheumatol*. 2018;14(5):269-278. doi:10.1038/nrrheum.2018.41
4. Podell M. Inflammatory myopathies. *Vet Clin North Am Small Anim Pract*. 2002;32(1):147-167. doi:10.1016/S0195-5616(03)00083-4
5. Prisco F, De Biase D, Piegari G, et al. Pathomechanism highlights of leishmania-associated myopathy in the dog. *J Comp Pathol*. 2019;166:110. doi:10.1016/j.jcpa.2018.10.033
6. Prisco F, Papparella S, Paciello O. The correlation between cardiac and skeletal muscle pathology in animal models of idiopathic inflammatory myopathies. *Acta Myol*. 2020;XXXIX:315-321. doi:10.36185/2532-1900-035
7. Shelton GD. From dog to man: The broad spectrum of inflammatory myopathies. *Neuromuscul Disord*. 2007;17(9-10):663-670. doi:10.1016/j.nmd.2007.06.466
8. King J, Lecouteur RA, Aleman M, et al. Vacuolar myopathy in a dog resembling human sporadic inclusion body myositis. *Acta Neuropathol*. 2009;118(5):711-717. doi:10.1007/s00401-009-0588-y
9. Moran EM, Mastaglia FL. Cytokines in immune-mediated inflammatory myopathies: Cellular sources, multiple actions and therapeutic implications. *Clin Exp Immunol*. 2014;178(3):405-415. doi:10.1111/cei.12445
10. Pagano TB, Prisco F, De Biase D, et al. Muscular Sarcocystosis in Sheep Associated With Lymphoplasmacytic Myositis and Expression of Major Histocompatibility Complex Class I and II. *Vet Pathol*. December 2019:030098581989125. doi:10.1177/0300985819891257
11. Evans J, Levesque D, Shelton GD. Canine inflammatory myopathies: A clinicopathologic review of 200 cases. *J Vet Intern Med*. 2004;18(5):679-691. doi:10.1892/0891-

6640(2004)18<679:CIMACR>2.0.CO;2
12. Hankel S, Shelton GD, Engvall E. Sarcolemma-specific autoantibodies in canine inflammatory myopathy. *Vet Immunol Immunopathol*. 2006;113(1-2):1-10. doi:10.1016/j.vetimm.2006.03.025
13. Paciello O, Oliva G, Gradoni L, et al. Canine inflammatory myopathy associated with Leishmania Infantum infection. *Neuromuscul Disord*. 2009;19(2):124-130. doi:10.1016/j.nmd.2008.10.013
14. Podell M, Chen E, Shelton GD. Feline immunodeficiency virus associated myopathy in the adult cat. *Muscle Nerve*. 1998;21(12):1680-1685. doi:10.1002/(SICI)1097-4598(199812)21:12<1680::AID-MUS9>3.0.CO;2-F
15. Pasolini MP, Pagano TB, Costagliola A, et al. Inflammatory Myopathy in Horses With Chronic Piroplasmosis. *Vet Pathol*. 2018;55(1):133-143. doi:10.1177/0300985817716262
16. Costagliola A, Piegari G, Otrocka-Domagala I, et al. Immunopathological features of canine myocarditis associated with leishmania infantum infection. *Biomed Res Int*. 2016;2016. doi:10.1155/2016/8016186
17. Silva-Almeida M, Carvalho LOP, Abreu-Silva AL, d'Escoffier LN, Calabrese KS. Leishsmania (Leishmania) amazonensis infection: Muscular involvement in BALB/c and C3H.HeN mice. *Exp Parasitol*. 2010;124(3):315-318. doi:10.1016/j.exppara.2009.11.006
18. Paciello O, Wojcik S, Gradoni L, et al. Syrian hamster infected with Leishmania infantum: a new experimental model for inflammatory myopathies. *Muscle Nerve*. 2010;41(3):355-361. doi:10.1002/mus.21502
19. Esteva L, Vargas C, Vargas de León C. The role of asymptomatics and dogs on leishmaniasis propagation. *Math Biosci*. 2017;293:46-55. doi:10.1016/j.mbs.2017.08.006
20. Dantas-Torres F, Miró G, Baneth G, et al. Canine leishmaniasis control in the context of one health. *Emerg Infect Dis*. 2019;25(12):E1-E4. doi:10.3201/eid2512.190164
21. Ribeiro RR, Suzan M, Michalick M, et al. Canine leishmaniasis: An overview of the current status and strategies for control. *Biomed Res Int*. 2018;2018(Cl):1-12.
22. Koutinas AF, Koutinas CK. Pathologic Mechanisms Underlying the

Clinical Findings in Canine Leishmaniosis due to Leishmania infantum/chagasi. *Vet Pathol*. 2014;51(2):527-538. doi:10.1177/0300985814521248

23. Baneth G, Yasur-Landau D, Gilad M, Nachum-Biala Y. Canine leishmaniosis caused by Leishmania major and Leishmania tropica: Comparative findings and serology. *Parasites and Vectors*. 2017;10(1):1-9. doi:10.1186/s13071-017-2050-7
24. Lopez R, Lucena R, Novales M, Ginel PJP, Martin E, Molleda JM. Circulating immune complexes and renal function in canine leishmaniasis. *J Vet Med Séries B*. 1996;43(8):469-474.
25. Ginel PJ, Camacho S, Lucena R. Anti-histone antibodies in dogs with leishmaniasis and glomerulonephritis. *Res Vet Sci*. 2008;85(3):510-514. doi:10.1016/j.rvsc.2008.01.007
26. Cortese L, Sica M, Piantedosi D, et al. Secondary immune-mediated thrombocytopenia in dogs naturally infected by Leishmania infantum. *Vet Rec*. 2009;164(25):778-782. doi:164/25/778 [pii]
27. Makaritsis KP, Gatselis NK, Ioannou M, Petinaki E, Dalekos GN. Polyclonal hypergammaglobulinemia and high smooth-muscle autoantibody titers with specificity against filamentous actin: consider visceral leishmaniasis, not just autoimmune hepatitis. *Int J Infect Dis*. 2009;13(4). doi:10.1016/j.ijid.2008.08.011
28. Paciello O, Shelton GD, Papparella S. Expression of major histocompatibility complex class I and class II antigens in canine masticatory muscle myositis. *Neuromuscul Disord*. 2007;17(4):313-320. doi:10.1016/j.nmd.2007.01.012
29. Cimmino I, Margheri F, Prisco F, et al. Prep1 regulates angiogenesis through a PGC-1α–mediated mechanism. *FASEB J*. October 2019:fj.201901230RR. doi:10.1096/fj.201901230RR
30. Cimmino I, Lorenzo V, Fiory F, et al. A peptide antagonist of Prep1-p160 interaction improves ceramide-induced insulin resistance in skeletal muscle cells. *Oncotarget*. 2017;8(42):71845-71858. doi:10.18632/oncotarget.18286
31. Chaabouni A, Boubaker Elandoulsi R, Mhadhbi M, Gharbi M, Sassi A. Comparative analysis of the Leishmania infantum-specific antibody repertoires and the autoantibody repertoires between asymptomatic and symptomatic dogs. *Vet Parasitol*. 2018;261:9-17. doi:10.1016/j.vetpar.2018.07.011
32. Lucena R, Ginel PJ, Lopez R, Novales M, Martin E, Molleda JM. Antinuclear Antibodies in Dogs with Leishmaniasis. *J Vet Med Ser*

A. 1996;43(1-10):255-259. doi:10.1111/j.1439-0442.1996.tb00451.x

33. Prisco F, De Biase D, Ilsami A, et al. Feline Immunodeficiency Virus-Associated Myopathy in Cats: An Autoimmune Disorder? *J Comp Pathol*. 2020;174:148. doi:10.1016/j.jcpa.2019.10.026
34. Stammers AN, Susser SE, Hamm NC, et al. The regulation of sarco (endo) plasmic reticulum. *Can J Physiol Pharmacol*. 2015;93(January):834–854. doi:10.1139/cjpp-2014-0463
35. Krishnan B, Massilamany C, Basavalingappa RH, et al. Epitope Mapping of SERCA2a Identifies an Antigenic Determinant That Induces Mainly Atrial Myocarditis in A/J Mice. *J Immunol*. 2018;200(2):523-537. doi:10.4049/jimmunol.1701090
36. Wu X, Li Z, Brooks R, et al. Autoantibodies in Canine Masticatory Muscle Myositis Recognize a Novel Myosin Binding Protein-C Family Member. *J Immunol*. 2007;179(7):4939-4944. doi:10.4049/jimmunol.179.7.4939
37. McHugh NJ, Tansley SL. Autoantibodies in myositis. *Nat Rev Rheumatol*. 2018;14(5):290-302. doi:10.1038/nrrheum.2018.56
38. Dubowitz V, Sewry CA, Oldfors A, Lane RJM. *Muscle Biopsy: A Practical Approach*. 4th Editio. Saunders; 2013.
39. Khaw BA, Narula J, Sharaf AR, Nicol PD, Southern JF, Carles M. SR-Ca2+ATPase as an autoimmunogen in experimental myocarditis. *Eur Heart J*. 1995;16(SUPPL. O):92-96. doi:10.1093/eurheartj/16.suppl_o.92
40. Sharaf AER, Narula J, Nicol PD, Southern JF, Khaw BA. Cardiac sarcoplasmic reticulum calcium ATPase, an autoimmune antigen in experimental cardiomyopathy. *Circulation*. 1994;89(3):1217-1228. doi:10.1161/01.CIR.89.3.1217
41. Ferrari BI, Levin MJ, Wallukat G, et al. Molecular Mimicry between the Immunodominant Ribosomal Protein PO of Trypanosoma crnzi and a Functional Epitope on the Human β1-Adrenergic Receptor. 1995;182(July).
42. Costanzo M, Caterino M, Cevenini A, et al. Proteomics reveals that methylmalonyl-coa mutase modulates cell architecture and increases susceptibility to stress. *Int J Mol Sci*. 2020;21(14):1-29. doi:10.3390/ijms21144998

Chapter 2

White Striping Myopathy in Broiler Chickens

Based on:

Histological and immunohistochemical characterization of white striping myopathy in broiler chickens. Francesco Prisco, Davide De Biase, Arianna Ilsami, Raffaelina Mercogliano, Ludovico Dipineto, Orlando Paciello and Serenella Papparella. LXXIII congresso SISVet, XVI Convegno AIPVet. Olbia dal 19 al 22 giugno 2019.

White striping myopathy in broiler chickens. Francesco Prisco, Davide De Biase, Giuseppe Piegari, Ilaria D'Aquino, Adriano Lama, Federica Comella, Raffaelina Mercogliano, Ludovico Dipineto, Serenella Papparella and Orlando Paciello. Submitted article.

2.1 Introduction

The increase in demand for chicken meat has been accompanied by intense genetic selection for growth rate, but on the other hand, it is accompanied by a variety of challenges, one of which is the white striping myopathy (WS).[3,19] WS is an emerging disease in broiler chickens, macroscopically characterized by white striations of the pectoralis and thighs muscles parallel to the muscle fibers.[21] WS is considered an esthetic and technological defect that devalues broiler breast fillets.[46] Many studies reported that the incidence of WS in broiler chickens increased dramatically from an average of 5% in 2012[15] to over 90% in the last years[21,27], with considerable economic losses for the poultry industry.[46]

There is little information available regarding the histological lesions associated with WS myopathy. The few studies have focused on abnormalities that can influence the chemical and textural properties of the meat, such as fibrosis and replacement with adipose tissue, and these studies only occasionally report microscopic changes such as necrosis and infiltration of lymphocytes and macrophages.[20,39]

To date, the pathomechanisms underlying WS are unclear. Recent studies suggested that hypoxia plays a major role in WS pathogenesis;[3,26] however, oxidative stress, fiber-type switching, and nutritional deficiencies may also contribute.[3] There is little information about the characteristics of the inflammatory response in WS.[45] Increasing evidence indicates that inflammatory responses including macrophages and T_H17 cell responses play a pivotal role in modulating the neovascularization, repair and

remodeling after muscle ischemia[4,13] For this reason, in addition to the morphological characterization of the inflammatory infiltrate, in the present study we explored the T_H1/T_H17 polarization of the inflammatory response.

Moreover, different ischemic injuries, such as myocardial infarctions[24], stroke and traumatic brain injury[16], have been recently associated with immune-mediated disorders. In an ischemia-induced inflammatory microenvironment, self-reactive lymphocytes and autoantibodies could be generated and may participate in inflammation and the progression of tissue injury.[16,24] Based on these observations, we hypothesized that an immune-mediated component may be part of the pathogenesis of WS. For this reason, in the present study, we evaluated the presence of the CD8/MHC I complexes, as hallmarks of immune-mediated muscle diseases, and assessed the expression of cytokines related to immune-mediated diseases.[33]

The aims of this study were to (1) characterize the histologic and histoenzymatic features of WS, (2) characterize the inflammatory infiltrate, (3) evaluate the expression of CD8/MHC I complexes, and (4) assess cytokine expression in order to understand the pathomechanisms underlying this myopathy.

2.2 Materials and Methods

2.2.1 Samples

The study included pectoralis muscles from 50 chickens randomly collected at a CE authorized slaughterhouse from five batches of 55 days old ROSS 308 broiler chickens with a mean weight of 3.5 Kg. The study did not require consent or ethical approval according to European Directive 2010/63/EU. The animals were slaughtered in strict accordance with European slaughter regulations (CE n° 1099/2009 of 24 September 2009) for the protection of animals at the time of killing (Ref. Official Journal of the European Union L 303/1). Permission to obtain the samples was granted from the owner of the abattoir and the veterinary inspector responsible for sanitary surveillance.

The gross severity of WS was graded in chicken pectoralis muscles following an established method[27]:

- Grade 0 (non-WS): no white striation on the meat surface;
- Grade 1 (mild-WS): 1 to 40 white lines with a thickness of < 1 mm;
- Grade 2 (moderate-WS): more than 40 white lines with a thickness of < 1 mm, or 1 to 5 white lines with a thickness of 1 mm to 2 mm;
- Grade 3 (severe-WS): more than 5 white lines with a thickness of 1 mm to 2 mm, or at least one line with a thickness ≥ 2 mm.

For this study, we avoided samples with wooden breast, “spaghetti meat”, and deep pectoral (green muscle disease) myopathies.[1] Two samples were collected from the cranial region on the ventral surface of each breast muscle, one of which was placed in RNAlater. All samples were immediately transported under refrigeration (2-4 °C) to the Laboratory of Comparative Neuromuscular Disorders of the Department of Veterinary Medicine of the University of Naples within 1-2 hours after sampling. Samples of 1 x 1 x 1 cm were snap-frozen in isopentane pre-cooled in liquid nitrogen for histology and the aliquots transported in RNAlater were frozen at -80°C for molecular examination.

2.2.2 Histopathology and immunohistochemistry

Frozen transverse sections (8 µm thick) were stained according to our routinely performed laboratory stains[30] including: i) hematoxylin and eosin (HE) and ii) Engel trichrome (ET) for a basic morphologic evaluation and mitochondria distribution; iii) reduced nicotinamide adenine dinucleotide-tetrazolium reductase (NADH-TR) to observe the intermyofibrillar pattern and secondary distribution of mitochondria; and iv) succinate dehydrogenase (SDH) and v) cytochrome oxidase (COX) to evaluate activity and distribution of mitochondria.[30]

A scoring system was designed to assess the degree of fiber atrophy as follows based on the assessment of at least 10 fields at 200X magnification (9.503 mm^2; 20× objective and a 10× ocular with a field number of 22 mm)[28]: normal (score 0), no atrophic fibers; mild (score 1),

<10% atrophic fibers; moderate (score 2), 10% to 50% atrophic fibers; and severe (score 3), >50% of atrophic fibers.[6,32,33] Muscle fibers were considered atrophic if the diameter was lower than 36 μm which is the minimum reported value for the cranial portion of the pectoral muscle of broiler chicken at slaughter-age.[7,40]

The number of lymphocytes and plasma cells was scored by light microscopy as: no infiltration (score 0); mild infiltration (score 1), on average 5 to 25 lymphocytes/plasma cells per high-power field (HPF; 0.237 mm^2; 40× objective and a 10× ocular with a field number of 22 mm)[28]; moderate infiltration (score 2), on average 26 to 50 lymphocytes/plasma cells per HPF; and severe infiltration (score 3), on average more than 50 lymphocytes/plasma cells per HPF. The average number was evaluated in at least 10 HPF for each sample.[33]

The degree of fiber necrosis was scored as follows based on the assessment of at least 10 fields at 200X magnification: normal (score 0), no necrotic fibers; mild (score 1), <10% necrotic fibers; moderate (score 2), 10% to 50% necrotic fibers; and severe (score 3), >50% of necrotic fibers.[6,32] For the evaluation of fiber necrosis, both the fibers with loss of the normal sarcoplasm structure and the necrotic fibers invaded by macrophages (sarcoclastosis) were counted. [7,33]

Fibrous and adipose tissue replacement were separately scored as follows using a system based on the assessment of 10 fields at 200X magnification: normal (score 0) no fibrous/adipose tissue replacement; mild (score 1), <10% of the skeletal muscle is replaced by fibrous/adipose tissue; moderate (score 2), 10% to 20% is replaced; and severe (score 3), >20% is replaced.

The alterations of intermyofibrillar pattern and alterations in mitochondrial activity and distribution have been studied with histoenzymatic stains to mark the following oxidative enzyme activities: reduced nicotinamide adenine dinucleotide-tetrazolium reductase (NADH-TR), succinate dehydrogenase (SDH) and cytochrome c oxidase (COX).[7,33] A scoring system was designed to assess the degree of alteration of intermyofibrillar pattern and alteration in mitochondrial activity and distribution. This score was based on the percentage of fibers showing abnormalities with the NADH-TR, SDH and COX stains, such as coarse intermyofibrillar pattern, "moth-eaten" fibers, target fibers, targetoid fibers, core fibers, pre-ragged blue fibers, whorled fibers, etc. The score was assessed on at least 10 fields at 200X magnification: normal (score 0), no evident alteration; mild (score 1), <10% of fibers showed morphological alterations; moderate (score 2), 10% to 20% of fibers showed morphological alterations; and severe (score 3), >20% of fibers showed morphological alterations.[6,32,44]

Sections were evaluated by 2 independent pathologists (F.P. and O.P.) under an optical microscope (Nikon E600; Nikon, Tokyo, Japan). Discordant results were reviewed with a multiheaded microscope to reach a consensus.

For immunohistochemistry (IHC), frozen sections (8 µm thick) were processed with the MACH1 Universal HPR Polymer Detection Kit (Biocare Medical LLC, Concord, CA) as previously described.[33] The primary antibodies used are summarized in Table 2.1. A quantitative assessment of immunohistochemically stained sections was performed on 5 randomly selected cases for each grade of severity of the gross lesions. For each case,

ten 20× fields were randomly photographed under an optical microscope (Leica DM6000B by Leica, Wetzlar, Germany) associated with a digital camera (Leica DFC450C digital camera by Leica). Each photo was elaborated with Fiji (ImageJ, National Institutes of Health): a color deconvolution filter (H DAB) was applied to each photo to permit discrimination of browns and blues; the obtained 8-bit browns level was binarized using a threshold manually adjusted (between 0-100 and 0-120), as needed, for each image sets to accurately reflect chromogen distribution in the regions of interest; and the positive area was measured.[5,17,23] The mean positive area of the 10 analyzed fields was calculated for each case and expressed in percentage of the area of an entire field (% units). Furthermore, the areas of the marked inflammatory cells were added to obtain, for each case, a total inflammatory cell area. The mean positive areas of the 5 selected cases were calculated for each group of macroscopic severity.

Table 2.1. Anti-chicken monoclonal antibodies used as primary antibodies for immunohistochemistry and immunofluorescence.[a]

Recognized chicken molecule	***Target***	***Clone***	***Dilution***
Bu-1	B lymphocytes	AV20	1:400
CD3	T lymphocytes	CT-3	1:100
CD4	T helper lymphocytes	CT-4	1:100
CD8α	T cytotoxic lymphocytes	CT-8	1:500
TCRγδ	γδ-T lymphocytes	TCR-1	1:200
Monocyte/Macrophage-antigen	Monocyte/Macrophage	KUL01	1:500
MHC I	Major histocompatibility complex class I	F21-2	1:500
MHC II	Major histocompatibility complex class II	2G11	1:500

[a]All primary antibodies were mouse monoclonal antibodies from SouthernBiotech, Birmingham, AL, USA.

2.2.3 Immunofluorescence

To determine if muscle fibers infiltrated by CD8+ lymphocytes expressed MHC I (CD8/MHC I complexes), immunofluorescence was carried out as follows. Cryosections were dried at room temperature for 1 hour, preincubated with normal mouse serum diluted 1:10, and overlaid overnight in a humid chamber at 4°C with primary antibody for MHC Class I (F21-2, mouse monoclonal antibody, dilution 1:500; SouthernBiotech). A TRITC fluorochrome-labeled rabbit anti-mouse secondary antibody was applied (1:300; Jackson Laboratories, Bar Harbor, ME, USA) on sections for 1 hour at room temperature. Slides were rinsed with PBS and a second primary antibody directed against CD8 (CT-8, mouse monoclonal antibody, dilution 1:400; SouthernBiotech) was applied overnight at 4°C. A FITC fluorochrome-labeled rabbit anti-mouse secondary antibody was applied (1:300; Jackson Laboratories) on sections for 2 hours at room temperature. Slides were rinsed with PBS and mounted with a solution of 1-part glycerol/1-part PBS. For scanning and photography was used a fluorescence microscope (Leica DM6000B by Leica, Wetzlar, Germany) associated with a digital camera (Leica DFC450C digital camera by Leica). To exclude autofluorescence, serial sections of muscle were incubated with PBS omitting the primary antibody. Frozen sections of normal chicken cecal tonsils were used as positive controls for anti-MHC I and anti-CD8 antibodies.

2.2.4 RNA extraction and Real-time semi-quantitative PCR

To explore the T_H1/T_H17 inflammatory response and to evaluate the expression of cytokines related to immune-mediated diseases, total RNA derived from 5 pectoralis muscles randomly selected for each severity grade was extracted using TRIzol Reagent (Bio-Rad Laboratories) using a specific RNA extraction kit (NucleoSpin®, MACHEREY-NAGEL GmbH & Co, Düren, Germany), according to the manufacturer's instructions. cDNA was synthesized using High-Capacity cDNA Reverse Transcription Kit (Applied Biosystems) from 6 µg total RNA. The applied PCR settings were previously described.[22] The gene primers were: IFNG (for IFN-γ), LITAF (for lipopolysaccharides-induced TNF-alpha factor), IL6 (for IL-6), IL12A (for IL-12A), IL17 (for IL-17) (Qiagen, Hilden, Germany) in a final volume of 25 µl. All mRNAs were normalized to GAPDH as housekeeping gene, and data were analyzed according to the $2^{-\Delta\Delta C}{}_T$ method.

2.2.5 Statistical analysis

Statistical analysis was performed using Prism 8 (Version 8.2.1) with a level of significance of 0.05. The D'Agostino-Pearson test was used to assess the normality of data. The differences among means of each histologic semi-quantitative score were evaluated using Kruskal–Wallis test and post-hoc multiple comparisons using Dunn's test. The differences among means of immunohistochemical quantitative assessments and Real-

time PCR quantitative assessments were evaluated using one-way analysis of variance (ANOVA) and post-hoc multiple comparisons using the Holm-Sidak's multiple comparisons test.

The following correlations were evaluated using Spearman's rank correlation coefficient: (1) the macroscopic grade of the WS vs histologic semi-quantitative scores and the immunohistochemical quantitative assessments; (2) among the various histologic semi-quantitative scores; (3) between histologic semi-quantitative scores vs immunohistochemical quantitative assessments.

2.3 Results

2.3.1 Gross examination

White striations were present in 45/50 (90%) samples, with characteristic white striations parallel to the muscle fibers and more severe lesions in the cranio-lateral parts of the pectoralis muscles where the muscles were thicker (Fig. 2.1). The other 5/50 pectoralis muscle samples were macroscopically normal (grade 0).

Grade 1 (mild) lesions were present in 20/50 (40%) pectoralis muscles, with few and thin (< 1 mm) white striations usually exclusively present in the cranio-lateral parts of the pectoralis muscles. Grade 2 (moderate) lesions were present in 16/50 (32%) of the pectoralis muscles, with numerous white striations some of which were 1-2 mm, and usually

more evident in the cranial two-thirds of the pectoralis muscles. Grade 3 (severe) lesions were present in 9/50 (18%) of the pectoralis muscles, several white striations, some thicker than 2 mm, usually evident in the whole pectoralis muscle and often associated with hemorrhages. Distribution data are summarized in Figure 2.2.

Figure 2.1. White striping myopathy (WS), left pectoralis major muscle, chicken. Scoring scale used for evaluation of histopathologic changes. Muscles classified as grade 0 (normal, case 3) do not show any distinct white lines. Muscles classified as grade 1 (mild, case 7) exhibit white lines, less than 1 mm thick, parallel to the muscle fibers. Muscles classified as grade 2 (moderate, case 35) exhibit white lines from 1 to 2 mm thick, parallel to the muscle fibers. Muscles classified as score 3 (severe, case 44) exhibit easily evident white lines, more than 2 mm thick, parallel to the muscle fibers and associated with hemorrhages on the muscle surface. **Figure 2.2. Gross lesion scores for WS in pectoralis muscles from 50 broiler chickens.** Only 10% of the muscles were morphologically normal and the most frequent lesions score was grade 1.

2.3.2 Histology and immunohistochemistry

Atrophy, inflammation, necrosis, fibrosis and adipose tissue replacement were prominent findings in all cases. Other associated myopathic features were: centralization of nuclei, fiber splitting, and endomysial and perimysial edema.

There was increased variability of muscle fiber diameter with numerous muscle fibers reduced in size (atrophy), mainly round, rarely with angular profiles, scattered or distributed in small groups. The atrophy was scored as mild in 8/50 (16%) cases, moderate in 26/50 (52%) cases, and severe in 16/50 (32%) cases (Figs. 2.3-2.5).

All examined cases showed endomysial and perivascular infiltration of macrophages, lymphocytes and plasma cells. Endomysium was multifocally expanded by numerous macrophages, which often invaded necrotic muscle fibers (sarcoclastosis), associated with fewer lymphocytes and plasma cells, and often surrounding intact myofibers. Rarely, morphologically normal muscle fibers were infiltrated by one or few lymphocytes. Furthermore, numerous blood vessels were surrounded by lymphocytes and plasma cells, often organized in follicular structures, with fewer macrophages. Sometimes, inflammatory cells infiltrated and disrupted the vessel walls. Lymphoplasmacytic and histiocytic inflammation was scored as mild in 14/50 (28%) cases, moderate in 15/50 (30%) cases, and severe in 21/50 (42%) cases (Figs. 2.6-2.8).

Often, frequent scattered muscle fibers were necrotic and invaded by numerous macrophages (sarcoclastosis). The number of necrotic fibers was

scored as mild in 14/50 (28%) cases, moderate in 22/50 (44%) cases and severe in 14/50 (28%) cases (Figs. 2.9-2.11).

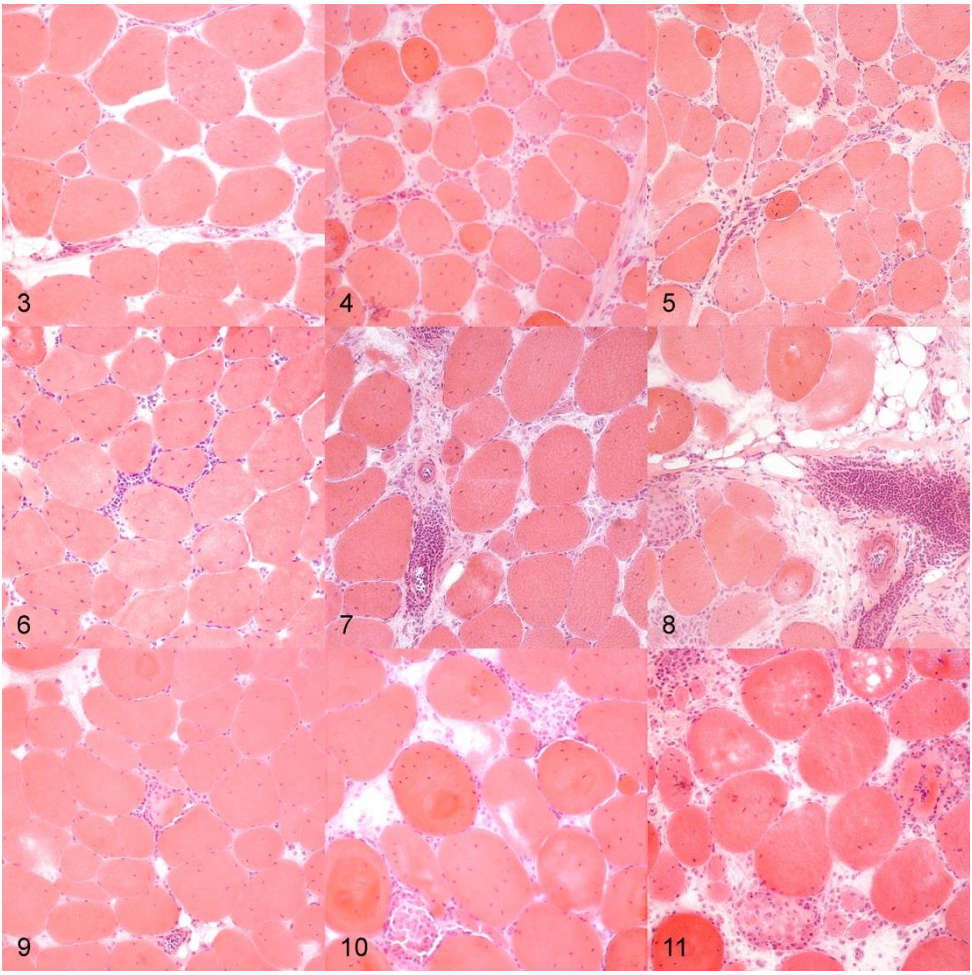

Figures 2.3-2.5. Atrophy, white striping myopathy (WS), skeletal muscle, chicken. Muscle fiber diameters are variable with numerous fibers reduced in size (atrophy). Atrophic fibers are mainly round or rarely had angular profiles. Hematoxylin and eosin (HE). **Figure 2.3.** Case 5. Mild atrophy (<10% atrophic fibers), centralization of muscle fibers nuclei, endomysial edema and scattered inflammatory cells. **Figure 2.4.** Case 16. Moderate atrophy (10% to 50%

atrophic fibers), centralization of muscle fibers nuclei, endomysial fibrosis and infiltrating inflammatory cells. **Figure 2.5.** Case 35. Severe atrophy (>50% of atrophic fibers), centralization of muscle fibers nuclei and severe inflammatory cells infiltration in the endomysium. **Figures 2.6-2.8. Inflammation, WS, skeletal muscle, chicken.** Infiltrates of lymphocytes and macrophages expand the endomysium and surround and infiltrate among muscle fibers. HE. **Figure 2.6.** Case 2. Mild inflammation (5 to 25 inflammatory cells per HPF), centralization of muscle fibers nuclei and endomysial edema. **Figure 2.7.** Case 31. Moderate inflammation (26 to 50 inflammatory cells per HPF), centralization of muscle fibers nuclei, scattered atrophic fibers and perimysial fibrosis. **Figure 2.8.** Case 42. Severe inflammation (>50 inflammatory cells per HPF), centralization of muscle fibers nuclei, perimysial fibrosis and replacement with adipose tissue. Inset: the inflammatory infiltrate is composed of lymphocytes and macrophages. **Figures 2.9-2.11. Myofiber necrosis, WS, skeletal muscle, chicken.** Necrotic fibers are present and are invaded by inflammatory cells, mainly macrophages. HE. **Figure 2.9.** Case 9. Mild myofiber necrosis (<10% necrotic fibers) with sarcoclastosis, centralization of muscle fibers nuclei, scattered atrophic fibers and scattered inflammatory cells in the endomysium. **Figure 2.10.** Case 24. Moderate myofiber necrosis (10% to 50% necrotic fibers) with sarcoclastosis, centralization of muscle fibers nuclei, scattered atrophic fibers and scattered inflammatory cells in the endomysium. **Figure 2.11.** Case 40. Severe myofiber necrosis (>50% of necrotic fibers) with sarcoclastosis, centralization of muscle fibers nuclei, scattered atrophic fibers and endomysial edema.

Fibrous and adipose tissue replacement of the skeletal muscle was also prominent. Fibrous replacement was absent in 3/50 (6%) cases, mild in 17/50 (34%) cases, moderate in 16/50 (32%) cases, and severe in 14/50 (28%) cases (Figs. 2.12-2.14). Adipose tissue replacement was absent in 3/50 (6%) cases, mild in 9/50 (18%) cases, moderate in 21/50 (42%) cases, and severe in 17/50 (34%) cases (Figs. 2.15-2.17).

Abnormalities of the intermyofibrillar pattern and mitochondrial activity and distribution were present in 49/50 cases, including coarse intermyofibrillar pattern and mitochondrial abnormalities such as “moth-eaten” fibers, target fibers, targetoid fibers, core fibers, pre-ragged blue fibers, and whorled fibers. Abnormalities of intermyofibrillar pattern and activity and distribution of mitochondria were scored as absent in 1 case (2%), mild in 15/50 (30%) cases, moderate in 25/50 (50%) cases and severe in 9/50 (19%) cases (Figs. 2.18-2.20).

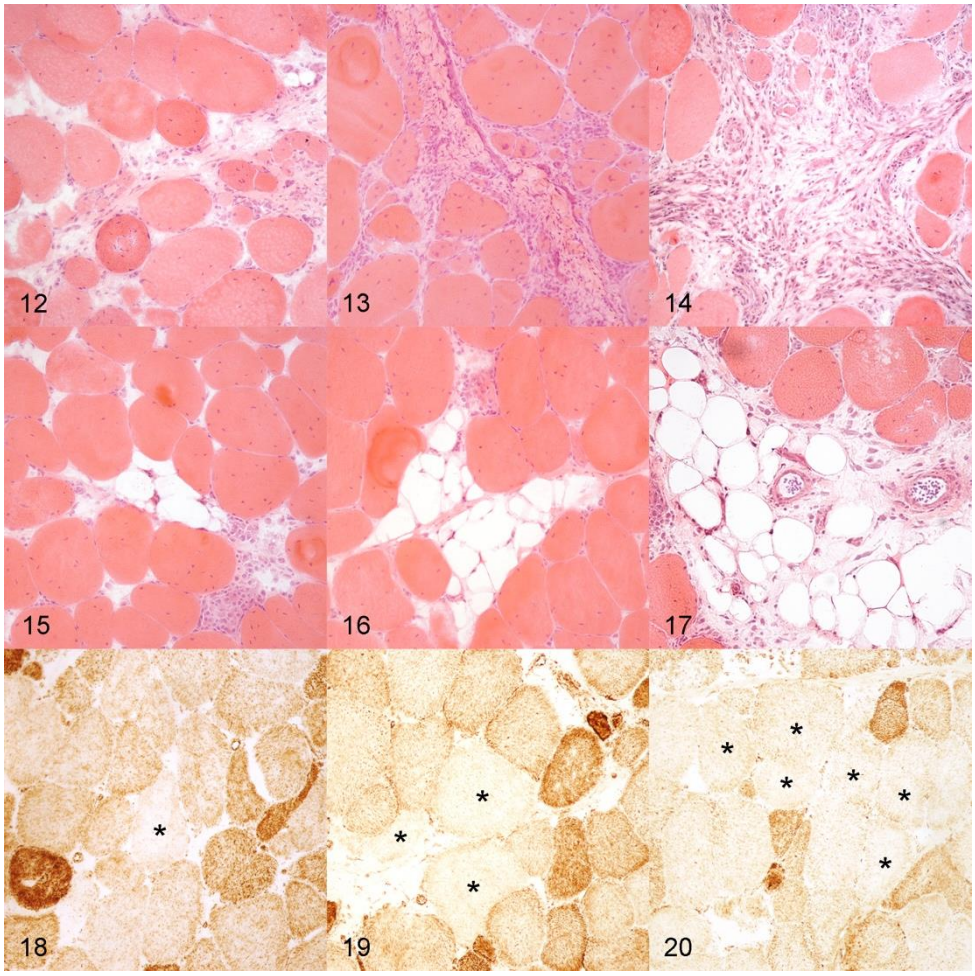

Figures 2.12-2.14. Fibrosis, White striping myopathy, skeletal muscle, chicken. The endomysium is expanded by fibrous tissue. HE. **Figure 2.12.** Case 23. Mild fibrosis (<10% of the skeletal muscle replaced), centralization of muscle fibers nuclei, scattered atrophic fibers and endomysial edema. **Figure 2.13.** Case 19. Moderate fibrosis (10% to 20% of the skeletal muscle replaced), centralization of muscle fibers nuclei, small groups of atrophic fibers and infiltration of inflammatory cells. **Figure 2.14.** Case 43. Severe fibrosis (>20% of the skeletal muscle replaced), centralization of muscle fibers nuclei, scattered atrophic fibers and severe infiltration of inflammatory cells. **Figures 2.15-2.17. Adipose tissue**

replacement, WS, skeletal muscle, chicken. The endomysium and perimysium are expanded by adipose tissue. HE. **Figure 2.15.** Case 9. Mild replacement with adipose tissue (<10% of the skeletal muscle replaced), centralization of muscle fibers nuclei, necrosis with sarcoclastosis of single muscle fiber and focal infiltration of inflammatory cells. **Figure 2.16.** Case 20. Moderate replacement with adipose tissue (10% to 20% of the skeletal muscle replaced), centralization of muscle fibers nuclei, necrosis with sarcoclastosis of single muscle fiber and scattered inflammatory cells infiltrating the endomysium. **Figure 2.17.** Case 26. Severe replacement with adipose tissue (>20% of the skeletal muscle replaced), centralization of muscle fibers nuclei and scattered inflammatory cells infiltrating the perimysium. **Figures 2.18-2.20. Mitochondrial alterations, WS, skeletal muscle, chicken.** Diffusely pale fibers (asterisks) show the absence of COX activity. Cytochrome oxidase stain. **Figure 2.18.** Case 10. Mild reduction in staining for cytochrome oxidase (<10% of fibers). **Figure 2.19.** Case 40. Moderate reduction in staining for cytochrome oxidase (10% to 20% of fibers). **Figure 2.20.** Case 47. Severe reduction in staining for cytochrome oxidase (>20% of fibers).

The atrophy score was higher in muscle with grade 3 WS compared with grade 0 (P<.05). Inflammation score was higher in muscle with grade 3 WS compared with grade 0 (P<.05) and grade 1 (P<.05). Necrosis score was higher in muscle with grade 3 WS compared with grade 0 (P<.01), grade 1 (P<.05), and grade 2 (P<.05). Fibrosis score was higher in grade 3 WS compared with grade 0 (P<.01) and grade 1 (P<.01). Fibrosis score was higher also in grade 2 WS compared with grade 0 (P<.05). Adipose tissue replacement score was lower in grade 0 WS compared with grade 3 (P<.001), grade 2 (P<.01) and grade 1 (P<.05). Mitochondrial alteration score was higher in muscle with grade 3 WS compared with grade 1 WS (P<.05) and grade 0 WS (P<.01). The differences between mean scores are summarized in Figure 2.21.

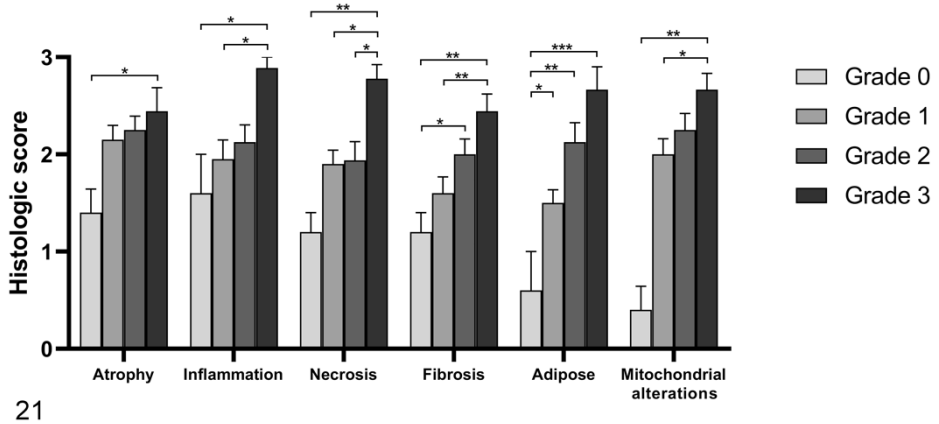

21

Figure 2.21. Relationships between histological lesion scores and macroscopic severity grade in muscles samples from 50 broiler chickens. Scores were determined for the histologic lesions shown and compared among samples with different macroscopic severity grades (grades 0-3, shown by different colored bars). The histological lesions were progressively more severe according

to the macroscopic severity grade of the white striping. Bars indicate means ± SEM. The means were compared using the Kruskal–Wallis test and post-hoc Dunn's multiple comparisons. Asterisks denote statistically differences between macroscopic lesion grades (*P<.05, **P<.01, ***P<.001).

The grade of gross severity of the WS was weakly positively correlated with atrophy score (r_s=0.325; P<.05), inflammation score (r_s=0.411; P<.01) and necrosis score (r_s=0.480; P<.001) and was moderately positively correlated with fibrosis score (r_s=0.621; P<.001), adipose tissue replacement score (r_s=0.530; P<.001) and mitochondrial alteration score (r_s=0.515; P<.001). Atrophy score was highly positively correlated with inflammation (r_s=0.757; P<.001), necrosis (r_s=0.757; P<.001) and adipose tissue replacement (r_s=0.434; P<.01) scores and was moderately positively correlated with fibrosis score (r_s=0.545; P<.001) and mitochondrial alteration score (r_s=0.603; P<.001). Inflammation score was also highly positively correlated with necrosis score (r_s=0.814; P<.001) and moderately positively correlated with fibrosis score (r_s=0.579; P<.001), adipose tissue replacement score (r_s=0.470; P=.001) and mitochondrial alteration score (r_s=0.663; P<.001). Necrosis score was moderately positively correlated with fibrosis score (r_s=0.639; P<.001), adipose tissue replacement score (r_s=0.568; P=.001) and mitochondrial alteration score (r_s=0.654; P<.001). Fibrosis score was low positively correlated with adipose tissue replacement score (r_s=0.436; P=.01) and moderately positively correlated with mitochondrial alteration score (r_s=0.585; P<.001). Adipose tissue

replacement score was also low positively correlated with mitochondrial alteration score (r_s=0.436; P<.01).

The inflammatory infiltrate expanding the endomysium and invading the necrotic muscle fibers was mainly composed of macrophages with fewer CD8+ lymphocytes and scattered or small groups of CD4+ lymphocytes, Bu1+ B cells and TCRγδ+ lymphocytes (Fig. 2.22). Otherwise, the inflammatory infiltrate surrounding the blood vessels was mainly composed of CD3+ T lymphocytes, predominantly CD8+ with less CD4+, associated with fewer Bu1+ B cells, TCRγδ+ lymphocytes and macrophages (Fig. 2.23).

The quantitative assessment of immunolabeled sections (Fig. 2.24) showed that the overall inflammatory population was mainly composed of macrophages and CD8+ lymphocytes. Furthermore, the distribution of the inflammatory infiltrate by each grade (Fig. 2.25) showed that for all markers the mean immunolabeling increased from grade 0 to grade 2 and decreased from grade 2 to grade 3. The exception was that immunolabeling of macrophages continuously increased from grade 0 to grade 3.

TCRγδ immunolabeling was higher in grade 3 WS compared with grade 0 (P.<.05) and was higher in grade 2 compared with grade 0 (P<.01) and grade 1 (P<.05). MAC immunolabeling was higher in grade 3 compared with grade 0 (P<.001) and grade 1 (P<.0001) and was higher in grade 2 compared with grade 0 (P<.01).

The macroscopic grade of the WS was moderately positively correlated with CD4 positivity (r_s=0.605; P<.01), Bu-1 positivity (r_s=0.523; P<.05) and TCRγδ positivity (r_s=0.690; P=.001). Furthermore, macroscopic grade was highly positively correlated with MAC positivity (r_s=0.845;

P<.001) and with total inflammatory cells (r_s=0.717; P=.001). Immunohistochemistry data are summarized in Figure 2.25.

Sarcolemmal and sarcoplasmic immunopositivity for MHC I was constantly observed in at least 90% of muscle fibers in all cases, both in fields with and without an evident inflammatory infiltrate (Fig. 2.26). Sarcolemmal and sarcoplasmic immunopositivity for MHC II were never observed (Fig. 2.27).

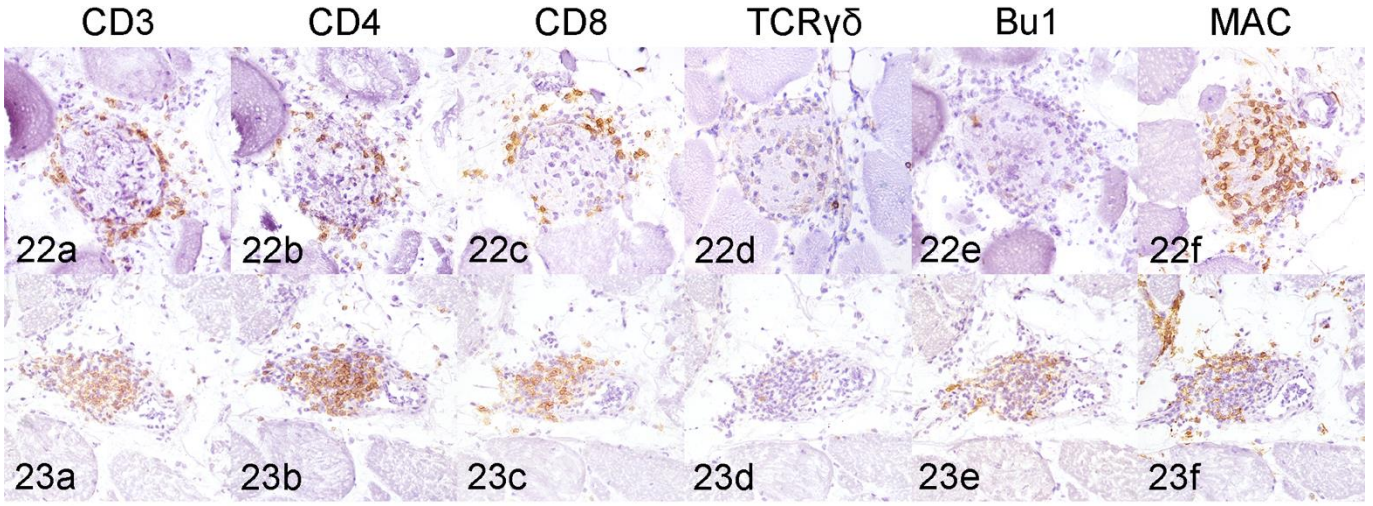
CD3
CD4
CD8
TCRγδ
Bu1
MAC
22a
22b
22c
22d
22e
22f
23a
23b
23c
23d
23e
23f

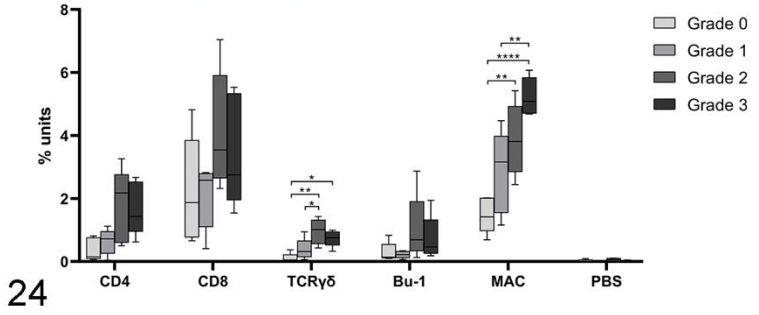
% units
CD4
CD8
TCRγδ
Bu-1
MAC
PBS
Grade 0
Grade 1
Grade 2
Grade 3

24

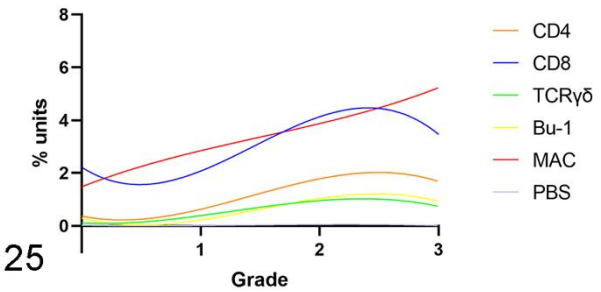
% units
Grade
CD4
CD8
TCRγδ
Bu-1
MAC
PBS

25

Figures 2.22 and 2.23. White striping myopathy, skeletal muscle, chicken. Immunohistochemistry, serial sections. Detection of CD3 (column a), CD4 (column b), CD8 (column c), TCRγδ (column d), Bu1 (column e) and MAC (column f). **Figure 2.22.** Case 26. The endomysial inflammatory infiltrate is mainly composed of macrophages with fewer CD8+ lymphocytes. There are scattered CD4+ lymphocytes, Bu1+ B cells, and TCRγδ+ lymphocytes. **Figure 2.23.** Case 6. The perivascular inflammatory infiltrate is mainly composed of CD3+ lymphocytes, with both CD8+ and CD4+ cells. There are a moderate number of Bu1+ B cells and macrophages and few TCRγδ+ lymphocytes. **Figures 2.24. Quantitative assessment of immunolabeling.** The inflammatory cell population was mainly composed of macrophages and CD8+ lymphocytes. Immunolabeling for most markers increased from macroscopic lesion grade 0 to grade 2 and decreased from grade 2 to grade 3. The exception was Immunolabeling for macrophages (MAC), which continually increased from grade 0 to grade 3. Five cases from each macroscopic lesion grade were tested (20 cases in total). Means were compared with one-way ANOVA and post-hoc Holm-Sidak's multiple comparisons. Asterisks denote statistically differences between grades (*P<.05, **P<.01, ***P<.001, ****P<.0001). **Figure 2.25. Immunohistochemical data trends according to macroscopic grade.** Non-linear regression. MAC positivity had the best positive correlation with macroscopic grade (r_s=0.845; P<.001; Spearman's rank correlation coefficient).

2.3.3 Immunofluorescence

To explore the possible overexpression of MHC I on the sarcolemma of the intact myofibers infiltrated by CD8-positive lymphocytes, immunofluorescence was performed. In all cases, the intact myofibers infiltrated by CD8-positive lymphocytes showed an intense sarcolemmal and diffuse sarcoplasmic immunofluorescence to MHC I (Fig. 2.28). No immunofluorescence was detected in sections incubated with PBS omitting the primary antibody.

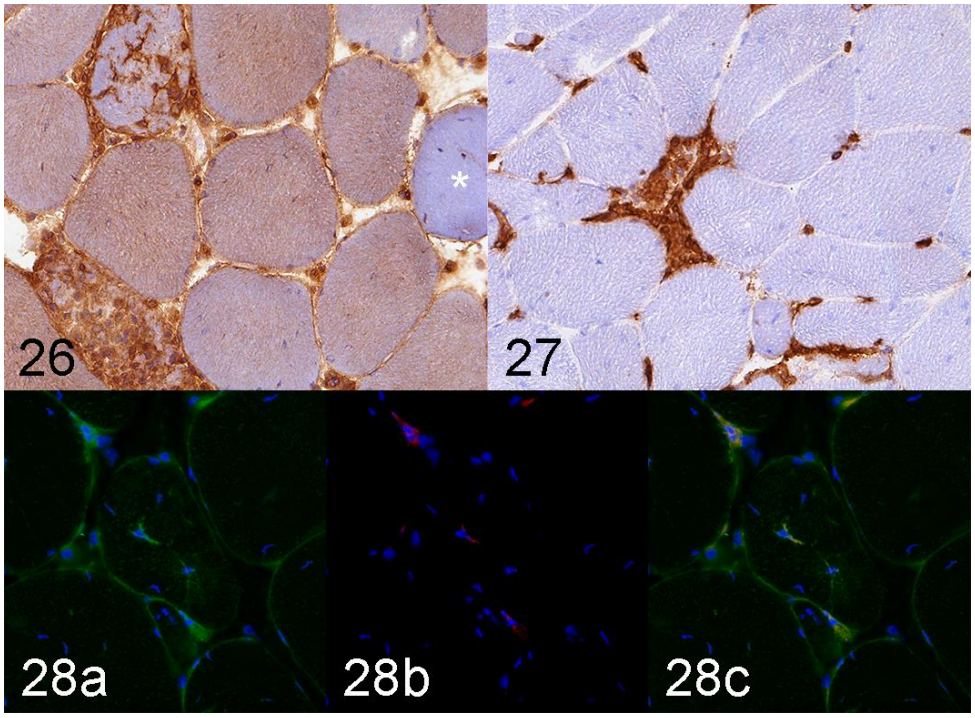

Figures 2.26 and 2.27. White striping myopathy, skeletal muscle, chicken. Immunohistochemistry. **Figure 2.26.** Case 9. Almost all muscle fibers

diffusely overexpress MHC I both on the sarcolemma and in the sarcoplasm. Negative muscle fibers are rare (asterisk). **Figure 2.27.** Case 9. The infiltrating inflammatory cells and the endothelial cells of the endomysial capillaries are MHC II-positive but no muscle fibers are positive. **Figure 2.28. White striping myopathy, skeletal muscle, chicken.** Immunofluorescence detection labeling of MHC I (a: green, FITC), CD8 (b: red, TRIC), and their colocalization (c: merge, orange color). Case 48. (a) Muscle fibers exhibit diffuse sarcolemmal and cytoplasmic immunolabeling of MHC I. (b) There are CD8-positive cells disseminated in the endomysium and rarely infiltrating morphologically normal muscle fibers. (c) Muscle fiber infiltrated by a CD8-positive cell intensely overexpresses MHC I (CD8/MHC I complex).

2.3.4 Cytokine expression

To molecularly characterize the inflammation in muscle samples, we evaluated inflammatory cytokine gene expression, including IFN- γ, LITAF, IL-6, IL-12A, and IL-17 (Fig. 2.29). There were no differences in the expression of IFN-γ among macroscopic grades. The expression of LITAF was higher in grade 3 compared with grade 1 ($P<.01$) and grade 0 ($P<.01$). The expression of IL-6 was higher in grade 3 compared with grade 2 ($P<.0001$), grade 1 ($P<.0001$) and grade 0 ($P=0001$). The expression of IL-17 was higher in grade 3 compared with grade 1 ($P<.05$) and grade 0 ($P<.05$).

The expression of LITAF was highly positively correlated with the WS grade ($r_s=0.818$; $P<.001$), inflammation score ($r_s=0.706$; $P<.01$) and mitochondrial alterations ($r_s=0.702$; $P<.01$). LITAF expression was also

moderately positively correlated with atrophy (r_s=0.646; P<.01) and necrosis (r_s=0.586; P<.05) and fibrosis (r_s=0.666; P<.01). The expression of IL-6 was moderately positively correlated with the WS grade (r_s= 0.559; P<.05), inflammation score (r_s=0.592; P<.01), necrosis (r_s=0.624; P<.01), mitochondrial alterations (r_s=0.505; P<.05) and low positively correlated with fibrosis (r_s=0.486; P<.05). The expression of IL-12A was moderately positively correlated with the atrophy (r_s=0.504; P<.05), inflammation score (r_s=0.631; P<.01), necrosis (r_s=0.529; P<.05), fibrosis (r_s=0.569; P<.05) and low positively correlated with mitochondrial alterations (r_s=0.497; P<.05). The expression of IL-17 was highly positively correlated with the WS grade (r_s= 0.808; P<.001) and moderately positively correlated with inflammation score (r_s=0.633; P<.01), necrosis (r_s=0.652; P<.01), fibrosis (r_s=0.668; P<.01) and mitochondrial alterations (r_s=0.607; P<.05).

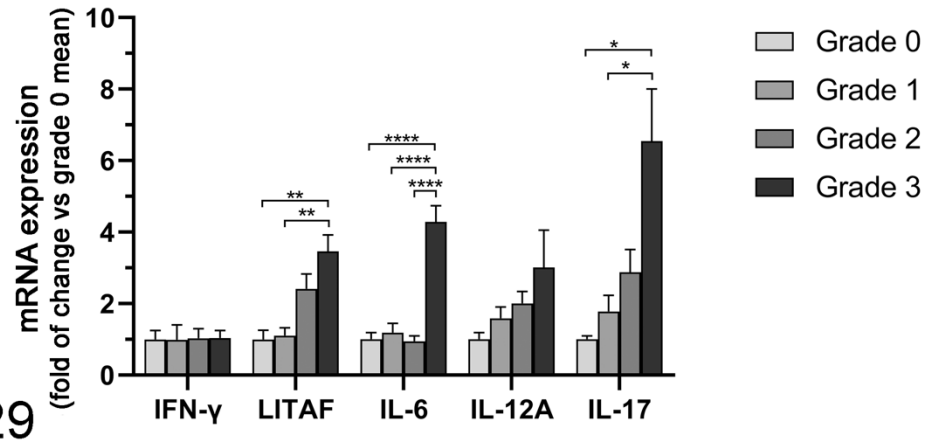

Figure 2.29. Quantitative RT-PCR analysis of inflammatory cytokine gene expression, in pectoralis muscle samples from 50 broiler chickens. Gene expression data are compared among samples with different macroscopic severity

grades (grades 0-3, shown by different colored bars) based on 5 tested samples for each grade (20 samples total). Gene expression data are expressed as fold-change from normal muscle samples (grade 0). Bars indicate means ± SEM. There are no differences in the IFN-γ gene expression among the different macroscopic grades. LITAF, IL-6, IL-12α, and IL-17 gene expression was higher in grade 3 pectoralis muscle compared with less severe grades. The means were compared by one-way ANOVA and post-hoc Holm-Sidak's multiple comparisons. Asterisks denote statistically differences between grades (*P<.05, **P<.01, ****P<.0001).

2.4 Discussion

WS is an emerging inflammatory myopathy affecting broiler chicken pectoral and thigh muscles with an increasing incidence at slaughter-age in recent years.[15,21,27] The morphologic appearance of this myopathy can adversely affect consumer acceptance of raw fillets and can cause a worsening of the chemical and textural properties of the meat, resulting in economic loss in the poultry industry.[19] The morphological and molecular characterization of this myopathy can lay the foundations for the development of genetic selection plans or therapies that may reduce the incidence of this condition with consequent reduction of the economic losses and improvement of animal welfare.

Our results showed that WS is a chronic inflammatory myopathy at slaughter-age, macroscopically characterized by white striations parallel to the muscle fibers,[19] and the striation thickness is related to the severity of

the disease. WS was observed in 90% of the examined pectoralis muscles in our study, most commonly as a grade 1 lesion. The reported incidence of WS in broiler chicken varies between published works but the most recent reported incidence data of WS in Ross 308 vary from 75.5% to 97.8% at slaughter age.[15,27] Incidence data variation could depend on confounding factors such as strain, age, sex, feed, etc.[19]

Histological lesions were observed in all animals, both with and without macroscopic evidence of WS, suggesting that the underlying disease process is even more frequent than reported. Macroscopically unaffected chickens generally showed mild microscopic lesions and may represent the early stages of the condition. Histologically, WS is mainly characterized by multifocal to coalescing endomysial and perivascular infiltrates of macrophages and CD8-positive T lymphocytes with severe myofiber atrophy, necrosis, fibrosis and replacement by adipose tissue. Other associated myopathic changes were endomysial and perimysial edema, centralization of nuclei, and fiber splitting.

The severity of the main histologic lesions was positively correlated with the macroscopic grade of WS. If we assume that a higher grade of WS corresponds to more advanced states of the condition[20], these data suggest concurrent progression of the histologic and macroscopic lesions in the pectoralis muscle. Inflammatory changes, fibrosis and adipose tissue replacement are the histologic lesions more strongly positively correlated with the macroscopic grade of WS. This observation suggests that these lesions may be mainly responsible for the macroscopic aspect of WS in chicken muscles. These results are supported by other studies where the

increased fat and decreased protein contents have been associated with the degree of white striping.[20]

The association between mitochondrial abnormalities and muscle inflammation is widely reported and it is frequently linked with damage of the mitochondrial DNA.[33] The grade of WS correlated with mitochondrial alterations suggesting a worsening of mitochondrial function according to the progression of the condition. In addition to an effect of inflammation, subsarcolemmal mitochondrial aggregates may also reflect chronic muscle hypoxia. It is reported that during hypoxia, skeletal muscle mitochondria shift position and localize preferentially in the subsarcolemmal region, where they are closer to capillaries. Moreover, the reduced COX-activity may reflect a hypoxia-related decrease in mitochondrial content, probably due to a combination of reduced mitochondrial biogenesis and increased mitophagy.[11] These findings are also supported by the reported increase in long- and medium-chain fatty acids and decrease in acylcarnitine esters in WS affected muscles, reflecting a defect in the beta-oxidation.[3]

The inflammatory infiltrate that characterizes WS is mainly composed of macrophages and CD8-positive lymphocytes. The quantitative assessment of immunolabeled sections showed that the number of lymphocytes in the lesions increased from grade 0 to grade 2 and decreased from grade 2 to grade 3. In contrast, the number of macrophages continuously increased from grade 0 to grade 3 and were highly positively correlated with macroscopic grade. Therefore, in the most advanced stages of the condition, macrophages tend to outnumber lymphocytes.

We hypothesize that histiocytic inflammation is triggered mainly by necrosis due to muscle hypoxia.[3] It has been suggested that the vascular

system in broiler chicken muscles may be marginal, supporting muscle growth under steady-state conditions, but inadequate to support the muscle under stress.[3] In this scenario, small stresses, such as minor trauma or sudden movements of wings[2], might destabilize an already precarious equilibrium and incite the development of this necrotizing and histiocytic myopathy. In addition to removing dead tissues and initiating the process of repair, macrophages can contribute to tissue injury in chronic inflammation by secreting cytokines and growth factors that act on various cells, notably T lymphocytes.[9,43]

T_H1 cytokines, including IL-12 and IFN-γ, are involved in the induction of cell-mediated immunity.[12,43] In the present study, there were no differences in IFN-γ and IL-12 mRNA expression among different grades of WS suggesting a constant production of these cytokines during disease progression.

We showed that LITAF was overexpressed in high-grade WS. LITAF is known as a TNF-α inducer in mammals[48], however, in chickens, the TNF-α homologous gene has been recently identified and the relationship with LITAF is not yet well defined.[14,37] Both in mammals and chickens, LITAF stimulates the expression of TNF-like ligand 1A (TL1A).[14,34,48] TL1A, also termed tumor necrosis factor superfamily member 15 (TNFSF15) and vascular endothelial growth inhibitor (VEGI), is an important negative regulator for endothelial cell proliferation, which may result in inhibition of vasculogenesis.[47] This activity might be part of the pathogenesis of ischemic muscle disease. This hypothesis is further supported by the positive correlation between LITAF expression and the observed necrosis and fibrosis. Moreover, the upregulation of LITAF

expression is reported in different immune-mediated disorders in humans, such as inflammatory bowel disease and rheumatoid arthritis.[48]

We observed that IL-6 is overexpressed in high-grade WS. IL-6 is generally considered a proinflammatory cytokine produced by T and B lymphocytes, macrophages and endothelial cells.[12] However, at least in mammals, IL-6 can also be produced by skeletal muscle fibers after physical exercise and, in this case, exerts an anti-inflammatory action. Conversely, in an inflammatory microenvironment with other proinflammatory cytokines such as TNF-α, IL-6 promotes inflammation.[36] Furthermore, the overproduction of IL-6 is considered important in the pathogenesis of multiple autoimmune inflammatory diseases, in which an imbalance between T_H17 cells and regulatory T cells and autoantibodies play a central role.[18]

IL-17 is another proinflammatory cytokine overexpressed in high-grade WS and principally released by activated T lymphocytes, specifically CD4+ T helper$_{17}$ (T_H17) and γδ-T cells. Moreover, IL-17 also induces IL-6 release by macrophages.[42] The functions of IL-17 are not yet well characterized in birds but, as for IL-6 and LITAF, IL-17 in mammals has been linked to several immune-mediated diseases such as rheumatoid arthritis, multiple sclerosis, lupus and Crohn's disease.[41,42] The IL-17 and IL-6 upregulation suggest an enhanced T_H17 response in severe degrees of WS.[41] The enhancement of the T_H17 response has been widely reported during muscle[8,10,25] and myocardial ischemia[38] where it has a critical role in angiogenesis, repair and remodelling.[4,13]

In addition to the overexpression of cytokines related to autoimmune inflammatory diseases, we also described morphologically normal MHCI

positive myofibers infiltrated by CD8-positive lymphocytes (CD8/MHC I complex), the hallmark of immune-mediated inflammatory myopathy in human, dogs, sheep and horses.[29,31,33,35] An association between ischemic injuries and immune-mediated disorders has been described in humans during myocardial infarctions[24], stroke and traumatic brain injury.[16] Thus, an immune-mediated mechanism should be considered as a component of the pathogenesis of the WS. We hypothesize that muscle necrosis might cause the release or the exposure of normally sequestered antigenic constituents that could potentially trigger an adaptive autoimmune response. Moreover, the persistent proinflammatory microenvironment following ischemic injuries could favor autoimmune responses to muscle antigens breaking tolerance mechanisms and triggering an immune-mediated myopathy.[16,24]

Our data are compatible with hypoxia-related damage to muscle tissue in WS, but further studies should consider other potential contributing mechanisms. In the present study, an immune-mediated component of the pathogenetic mechanism of WS has been suggested. Further studies are needed to evaluate the presence of circulating autoantibodies against muscle-antigens or the presence of autoreactive T cells.[16,41]

2.5 Conclusions

WS is a frequent chronic inflammatory and necrotizing myopathy of broiler chickens at slaughter-age. Macroscopically, it is characterized by white striation parallel to the muscle fibers. Histological lesions were

observed in all broiler chickens examined in this study, both with and without macroscopic evidence of WS. Histologically, WS was mainly characterized by multifocal to coalescing endomysial and perivascular inflammatory infiltrates of macrophages and CD8-positive T lymphocytes with severe myofiber atrophy, necrosis, fibrosis and replacement by adipose tissue. Other associated myopathic changes were endomysial and perimysial edema, centralization of nuclei, and fiber splitting, and there was a diffuse sarcoplasmic and sarcolemmal overexpression of MHC I. The severity of the histologic lesions was positively correlated with the macroscopic degree of white striations. The data suggest that the striations were mainly due to inflammation, fibrosis and adipose tissue replacement. The observation of CD8/MHC I complexes, together with the higher expression of IL-6, IL-17 and LITAF in severe WS, suggest an immune-mediated component may contribute to this myopathy. Given the increase in the incidence of WS, there is a pressing need to find a solution to reduce the incidence of WS and other hypoxia-induced myopathies of broiler chickens both to reduce economic losses in the poultry industry and for the chicken's welfare. Moreover, further studies are needed to explore the immune-mediated component of WS pathogenesis.

Chapter 2 References

1. Bailey RA, Watson KA, Bilgili SF, Avendano S. The genetic basis of pectoralis major myopathies in modern broiler chicken lines. *Poult Sci*. 2015;94:2870–2879.
2. Bianchi M, Petracci M, Franchini A, Cavani C. The occurrence of deep pectoral myopathy in roaster chickens. *Poult Sci*. 2006;85:1843–1846.
3. Boerboom G, van Kempen T, Navarro-Villa A, Pérez-Bonilla A. Unraveling the cause of white striping in broilers using metabolomics. *Poult Sci*. 2018;97:3977–3986.
4. Chen Z, Yan W, Mao Y, et al. Effect of Aerobic Exercise on Treg and Th17 of Rats with Ischemic Cardiomyopathy. *J Cardiovasc Transl Res*. 2018;11:230–235.
5. Cimmino I, Margheri F, Prisco F, et al. Prep1 regulates angiogenesis through a PGC-1α–mediated mechanism. *FASEB J*. 2019;fj.201901230RR.
6. Costagliola A, Wojcik S, Pagano TB, et al. Age-Related Changes in Skeletal Muscle of Cattle. *Vet Pathol*. 2016;53:436–446.
7. Dubowitz V, Sewry CA, Oldfors A, Lane RJM. *Muscle biopsy: a practical approach*. Saunders; 2013.
8. Ege T, Us MH, Sungun M, Duran E. Cytokine response in lower extremity ischaemia/reperfusion. *J Int Med Res*. 2004;32:124–131.
9. Fernández M, Benavides J, Castaño P, et al. Macrophage Subsets Within Granulomatous Intestinal Lesions in Bovine Paratuberculosis. *Vet Pathol*. 2017;54:82–93.
10. Gaines GC, Welborn MB, Moldawer LL, Huber TS, Harward TRS, Seeger JM. Attenuation of skeletal muscle ischemia/reperfusion injury by inhibition of tumor necrosis factor. *J Vasc Surg*. 1999;29:370–376.
11. Gamboa JL, Andrade FH. Mitochondrial content and distribution changes specific to mouse diaphragm after chronic normobaric hypoxia. *Am J Physiol - Regul Integr Comp Physiol*. 2010;298:575–583.
12. Giansanti F, Giardi M, Botti D. Avian Cytokines - An Overview.

Curr Pharm Des. 2007;12:3083–3099.
13. Hata T, Takahashi M, Hida S, et al. Critical role of Th17 cells in inflammation and neovascularization after ischaemia. *Cardiovasc Res*. 2011;90:364–372.
14. Hong YH, Lillehoj HS, Hyen Lee S, Woon Park D, Lillehoj EP. Molecular cloning and characterization of chicken lipopolysaccharide-induced TNF-α factor (LITAF). *Dev Comp Immunol*. 2006;30:919–929.
15. Huang X, Ahn DU. The Incidence of Muscle Abnormalities in Broiler Breast Meat – A Review. *Korean J food Sci Anim Resour*. 2018;38:835–850.
16. Javidi E, Magnus T. Autoimmunity After Ischemic Stroke and Brain Injury. *Front Immunol*. 2019;10:1–12.
17. Johnson SJ, Walker FR. Strategies to improve quantitative assessment of immunohistochemical and immunofluorescent labelling. *Sci Rep*. 2015;5:3–6.
18. Jones BE, Maerz MD, Buckner JH. IL-6: a cytokine at the crossroads of autoimmunity. *Curr Opin Immunol*. 2018;55:9–14.
19. Kuttappan VA, Hargis BM, Owens CM. White striping and woody breast myopathies in the modern poultry industry: A review. *Poult Sci*. 2016;95:2724–2733.
20. Kuttappan VA, Shivaprasad HL, Shaw DP, et al. Pathological changes associated with white striping in broiler breast muscles. *Poult Sci*. 2013;92:331–338.
21. Kuttappan VA, Owens CM, Coon C, Hargis BM, Vazquez-Añon M. Incidence of broiler breast myopathies at 2 different ages and its impact on selected raw meat quality parameters. *Poult Sci*. 2017;96:3005–3009.
22. Lama A, Annunziata C, Coretti L, et al. N-(1-carbamoyl-2-phenylethyl) butyramide reduces antibiotic-induced intestinal injury, innate immune activation and modulates microbiota composition. *Sci Rep*. 2019;9.
23. Law AMK, Yin JXM, Castillo L, et al. Andy's Algorithms: New automated digital image analysis pipelines for FIJI. *Sci Rep*. 2017;7:1–11.
24. Liao YH, Cheng X. Autoimmunity in myocardial infarction. *Int J Cardiol*. 2006;112:21–26.
25. Lopes RD, Batista ML, Rosa JC, et al. Changes in the production of IL-10 and TNF-α in skeletal muscle of rats with heart failure

secondary to acute myocardial infarction (Arquivos Brasileiros de Cardiologia (2010) 94, 3, (313-320)). *Arq Bras Cardiol*. 2010;95:279.
26. Malila Y, Thanatsang K, Arayamethakorn S, et al. Absolute expressions of hypoxia-inducible factor-1 alpha (HIF1A) transcript and the associated genes in chicken skeletal muscle with white striping and wooden breast myopathies. *PLoS One*. 2019;14:1–23.
27. Malila Y, U-Chupaj J, Srimarut Y, et al. Monitoring of white striping and wooden breast cases and impacts on quality of breast meat collected from commercial broilers (Gallus gallus). *Asian-Australasian J Anim Sci*. 2018;31:1807–1817.
28. Meuten DJ, Moore FM, George JW. Mitotic Count and the Field of View Area. *Vet Pathol*. 2016;53:7–9.
29. Paciello O, Oliva G, Gradoni L, et al. Canine inflammatory myopathy associated with Leishmania Infantum infection. *Neuromuscul Disord*. 2009;19:124–130.
30. Paciello O, Papparella S. Histochemical and immunohistological approach to comparative neuromuscular diseases. *Folia Histochem Cytobiol*. 2009;47:143–152.
31. Paciello O, Shelton GD, Papparella S. Expression of major histocompatibility complex class I and class II antigens in canine masticatory muscle myositis. *Neuromuscul Disord*. 2007;17:313–320.
32. Pagano TB, Wojcik S, Costagliola A, et al. Age related skeletal muscle atrophy and upregulation of autophagy in dogs. *Vet J*. 2015;206:54–60.
33. Pagano TB, Prisco F, De Biase D, et al. Muscular Sarcocystosis in Sheep Associated With Lymphoplasmacytic Myositis and Expression of Major Histocompatibility Complex Class I and II. *Vet Pathol*. 2019;030098581989125.
34. Park SS, Lillehoj HS, Hong YH, Lee SH. Functional characterization of tumor necrosis factor superfamily 15 (TNFSF15) induced by lipopolysaccharides and Eimeria infection. *Dev Comp Immunol*. 2007;31:934–944.
35. Pasolini MP, Pagano TB, Costagliola A, et al. Inflammatory Myopathy in Horses With Chronic Piroplasmosis. *Vet Pathol*. 2018;55:133–143.
36. Pedersen BK, Febbraio MA. Muscle as an Endocrine Organ: Focus on Muscle-Derived Interleukin-6. *Physiol Rev*. 2008;88:1379–1406.

37. Rohde F, Schusser B, Hron T, et al. Characterization of chicken tumor necrosis factor-α, a long missed cytokine in birds. *Front Immunol*. 2018;9:1–14.
38. Saini HK, Xu YJ, Zhang M, Liu PP, Kirshenbaum LA, Dhalla NS. Role of tumour necrosis factor-alpha and other cytokines in ischemia-reperfusion-induced injury in the heart. *Exp Clin Cardiol*. 2005;10:213–222.
39. Salles GBC, Boiago MM, Silva AD, et al. Lipid peroxidation and protein oxidation in broiler breast fillets with white striping myopathy. *J Food Biochem*. 2019;43:1–7.
40. Smith DP, Fletcher DL. Chicken breast muscle fiber type and diameter as influenced by age and intramuscular location. *Poult Sci*. 1988;67:908–913.
41. Tabarkiewicz J, Pogoda K, Karczmarczyk A, Pozarowski P, Giannopoulos K. The Role of IL-17 and Th17 Lymphocytes in Autoimmune Diseases. *Arch Immunol Ther Exp (Warsz)*. 2015;63:435–449.
42. Walliser I, Göbel TW. Chicken IL-17A is expressed in αβ and γδ T cell subsets and binds to a receptor present on macrophages, and T cells. *Dev Comp Immunol*. 2018;81:44–53.
43. Wigley P, Kaiser P. Avian cytokines in health and disease. *Rev Bras Ciência Avícola*. 2003;5:1–14.
44. Zaghini A, Sarli G, Barboni C, et al. Long term breeding of the Lmna G609G progeric mouse: Characterization of homozygous and heterozygous models. *Exp Gerontol*. 2020;130:110784.
45. Zambonelli P, Zappaterra M, Soglia F, et al. Detection of differentially expressed genes in broiler pectoralis major muscle affected by White Striping - Wooden Breast myopathies. *Poult Sci*. 2016;95:2771–2785.
46. Zanetti MA, Tedesco DC, Schneider T, et al. Economic losses associated with Wooden Breast and White Striping in broilers. *Semin Agrar*. 2018;39:887–891.
47. Zhang ZH, Chen QZ, Jiang F, et al. Changes in TL1A levels and associated cytokines during pathogenesis of diabetic retinopathy. *Mol Med Rep*. 2017;15:573–580.
48. ZOU J, GUO P, LV N, HUANG D. Lipopolysaccharide-induced tumor necrosis factor-α factor enhances inflammation and is associated with cancer (Review). *Mol Med Rep*. 2015;12:6399–6404.

Chapter 3

Feline Immunodeficiency Virus-Associated Myopathy in Cats

Based on:
Feline Immunodeficiency Virus-Associated Myopathy in Cats: An Autoimmune Disorder? F. Prisco, D. De Biase, A. Ilsami, L. Cardillo, G. Fusco, P. Santoro, S. Papparella and O. Paciello. J Comp Pathol. 2020;174:148. doi:10.1016/j.jcpa.2019.10.026.

3.1 Introduction

In cats, Feline immunodeficiency virus (FIV) has been shown to induce IM after experimental infection[10], however, according to the authors' knowledge cases of IM associated with natural FIV infection have never been investigated. Moreover, myocarditis and hypertrophic cardiomyopathy associated with FIV infection have been described in five naturally infected cats.[11]

Information regarding retroviral-associated IMs and myocarditis is much stronger in humans and non-human primates.[10–13] Human Immunodeficiency Virus (HIV) and Simian Immunodeficiency Virus (SIV) have been associated with different forms of T cell-mediated IMs (polymyositis, dermatomyositis and inclusion body myositis) and some form of cardiac disorders.[10–13] The latter can be represented by mild inflammatory infiltrates that are found incidentally upon microscopic examination of autopsy cases but can also manifest as a clinically significant cardiac disease with chronic cardiac dysfunction.[13] There is great attention on HIV-associated heart diseases in human medicine because these greatly increase the risk of death in HIV-positive patients.[14] The pathogenetic mechanism underlying retrovirus-associated skeletal and cardiac disorders both in cats and humans are still not clear[10,12], however, a common pathogenetic mechanism can be hypothesized and cats can represent a valid spontaneous model of human disease.[3]

IMs are often characterized by a significant immune-mediated pathogenetic component, and usually associated anti-skeletal muscle autoantibody can be identified.[15] The role of autoantibodies in causing muscle damage and dysfunction is debated because most of the autoantigens are intracellular and thus not easily accessible to circulating autoantibodies.[1,15] Moreover, different forms of IM are characterized by specific anti-muscle autoantibodies that are considered ideal biomarkers for the diagnosis and prognosis and can have potential implications for personalized therapy options.[1,15]

HIV positive humans, and particularly those with cardiomyopathy, show circulating cardiac-specific autoantibodies, some of which also react with skeletal muscle (notably anti-β-myosin autoantibody).[16,17]

Based on this background, we hypothesize that circulating anti-muscle autoantibodies can be present also in FIV-infected cats and justify the associated IM. Furthermore, considering that the myocardium shares many proteins with skeletal muscle, we also hypothesize that the same autoantibodies may similarly target myocardial proteins.

The aims of the present study were: (1) investigate the occurrence of IM and myocarditis in cats naturally infected with FIV; (2) morphologically and molecularly characterize IM and myocarditis associated with natural FIV infection; and (3) investigate the presence of circulating autoantibodies targeting the skeletal muscle in sera of FIV-positive cats.

3.2 Materials and Methods

3.2.1 Sera and skeletal muscle samples

Sera, skeletal muscle and myocardium samples included in this study were retrospectively selected from the sera and tissue bank of the Comparative Neuromuscular Laboratory at the Department of Veterinary Medicine of the University Federico II in Napoli (UNINA).

The study included sera from 10 serologically FIV-positive, Feline Leukemia Virus (FeLV)-negative and Feline Coronavirus (FCoV)-negative cats and 5 negative control cats. Snap-frozen skeletal muscle samples from quadriceps femoris (vastus lateralis; QF) and triceps brachii (lateral head; TB) muscles and myocardium samples from interventricular septum were retrospectively selected from 20 cats PCR-positive for FIV and negative for FeLV and FCoV and 20 negative controls.

Corresponding frozen samples in RNA-later for assessment of cytokine expression were available for all 20 QF from FIV-positive cats and the 20 negative controls. Differently, the interventricular septum was available for 13 FIV-positive cats and all 20 negative controls.

3.2.2 Histopathology and immunohistochemistry

Frozen transverse sections (8 µm thick) were stained according to our routinely performed laboratory stains[18] including: i) hematoxylin and eosin (HE) and ii) Engel trichrome (ET) for a basic morphologic evaluation

and mitochondria distribution; iii) reduced nicotinamide adenine dinucleotide-tetrazolium reductase (NADH-TR) to observe the intermyofibrillar pattern and secondary distribution of mitochondria; and iv) succinate dehydrogenase (SDH) and v) cytochrome oxidase (COX) to evaluate activity and distribution of mitochondria.[18]

Sections were evaluated by 2 independent pathologists (F.P. and O.P.) under an optical microscope (Nikon E600; Nikon, Tokyo, Japan). Discordant results were reviewed with a multiheaded microscope to reach a consensus.

Skeletal muscle and myocardial sample were considered inflamed when at least one focus of inflammatory cells was evident.

For immunohistochemistry (IHC), frozen sections (8 µm thick) were processed with the MACH1 Universal HPR Polymer Detection Kit (Biocare Medical LLC, Concord, CA) as previously described.[20] The primary antibodies used are summarized in Table 3.1. Sections of QF and myocardium stained for CD3, CD20 and Iba-1 were used for a quantitative assessment of the inflammatory cell number using the computer program VIS (Visiopharm Integrator System, Version 5.0.4.1382; Visiopharm, Hoersholm, Denmark). For all quantitative approaches, the whole section was selected as the region of interest (ROI). A threshold classification allowed recognition of positive (intense brown staining of the entire cytoplasm) and negative cells in each ROI. To prevent groups of positive cells from being counted as a single cell, the nuclei present in each identified positive area were counted. In a post-processing step, very small nuclei (nuclear area $< 5\ \mu m^2$) were excluded from counting in order to avoid falsely classifying areas of increased background staining as nuclei. The results

were expressed as number of positive cells for μm^2 dividing the absolute number of detected positive nuclei by the area of the analyzed ROI.

Table 3.1. List of primary antibodies used for immunohistochemistry.

Recognized molecule	***Target***	***Host***	***Clone***	***Dilution***	***Manufacturer***
CD20	B lymphocytes	Rabbit	Polyclonal	1:200	BioCare Medical[a]
CD3	T lymphocytes	Rabbit	Polyclonal	1:200	Dako[b]
Iba-1	Monocyte/Macrophage	Rabbit	Polyclonal	1:500	Wako[d]
FIV-p24-gag	FIV group-specific antigen	Mouse	PAK3-2C1	1:200	Novus Biologicals[e]
MHC I	Major histocompatibility complex class I	Mouse	H58A	1:200	VMRD[c]
MHC II	Major histocompatibility complex class II	Mouse	H42A	1:500	VMRD[c]

[a]BioCare Medical, Pacheco, CA, USA.

[b]Dako, Milan, Italy.

[c]VMRD, Pullman, WA, USA.

[d]Wako, Neuss, Germany.

[e]Novus Biologicals, Centennial, CO, USA.

3.2.3 Indirect immunofluorescence

Three QF specimens were randomly selected from the control group for the indirect immunofluorescence assay (IIF). Eight micrometers transversal cryosections were cut and dried at room temperature for 45 minutes. Sections were fixed in acetone for 10 minutes at 4 °C. After 3 wash of 5 minutes in PBS, sections were incubated with 10% normal rabbit sera in PBS for 30 minutes at room temperature. To block endogenous feline IgG, after 3 wash of 5 minutes in PBS, sections were preincubated with F(ab')2 fragments of rabbit anti-feline IgG (H+L) (1:50; Rockland Immunochemicals, Limerick, PA, USA) for 1 hour. Sera from FIV-positive cats were serially diluted in PBS (1:100, 1:300, 1:1000, 1:3000, 1:10000) and, after 3 wash of 5 minutes in PBS, were added to each section for incubation overnight at 4 °C. Control sections were incubated with PBS. After washing three times with PBS for 5 minutes, FITC-conjugated rabbit anti-feline IgG (H+L) (1:300; Jackson Laboratories, West Grove, PA, USA) was added to each section and incubated for 40 minutes at room temperature. Sections were washed three times with PBS for 5 minutes and mounted under coverslips in VECTASHIELD® H-1200 (Vector, Burlingame, CA, USA) to prevent fading of fluorescence.

A quantitative assessment of immunofluorescence-stained sections was performed for each dilution for each serum. Ten 40× fields were randomly photographed under an optical microscope (Leica DM6000B by Leica, Wetzlar, Germany) associated with a digital camera (Leica DFC450C digital camera by Leica). The intensity of the fluorescence signal was

measured for each photo with Fiji (ImageJ, National Institutes of Health). The mean stain intensity of the 10 analyzed fields was calculated for each dilution for each serum. Background signal intensity was measured on sections incubated with PBS and was considered as a basal value.

3.2.4 RNA Extraction and cDNA Synthesis

RNA extraction was carried out using the RNeasy Fibrous Tissue Mini Kit® (Qiagen) according to the manufacturer's protocol. Before on-column extraction and elution of RNA, 30 mg of skeletal muscle or myocardium tissue were disrupted in extraction buffer using a tissue homogenizer (Mixer-Mill 300, Retsch, Haan, Germany) two times for 40 sec at 55 Hz with a 20-second pause between the two cycles.

RNA levels were measured using a NanoDrop 2000® (ThermoFisher Scientific) and cDNA was synthesized using the High-Capacity cDNA Reverse Transcription Kits (ThermoFisher Scientific, Waltham, Massachusetts, USA) following the manufacturer's instructions. Ending cDNA levels were equilibrated between samples to 15 ng/ml prior to RT-RT-qPCR.

3.2.5 Reverse Transcriptase Quantitative Polymerase Chain Reaction

TaqMan RT-RT-qPCR was performed on an Applied Biosystems 7500 Fast PCR System® (ThermoFisher Scientific) using newly developed,

or previously published[21,22], primer and probe protocols for: interferon (IFN)-γ, tumor necrosis factor (TNF)-α, Interleukin (IL)-1β, IL-4, IL-6, IL-10, IL-13, IL-17, transforming growth factor (TGF)-β and glyceraldehyde 3-phosphate dehydrogenase (GAPDH). All primers and probes were manufactured by Microsynth (Balgach, Switzerland). The hydrolysis probes were labeled with a 50 reporter dye FAM (6-carboxyfluorescein) and a 30 quencher TAMRA (6-carboxy-tetramethylrhodamine).

Those primers and probes that were newly developed were designed using Primer Express® software (v3.0.1, Thermo Fisher Scientific) to span an exon-exon junction. These were tested for specificity by conventional PCR of a test sample, gel electrophoresis, sequencing of the resulting extracted band (Microsynth) and evaluation using NCBI BLAST. Conditions were as for RT-RT-qPCR except for the omission of the probe. Primer concentrations for this step were 900 nM. Varying primer/probe concentrations were then tested to determine the optimal efficiency and dynamic range as well as replicability using a sample dilution series. All final protocols (Table 3.2) had an efficiency >95%. Those previously published were tested again in our system, omitting the conventional RT-PCR step. Each reaction comprised 10 µl Taq-Man Fast Universal Master Mix® (ThermoFisher Scientific), with 2 µl cDNA, primer and probe volumes as per Table 3.2, made up to 20 µl with RNase-free water. The thermal profile for all RT-RT-qPCRs was: 50°C for 2 min, 95°C for 10 min, and 45 cycles of 95°C for 10 sec and 60°C for 1 min. All samples were run in duplicate and any samples with discordant results were repeated. Data collection occurred during the extension phase at 60°C. Appropriate controls were included in each run.

The Applied Biosystems 7500 Software® v2.0.6 was used to visualize results and allocate a quantification cycle (C_q) to each sample, and the threshold was equilibrated between runs for each target. Relative mRNA transcription levels were calculated using the comparative C_q method.[21] The C_q of each target was first normalized to GAPDH as the endogenous reference (ΔC_q) and then expressed relative to the control group ΔC_q mean as the calibrator ($2^{-\Delta\Delta Cq}$).[21]

Table 3.2. Primer and probe sequences used for RT-RT-qPCR. Accession number, NCBI accession number; F, forward primer and start site; R, reverse primer and start site; P, probe and start site.[a]

Gene	Reference or accession number		Primer and probe sequences (5'-3') where not previously published	PCR product length (base pairs)
INFα, IFN-γ, TNF-α, IL-1β, IL-6, IL-10, IL-17, TGF-β, GAPDH	A.J. Malbon et al. (2019)[21]			
IL-4	C.M. Leutenegger et al. (1999)[22]			
IL-13	XM_006927586.3	F-1495 R-1562 P-1516	CAACCGGCATGCAGTACTGT TTGGATGGCAGTGCAGTCA CAGCCCTAGAATCTCTCAT	67

[a]All final reactions contained equivalent F and R concentrations of 900 nM and 250 nM for P, with the exception of TGF-β, 200 nM and 50 nM; IL-4, 400 nM and 80 nM, respectively.

3.2.6 Statistical Analysis

The statistical software SPSS Statistics v.25® (IBM, Armonk, New York, USA) was used for all analyses. Data were first assessed for normality using a Shapiro-Wilk test. As almost all data failed the test, non-parametric tests were applied. A two-tailed Mann-Whitney test with a significance level of 0.05 was used to compare results between groups for the number of inflammatory cells and means of mRNA expression for each target molecule. Correlation between the number of inflammatory cells and inflammatory mediator gene expression levels was evaluated using Spearman's rank test with a significance level of 0.05.

3.3 Results

3.3.1 Histology and Immunohistochemistry

8/20 (40%) of cats naturally infected with FIV showed a multifocal, endomysial lymphoplasmacellular infiltrate in quadriceps femoris (QF) and triceps brachii (TB) muscles. The severity of muscle inflammation ranged from minimal to moderate and often the inflammatory infiltrate is arranged around non-necrotic muscle fibers (Fig. 3.1). Differently, control cats showed only few scattered endomysial leukocytes.

There was no difference in the frequency of morphologically evident muscular inflammation between both muscle localizations, QF and TB, in FIV-positive cats (p=0.4470).

6/20 (30%) of FIV-positive cats showed a multifocal lymphoplasmacellular infiltrate in the myocardium. The severity of myocardial inflammation ranged from minimal to moderate.

Inflammatory changes are more frequent bot in skeletal muscle (p=0.0033) and myocardium (p=0.0083) compared with controls. Moreover, inflammation of skeletal muscle and myocardium were not independent, the two events occurred more frequently together (p=0.0116).

Both in skeletal muscle samples and myocardium, lymphocytic infiltrate was mainly characterized by CD3+ T cells and fewer CD20+ B cells. The Major histocompatibility complex (MHC) class I and II were also overexpressed in scattered skeletal muscle fibers and cardiomyocytes of FIV-positive cats. Furthermore, numerous scattered endomysial lymphocytes showed an intense cytoplasmatic and nuclear IHC-positivity for the FIV-p24-gag antigen.

In QF the number of both T (p=0.001) and B (p=0.048) lymphocytes was higher in FIV-positive cats compared with controls. The number of T (p=0.016) cells was higher also in the myocardium of FIV-positive cats compared with controls, but no differences in the number of B cells were observed. No differences have been observed regarding the number of macrophages both in QF and myocardium samples (Fig. 3.2). Furthermore, the total numbers of inflammatory cells in QF and myocardium were positively correlated (r_s=0.6140, p=0.0067) as well as the number of T cells (r_s=0.5344, p=0.0184).

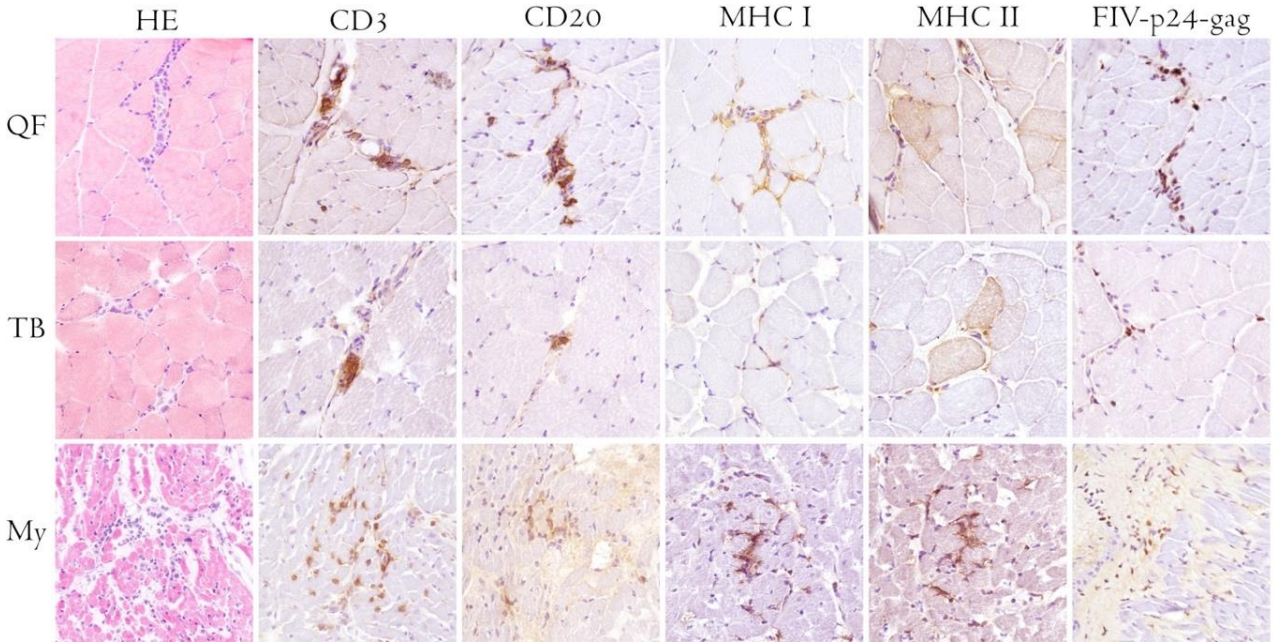

Figure 3.1. Inflammatory myopathy and myocarditis associated with naturally occurred FIV infection, cats.

A moderate multifocal, endomysial and perivascular lymphoplasmacellular infiltrate was evident both in quadriceps femoris (QF) and triceps brachii (TB) muscles and myocardium (My) of FIV infected cats. Lymphocytic infiltrate was mainly characterized by CD3+ T cells with fewer CD20+ B cells. T cells infiltrate was mainly composed of CD8+ with fewer CD4+ cells. MHC I and II-positivity were also observed in FIV-positive muscles and myocardium. Numerous scattered inflammatory cells with an intense cytoplasmatic and nuclear IHC-positivity for FIV-p24-gag antigen were also evident.

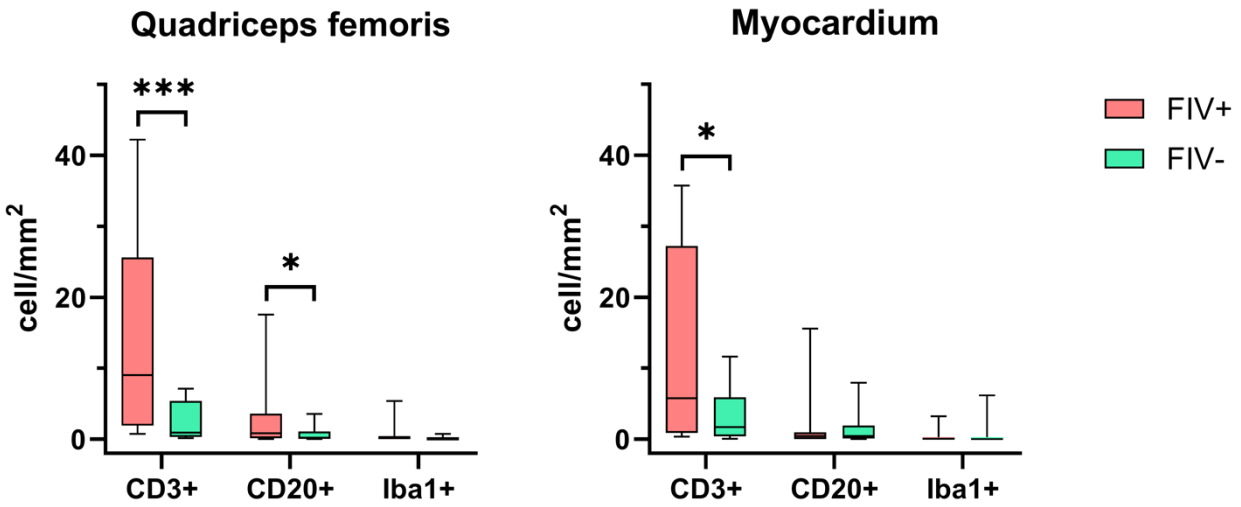

Figure 3.2. Boxplots of inflammatory cells infiltrate composition in quadriceps femoris and myocardium. The number of inflammatory cells has been determined with image analysis and expressed as number of cells per mm^2. The boxes depict the median and interquartile (IQ) range with whiskers extending to the highest and lowest values, which are within 1.5× the IQ range. Asterisks represent statistical differences between groups (*$p \leq 0.05$, ***$p \leq 0.001$).

3.3.2 Reverse Transcription Quantitative Polymerase Chain Reaction

QF samples from FIV-positive animals showed a higher expression of INFγ (p=0.010), TNFα (p=0.041), IL-17 (p=0.041), IL-6 (p=0.038), IL-13 (p=0.048), TGFβ (p=0.006) and IL-10 (p=0.041) compared with controls. No differences in the expression of IL-1β has been found in QF (p=0.303). IL-4 was not amplified in any of the QF samples (Fig. 3.3).

Myocardial samples from FIV-positive animals showed in average a high expression of INFγ, TNFα, IL-1β, IL-17, IL-6, TGFβ and IL-10 compared with controls, but no statistically significant differences were observed. Differently, IL-4 and IL-13 were less expressed in the myocardium of FIV-positive cats compared with controls, however, a statical significant difference was evident only for IL-13 (p=0.003; Fig. 3.3).

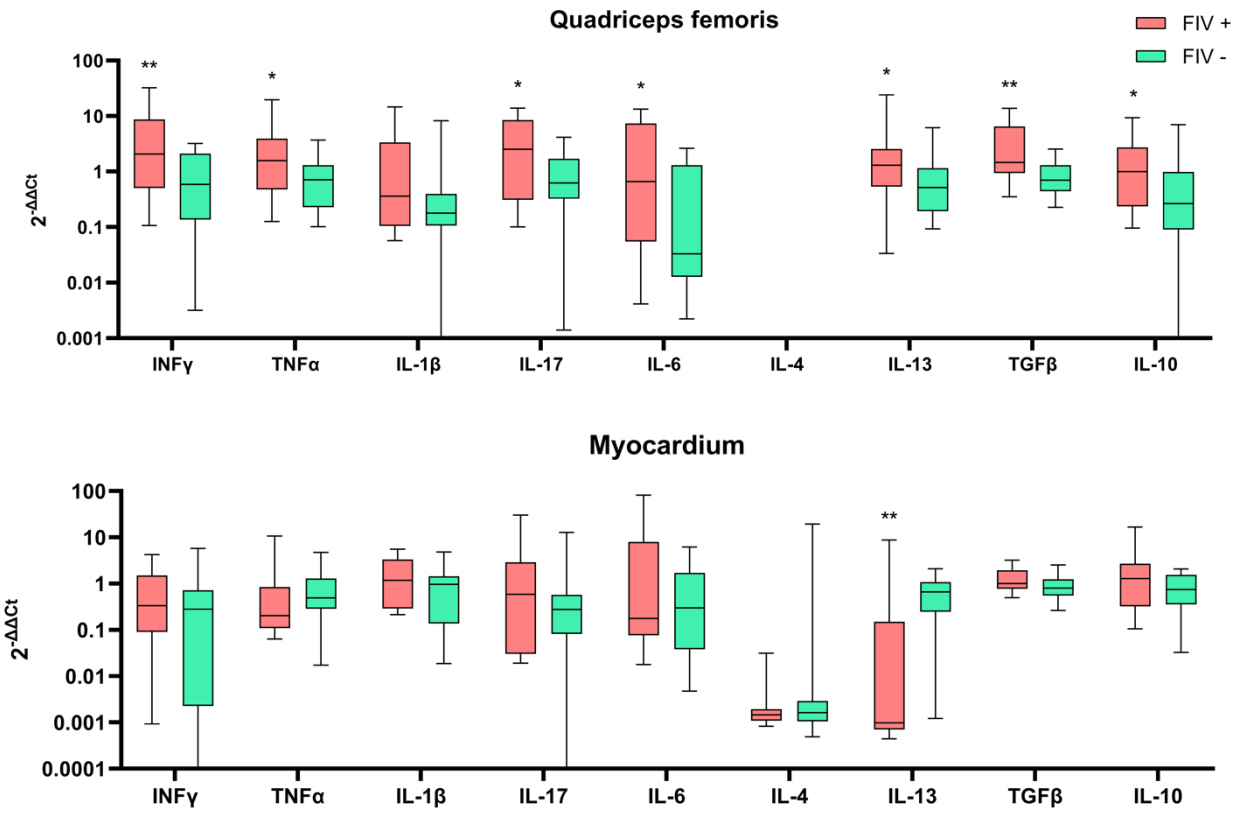
Quadriceps femoris
FIV +
FIV -
2-ΔΔCt
100
10
1
0.1
0.01
0.001
**
*
*
*
*
**
*
INFγ
TNFα
IL-1β
IL-17
IL-6
IL-4
IL-13
TGFβ
IL-10
Myocardium
2-ΔΔCt
100
10
1
0.1
0.01
0.001
0.0001
**
INFγ
TNFα
IL-1β
IL-17
IL-6
IL-4
IL-13
TGFβ
IL-10

Figure 3.3. Boxplots of relative levels of cytokine gene expression in quadriceps femoris and myocardium. The amount of target was calculated by $2^{-\Delta\Delta Cq}$, using GAPDH as the internal reference gene and expressed as an n fold difference relative to the control group mean as a calibrator. The boxes depict the median and interquartile (IQ) range with whiskers extending to the highest and lowest values, which are within 1.5× the IQ range. Asterisks represent statistical differences between groups (*$p \leq 0.05$, **$p \leq 0.01$).

3.3.3 Immunofluorescence

All sera from FIV-positive cats showed antibodies against skeletal muscle in titers up to 1:300. The IF showed mainly a sarcoplasmic positivity. No specific staining has been found using sera from normal control cats (Fig. 3.4).

Fisher's Exact test confirmed a statistically significant difference between FIV-positive and FIV-negative cats ($p=0.0119$).

Sera from FIV-positive cats showed a higher mean intensity of fluorescence both at 1:100 ($p=0.0052$) and 1:300 ($p=0.0149$) compared with controls (Fig. 3.5). Despite the R index of Spearman's rank correlation test is high ($r_s=0.8286$), the p-value is not low enough ($p=0.0583$) to define a correlation between IIF positivity and serum dilution of the FIV-positive group. No correlation was evident in the control group ($r_s= -0.7143$; $p=0.1361$).

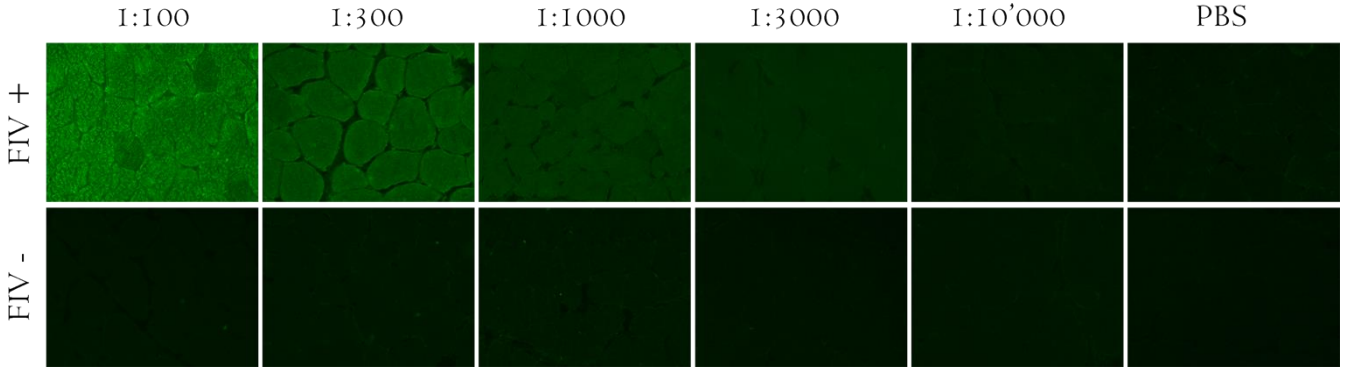

Figure 3.4. FIV-positive cats carry circulating antibodies against muscle proteins. Indirect immunofluorescence using cat sera as primary antibody on sections of normal quadriceps femoris muscle. Dilution-dependent immunofluorescent staining is evident in M. quadriceps femoris sections incubated with serum from FIV-positive cats in up to 1:300 dilutions. No specific staining is evident when the muscle sections are incubated with sera from FIV-negative control cats.

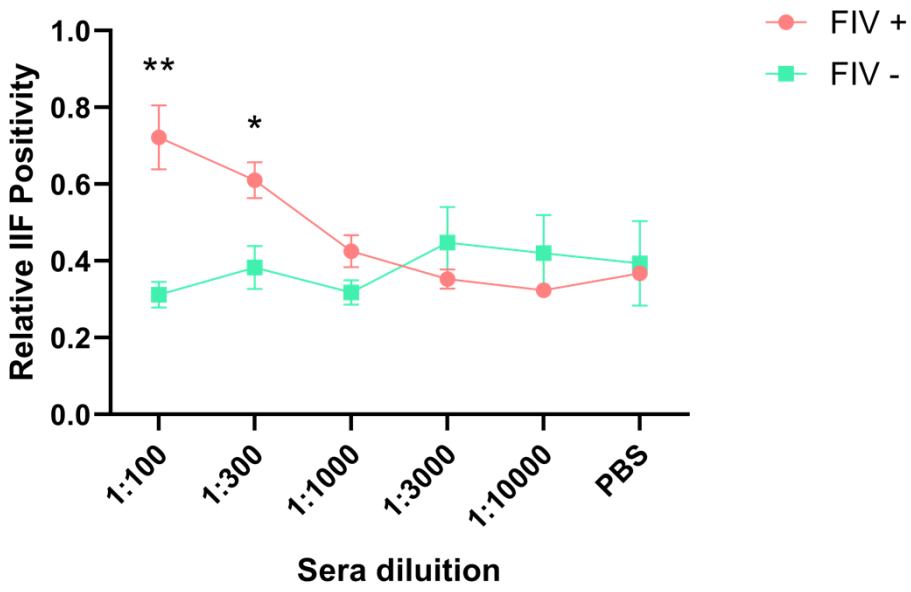

Figure 3.5. Quantitative assessment of the IIF assay. The intensity of the fluorescence was assessed with image analysis and was expressed as relative to the maximum intensity measured. FIV-positive cat sera showed a higher mean intensity of fluorescence (up to 1:300 dilution) compared to controls. Asterisks represent statistical differences between groups (*$p \leq 0.05$, **$p \leq 0.01$).

3.4 Discussion

Our results showed that an inflammatory myopathy is a relatively common condition in FIV-positive cats, affecting 40% of the examined

animals. This myopathy is associated with myocarditis, observed in 30% of the FIV-infected cats in the present study.

In a previous study in which 6 adult cats were experimentally infected with FIV, skeletal muscle inflammation was observed in all FIV-infected animals in at least one of the four sampled muscles.[10] In the present study we collected retrospectively quadriceps femoris and triceps brachii samples, differently, in the previous experimental study the investigators also examined extensor carpi radialis and cranial tibialis muscles, likely increasing the chances of finding muscle inflammation.[10] In a relatively large biopsy-based study, muscular disorders have been reported 92% (46/50) of biopsy form HIV-infected humans, where 68% (34/50) consisted in an IM and 24% (12/50) in isolated mitochondrial abnormalities without inflammatory changes.[23]

Histologically, the skeletal muscle of the FIV-positive cats with IM is characterized by multifocal mild-to-moderate chronic endomysial and perivascular muscle infiltration mainly composed of T lymphocytes associated with a lower number of B lymphocytes and rare macrophages. The high number of T cells and the rare macrophages are consistent with the already reported muscular inflammatory infiltrate phenotype in experimentally FIV-infected cats[10], however, differently from the previous study, we also observed a small number of B cells admixed in the principal cell population. These findings are also consistent with the inflammatory infiltrate described in HIV-associated IM in humans.[24]

In the present study, the expression of MHC I and MHC II in the muscle of FIV-infected cats was explored for the first time. In inflamed muscles, we observed some disseminated fibers with sarcolemmal

overexpression of MHC I and II. Sarcolemmal MHC I overexpression has been already reported in human HIV-related myopathy[24], differently, the overexpression of MHC II is a novel reported finding. Overexpression of these markers is common in IMs and is also considered an excellent diagnostic marker when the inflammatory infiltrate is not evident in the examined sections.[18,20]

HIV DNA has been identified with the use of in situ reverse-transcriptase polymerase chain reaction within endomysial macrophages and myocyte nuclei, raising the possibility that myopathies may be due in part to direct HIV infection of myocytes.[24] Differently, immunohistochemical positivity for HIV antigens has been described only in infiltrating inflammatory cells.[24] We also described immunohistochemically positive cells for FIV-p24-gag antigen within the infiltrating inflammatory cells and no positivity has been observed in muscle fibers.

In the present study, we observed myocarditis in 30% of FIV-infected cats. Data on FIV-associated myocarditis in literature are restricted to one report on five cases, all in cats that suffered from hypertrophic cardiomyopathy.[11] Given the difficulty of performing a myocardial biopsy, there are few studies in human medicine that describe the prevalence of myocarditis in HIV-infected patients.[25] Moreover, this prevalence is probably reduced by the extensive use of antiretroviral therapy (ART).[13,25] In an autopsy series performed in the pre-ART era, myocarditis was documented in 40-52% of HIV-infected patients.[25]

Histologically, the myocardium of the FIV-positive cats with myocarditis is characterized by a multifocal mild-to-moderate inflammatory

infiltrate with the same immunophenotype found in skeletal muscle. The inflammatory infiltrate mainly composed of CD3+ T cells is consistent with the inflammatory infiltrate phenotype already reported in the previously mentioned case series of five cats.[11] Moreover, the same inflammatory infiltrate has been reported also in human myocarditis associated with HIV infection.[26]

As previously reported, we also observed immunohistochemically positive cells for FIV-p24-gag antigen among the inflammatory cells infiltrating the myocardium and no positivity has been observed in cardiomyocytes.[11]

The over-expression of T helper type 1 (T_H1) cytokines such as INFγ and TNFα and T helper type 17 (T_H17) cytokines such as IL-17 and IL-6 in the skeletal muscle of FIV-positive cats implicate a T_H1/T_H17 lymphocytes polarization in the inflamed muscle.[4] The T_H1/T_H17 immune response is central in the pathogenesis of the majority of the IMs both in human and in other animals and suggest an autoimmune pathomechanism.[3,4,9,27] T_H1 and T_H17 cells secrete cytokines that mediate muscle damage and inflammation and the activation of additional immune cells.[4] IL-13 overexpression was also found in the skeletal muscle of FIV-infected cats, differently, no detectable expression of IL-4 was found. IL-13 and IL-4 are T helper type 2 (T_H2) cytokines and modulate B cell function and differentiation into antibody-producing plasma cells potentially contributing to the production of autoantibodies.[4] We also observed overexpression of regulatory T cells (T_{reg}) cytokines such as TGFβ and IL-10. The presence of regulatory T cells (Treg) reduces inflammation and tissue damage by inhibiting CD4+ and CD8+ effector T cells.[4] The overexpression of T_{reg} cytokines is described in

several inflammatory myopathies and is supposed to have the role of balancing the inflammatory response; however, cytokines can display both pro- and anti-inflammatory properties depending on the context.[4] Notably, in *Toxoplasma gondii* infection, regulatory T cells promote myositis and muscle damage.[28]

Differently, despite on average most of the markers of the T_H1/T_H17 inflammatory response are over-expressed also in the myocardium of FIV-positive cats and T_H2 markers are downregulated, we observed statistically significant difference with the control group only in IL-13 expression.[4] This is probably due to the smaller number of samples examined, so further advances are needed to better define the polarization of the inflammatory response in this tissue.

In this study, we identified circulating IgG autoantibodies specific for the skeletal muscle in cats infected with FIV. We found mainly a sarcoplasmic positivity with indirect immunofluorescence suggesting that the major antigen is intracellular. Circulating autoantibodies are a common finding in IM, both in humans and other animals.[3,9,15] Most of the reported autoantigens are intracellular and, for this reason, the role of autoantibodies in causing muscle damage and dysfunction is debated.[1,15] Further studies are needed to define if these circulating autoantibodies cross-react with the myocardium and to identify precisely the target antigen(s).

Autoimmune manifestations are common in HIV patients, an increased prevalence and titer of circulating autoantibodies have been reported.[29] Up to 68.1% of HIV patients have circulating antinuclear antibodies (ANAs), furthermore, autoantibodies against peripheral blood cells, MHC II, and phospholipids have also been frequently observed in HIV

patients.[29] HIV positive humans, and particularly those with cardiomyopathy, show circulating cardiac-specific autoantibodies, some of which also react with skeletal muscle (notably anti-β-myosin autoantibody).[16,17] The increased incidence and titer of autoantibodies are associated with lower CD4+ T cell count and higher mortality in HIV patients who are naive to antiretroviral therapy, indicating that autoantibodies may play a pathogenic role or can serve as a prognostic indicator in HIV infection.[29]

Traditionally, autoantibodies found in patients with myositis are described as being myositis-specific autoantibodies (MSAs) or myositis-associated autoantibodies (MAAs), depending on their prevalence in other related conditions. An intriguing aspect of MSAs is that the detection of more than one such autoantibody in the same individual patient is extremely rare, although MAAs can sometimes coexist.[3,9,15] As such, MSAs are ideal biomarkers, not only for identifying homogeneous subsets of myositis but also for exploring more precisely the potential environmental and genetic factors contributing to the disease.[3,15] Therefore, the identification of FIV myopathy-associated MSAs can be relevant because they can become an excellent diagnostic tool helping the clinician in the decision to perform a muscle biopsy.[15,30]

3.5 Conclusions

Our study provides evidence that FIV is associated with an IM also in naturally infected cats. FIV-associated IM is characterized by a mild-to-

moderate endomysial and perivascular inflammatory infiltrate composed of mainly T lymphocytes.

Moreover, this pathology can be complicated by myocarditis also characterized by a mild-to-moderate interstitial inflammatory infiltrate mainly composed of T lymphocytes.

Both inflammatory processes sesames to be characterized by a T_H1/T_H17 lymphocyte polarization, suggesting an autoimmune pathogenesis.[27]

We also demonstrated the presence of circulating anti-skeletal muscle autoantibodies and hypostasized that these autoantibodies may cross-react also with the myocardium.

Further studies are needed to better elucidate the pathomechanisms underlying FIV-associated IM and myocarditis in cats. The identification of the specific target of the circulating autoantibodies may be helpful for diagnosis, therapy, monitoring of the disease and prognosis.[15] Furthermore, considering the overlapping features with HIV-related IM and myocarditis in humans, FIV infection in cats could also serve as a natural model for HIV infection.

Chapter 3 References

1. Dubowitz V, Sewry CA, Oldfors A, Lane RJM. *Muscle Biopsy: A Practical Approach*. 4th Editio. Saunders; 2013.
2. Miller FW, Lamb JA, Schmidt J, Nagaraju K. Risk factors and disease mechanisms in myositis. *Nat Rev Rheumatol*. 2018;14(5):255-268. doi:10.1038/nrrheum.2018.48
3. Prisco F, Papparella S, Paciello O. The correlation between cardiac and skeletal muscle pathology in animal models of idiopathic inflammatory myopathies. 2020:315-321. doi:10.36185/2532-1900-035
4. Moran EM, Mastaglia FL. Cytokines in immune-mediated inflammatory myopathies: Cellular sources, multiple actions and therapeutic implications. *Clin Exp Immunol*. 2014;178(3):405-415. doi:10.1111/cei.12445
5. Shelton GD. From dog to man: The broad spectrum of inflammatory myopathies. *Neuromuscul Disord*. 2007;17(9-10):663-670. doi:10.1016/j.nmd.2007.06.466
6. Paciello O, Oliva G, Gradoni L, et al. Canine inflammatory myopathy associated with Leishmania Infantum infection. *Neuromuscul Disord*. 2009;19(2):124-130. doi:10.1016/j.nmd.2008.10.013
7. Costagliola A, Piegari G, Otrocka-Domagala I, et al. Immunopathological features of canine myocarditis associated with leishmania infantum infection. *Biomed Res Int*. 2016;2016. doi:10.1155/2016/8016186
8. Prisco F, De Biase D, Piegari G, et al. Pathomechanism highlights of leishmania-associated myopathy in the dog. *J Comp Pathol*. 2019;166:110. doi:10.1016/j.jcpa.2018.10.033
9. Pasolini MP, Pagano TB, Costagliola A, et al. Inflammatory Myopathy in Horses With Chronic Piroplasmosis. *Vet Pathol*. 2018;55(1):133-143. doi:10.1177/0300985817716262
10. Podell M, Chen E, Shelton GD. Feline immunodeficiency virus associated myopathy in the adult cat. *Muscle Nerve*. 1998;21(12):1680-1685. doi:10.1002/(SICI)1097-4598(199812)21:12<1680::AID-MUS9>3.0.CO;2-F
11. Rolim VM, Casagrande RA, Wouters ATB, Driemeier D, Pavarini SP. Myocarditis caused by Feline Immunodeficiency Virus in Five

Cats with Hypertrophic Cardiomyopathy. *J Comp Pathol*. 2016;154(1):3-8. doi:10.1016/j.jcpa.2015.10.180

12. Hiniker A, Daniels BH, Margeta M. T-cell-mediated inflammatory myopathies in HIV-positive individuals: A histologic study of 19 cases. *J Neuropathol Exp Neurol*. 2016;75(3):239-245. doi:10.1093/jnen/nlv023
13. Sani MU. Myocardial disease in human immunodeficiency virus (HIV) infection: A review. *Wien Klin Wochenschr*. 2008;120(3-4):77-87. doi:10.1007/s00508-008-0935-3
14. Hsue PY, Waters DD. Heart failure in persons living with HIV infection. *Curr Opin HIV AIDS*. 2017;12(6):534-539. doi:10.1097/COH.0000000000000409
15. McHugh NJ, Tansley SL. Autoantibodies in myositis. *Nat Rev Rheumatol*. 2018;14(5):290-302. doi:10.1038/nrrheum.2018.56
16. Currie PF, Goldman JH, Caforio ALP, et al. Cardiac autoimmunity in HIV related heart muscle disease. *Heart*. 1998;79(6):599-604. doi:10.1136/hrt.79.6.599
17. Huck DM, Okello E, Mirembe G, et al. Role of Natural Autoantibodies in Ugandans With Rheumatic Heart Disease and HIV. *EBioMedicine*. 2016;5:161-166. doi:10.1016/j.ebiom.2016.02.006
18. Paciello O, Papparella S. Histochemical and immunohistological approach to comparative neuromuscular diseases. *Folia Histochem Cytobiol*. 2009;47(2):143-152. doi:10.2478/v10042-009-0066-3
19. Meuten DJ, Moore FM, George JW. Mitotic Count and the Field of View Area. *Vet Pathol*. 2016;53(1):7-9. doi:10.1177/0300985815593349
20. Pagano TB, Prisco F, De Biase D, et al. Muscular Sarcocystosis in Sheep Associated With Lymphoplasmacytic Myositis and Expression of Major Histocompatibility Complex Class I and II. *Vet Pathol*. December 2019:030098581989125. doi:10.1177/0300985819891257
21. Malbon AJ, Meli ML, Barker EN, Davidson AD, Tasker S, Kipar A. Inflammatory Mediators in the Mesenteric Lymph Nodes, Site of a Possible Intermediate Phase in the Immune Response to Feline Coronavirus and the Pathogenesis of Feline Infectious Peritonitis? *J Comp Pathol*. 2019;166:69-86. doi:10.1016/j.jcpa.2018.11.001
22. Leutenegger CM, Mislin CN, Sigrist B, Ehrengruber MU, Hofmann-Lehmann R, Lutz H. Quantitative real-time PCR for the measurement

of feline cytokine mRNA. *Vet Immunol Immunopathol*. 1999;71(3-4):291-305. doi:10.1016/S0165-2427(99)00100-2

23. Myalgia I, Prism G, Hiv-positive MA. Expanding the spectrum of HIV- associated myopathy. :1-2. doi:10.1136/jnnp-2018-319419
24. Tien-Auh Chan A, Kirton C, Estanislao L, Simpson DM. Myopathy in HIV infection. *Handb Clin Neurol*. 2007;85(Actg 016):139-145. doi:10.1016/S0072-9752(07)85010-X
25. Ntusi NAB. HIV and myocarditis. *Curr Opin HIV AIDS*. 2017;12(6):561-565. doi:10.1097/COH.0000000000000416
26. Barbaro G, Di Lorenzo G, Grisorio B, et al. Cardiac involvement in the acquired immunodeficiency syndrome: A multicenter clinical-pathological study. *AIDS Res Hum Retroviruses*. 1998;14(12):1071-1077. doi:10.1089/aid.1998.14.1071
27. Tabarkiewicz J, Pogoda K, Karczmarczyk A, Pozarowski P, Giannopoulos K. The Role of IL-17 and Th17 Lymphocytes in Autoimmune Diseases. *Arch Immunol Ther Exp (Warsz)*. 2015;63(6):435-449. doi:10.1007/s00005-015-0344-z
28. Jin RM, Blair SJ, Warunek J, Heffner RR, Blader IJ, Wohlfert EA. Regulatory T Cells Promote Myositis and Muscle Damage in Toxoplasma gondii Infection. *J Immunol*. 2017;198(1):352-362. doi:10.4049/jimmunol.1600914
29. Meng Z, Du L, Hu N, et al. Antiretroviral Therapy Normalizes Autoantibody Profile of HIV Patients by Decreasing CD33+ CD11b+ HLA-DR+ Cells. *Med (United States)*. 2016;95(15):1-9. doi:10.1097/MD.0000000000003285
30. Lundberg IE, De Visser M, Werth VP. Classification of myositis. *Nat Rev Rheumatol*. 2018;14(5):269-278. doi:10.1038/nrrheum.2018.41

Final conclusions

Inflammatory myopathies (IM) are muscle diseases characterized by complex and fascinating pathomechanisms. To date, many of the factors responsible for disease initiation and perpetuation remain unknown.

The objective of this thesis was to contribute to shedding light on these complex mechanisms and validating animal models for comparative medicine.

The main innovative aspects of this thesis are:

1. the identification of circulating autoantibodies that recognize the muscle protein sarcoplasmic/endoplasmic reticulum calcium ATPase 1 (SERCA1) in leishmania-infected dogs, supporting the autoimmune mechanism underlying this myopathy and the antigen mimicry pathogenesis;
2. the immune-mediated muscle damage in the white striping myopathy of the broiler chicken;
3. the identification of circulating anti-skeletal muscle autoantibodies as part of the pathomechanisms underlying the inflammatory myopathy associated with natural Feline Immunodeficiency Virus infection in cats.

The study of IM in veterinary medicine is a relatively young field of research. Studies in the past decade have elucidated possible genetic and environmental risk factors, as well as possible immune and non-immune mechanisms, that result in the development of the various IM phenotypes.

Conclusions

As shown in the present thesis, mounting evidence suggests that infectious agents are the main actors in the environmental factors which modulate the development of autoimmune diseases. The underlying mechanisms are multiple and complex, probably different according to the involved pathogens.

The presence of circulating autoantibodies in the majority of humans and other animals with IMs is of crescent interest. Despite the role of autoantibodies in causing muscle damage and dysfunction is still debated, myositis specific autoantibodies are ideal biomarkers, not only for identifying homogeneous subsets of myositis but also for exploring more precisely the potential environmental and genetic factors contributing to the disease.

In the future, emphasis needs to be placed on multidisciplinary, collaborative investigations of etiologies and pathomechanisms underlying IMs and of the diagnostic accuracy and utility of myositis-specific autoantibodies in animals.